


For Reference

NOT TO BE TAKEN FROM THIS ROOM

Ex LIBRIS
UNIVERSITATIS
ALBERTAENSIS





Digitized by the Internet Archive
in 2024 with funding from
University of Alberta Library

<https://archive.org/details/McLarnon1973>

THE UNIVERSITY OF ALBERTA

RELEASE FORM

NAME OF AUTHOR Barry David McLarnon
TITLE OF THESIS A Multiplexed Feeder System for Accurate
..... Excitation of a Large Antenna Array
.....
DEGREE FOR WHICH THESIS WAS PRESENTED Master of Science
YEAR THIS DEGREE GRANTED Fall 1973

Permission is hereby granted to THE UNIVERSITY OF
ALBERTA LIBRARY to reproduce single copies of this
thesis and to lend or sell such copies for private,
scholarly or scientific research purposes only.

The author reserves other publication rights, and
neither the thesis nor extensive extracts from it may
be printed or otherwise reproduced without the author's
written permission.

THE UNIVERSITY OF ALBERTA

A MULTIPLEXED FEEDER SYSTEM FOR ACCURATE
EXCITATION OF A LARGE ANTENNA ARRAY

by



BARRY DAVID McLARNON

A THESIS

SUBMITTED TO THE FACULTY OF GRADUATE STUDIES AND RESEARCH
IN PARTIAL FULFILMENT OF THE REQUIREMENTS FOR THE DEGREE
OF MASTER OF SCIENCE
IN
ELECTRICAL ENGINEERING

DEPARTMENT OF ELECTRICAL ENGINEERING

EDMONTON, ALBERTA

FALL, 1973

THE UNIVERSITY OF ALBERTA
FACULTY OF GRADUATE STUDIES AND RESEARCH

The undersigned certify that they have read, and recommend to the Faculty of Graduate Studies and Research, for acceptance, a thesis entitled "A Multiplexed Feeder System for Accurate Excitation of a Large Antenna Array" submitted by Barry David McLarnon in partial fulfilment of the requirements for the degree of Master of Science in Electrical Engineering.

DEDICATION

To My Mother

ABSTRACT

Details of a proposed Tee-shaped radio telescope array are presented, with particular emphasis placed on the demands of accuracy and versatility which are made concerning the array feeder system. The feeder systems of existing arrays are examined, and their advantages and shortcomings are pointed out. A general survey of feeder techniques follows, including a thorough examination of signal transmission methods and their effects on system noise temperature and errors in array excitation. Methods of reducing the number of transmission lines by the use of multiplexing are considered, and a frequency-division multiplexing scheme is shown to be the most practicable. An assessment of excitation errors is made, together with discussions concerning various means by which these errors can be reduced and maintained at a low level. The errors are also studied from the standpoint of their effect on the sidelobe levels of the Tee array radiation pattern. It is concluded that an automatic compensation system for maintenance of excitation accuracy should be included in the feeder system design. Preliminary details on the implementation of such a system are given; compensation for time delay errors is also considered briefly.

ACKNOWLEDGEMENTS

The author wishes to thank Dr. D. Routledge and Dr. C.G. Englefield, thesis supervisors, for their encouragement and guidance during the course of this work. The author also wishes to thank Dr. W.R. Goddard and D.A. Wynne for useful discussions.

The financial support provided by the National Research Council of Canada and the Department of Electrical Engineering is gratefully acknowledged.

TABLE OF CONTENTS

CHAPTER		PAGE
1.	INTRODUCTION AND PRELIMINARY DESIGN DETAILS	1
1.1	Introduction	1
1.2	Basic Configuration	2
1.3	Specifications and Performance Objectives	4
1.3.1	System Bandwidth	4
1.3.2	Array Pattern and Sidelobe Levels	5
1.3.3	Excitation Errors	7
1.3.4	Multibeaming	7
1.3.5	Subarray Size	10
1.4	A Survey of Large Phased-Array Radio Telescopes	14
1.4.1	Characteristics of Selected Installations	14
1.4.2	Other Radio Telescope Arrays	18
	(a) The Early Mills Crosses	18
	(b) The "Moving Tee" Aperture Synthesis Instruments	18
	(c) The Culgoora Radioheliograph	19
1.5	Summary of Available Options	20
1.5.1	Receiver Type	20
1.5.2	System Bandwidth	21
1.5.3	Feeder Systems	22
1.5.4	Signal Transmission Techniques	23
1.5.5	Control of Phase Errors	24
1.5.6	Subarrays	25

1.5.7	Multibeam Capability	26
2.	THE FEEDER SYSTEM	28
2.1	Basic Types of Feeder Systems	28
2.1.1	Single-Line Feeders	28
2.1.2	Binary Branching Feeders	31
2.1.3	Independent Equal-Length Feeders	33
2.2	Choice of a Feeder System	34
2.3	Signal Transmission Without Frequency Conversion	35
2.3.1	Attenuation and Noise Considerations	36
	(a) Transmission Without Preamplification	36
	(b) Transmission With Preamplification	40
2.3.2	Excitation Errors	44
	(a) Thermal Effects: Transmission Lines	44
	(b) Thermal Effects: Preamplifiers	48
	(c) Moisture and Other Environmental Factors	49
	(d) Component Aging	49
	(e) Cable Trimming	50
	(f) Shielding Efficiency and Crosstalk	53
2.3.3	Summary and Evaluation	59
2.4	Signal Transmission With Frequency Conversion	63
2.4.1	Receiver Type: SSB Versus DSB	63
2.4.2	Image Rejection and Choice of IF	67
2.4.3	Attenuation and Noise Considerations	70
2.4.4	Excitation Errors	72
2.4.5	Local Oscillator Distribution	74

2.4.6	Beam Pointing Error Compensation	78
2.5	Protection from Lightning	80
3.	MULTIPLEXING IN THE FEEDER SYSTEM	82
3.1	Multiplexing: An Overview	82
3.2	Time-Division Multiplexing	83
3.3	Frequency-Division Multiplexing	93
3.3.1	Basic System Design	93
3.3.2	Crosstalk from Intermodulation Distortion	99
3.3.3	Local Oscillator Distribution and Phase Equalization	108
3.3.4	Dispersion in the Transmission Lines	111
3.3.5	Amplitude Equalization	112
3.3.6	Summary	115
3.4	Quadrature Multiplexing	116
3.4.1	Basic System Design	116
3.4.2	Crosstalk from Phase Errors	118
3.4.3	Crosstalk from Amplitude Errors	120
4.	ASSESSMENT OF ARRAY EXCITATION ERRORS	123
4.1	The Remote Electronic Components	123
4.1.1	The Input Bandpass Filter	123
4.1.2	The Preamplifier/Mixer and Local Oscillator	128
4.2	The Transmission Lines	131
4.2.1	Measurement Errors	131
4.2.2	Phase and Amplitude Stability	132

4.2.3	Inter-Cable Crosstalk	133
4.2.4	Impedance Mismatches and Inhomogeneities	133
4.3	The Multiplexing System	136
4.3.1	Inter-Channel Crosstalk	136
4.3.2	Intermodulation Crosstalk	136
4.3.3	Equalization	137
4.4	The Second Mixer	138
4.5	Signal Processing After the Second Mixer	139
4.5.1	The Output Bandpass Filter and IF Amplifier	139
4.5.2	Beam Formation and Other Signal Processing	141
4.6	Summation of Excitation Errors	142
4.7	Other Sources of Error	144
4.7.1	Positional Errors	144
4.7.2	Mutual Coupling of the Array Elements	147
4.7.3	Miscellaneous Error Sources	148
5.	ERROR COMPENSATION SYSTEMS AND SIDELobe CALCULATIONS	150
5.1	Reduction of Excitation Errors	150
5.1.1	Continuous Phase Error Compensation	151
5.1.2	Discontinuous Compensation Systems	161
5.2	The Effects of Excitation Errors on Sidelobe Levels	173
5.2.1	Sidelobe Levels Off the Array Planes	173
5.2.2	Sidelobe Levels In the Array Planes	180
5.3	Decorrelation and Delay Error Compensation	182
6.	SUMMARY AND CONCLUSIONS	190
	REFERENCES	194

LIST OF TABLES

Table		Page
1.1a	Characteristics of Some Existing Radio Telescopes: General	16
1.1b	Characteristics of Some Existing Radio Telescopes: Feeder Systems	17
2.1	Characteristics of Common Coaxial Transmission Lines	41
2.2	Properties of Standard Telephone Cable (19 AWG twisted pairs, measured at 27°C)	66
2.3	Attenuation (dB) vs Frequency for 2.5 km Cable Runs	71
3.1	Normalization Factor for Cables	88
3.2	FDM System Parameters for Various Input Filters	95
3.3	Cable Attenuation (dB) for Two Typical IF Channels	113
4.1	Summary of Error Estimates	143
5.1	Predicted Sidelobe Levels With and Without Compensation	179

LIST OF FIGURES

Figure		Page
1.1	Tee Array Configuration	3
2.1a	Single-Line Feeder Systems: Series Feed	29
2.1b	Single-Line Feeder Systems: Parallel Feed	29
2.2	Binary Branching Feeder System	32
2.3	Independent Equal-Length Feedlines	32
2.4	System Noise Temperature Versus Cable Attenuation	43
2.5	Spectral Relationships in Frequency Conversion Systems	64
2.6	Local Oscillator Distribution System	76
3.1	Section of Sampled Signal Output Spectrum	84
3.2	Normalized Pulse Response of RG-218/U Cable	89
3.3	Basic Two-Channel Frequency-Division Multiplex System	94
3.4	Modified Two-Channel Frequency-Division Multiplex System	97
3.5	Intermodulation Products of a Mixer	103
3.6	Test Set-Up for Intermodulation Measurements	105
3.7	Quadrature Multiplexing System	117
3.8	Phasor Representation of QM Crosstalk	119
5.1	FDM System With Transmission Line Phase Compensation	152
5.2	Temperature Characteristics of Cable Delays	154
5.3	FDM System With Discontinuous Phase and Amplitude Compensation	163
5.4	Probability Density Function for Sidelobe Level Far from the Array Planes	177
5.5	Probability of Exceeding a Given Sidelobe Level	179
5.6	Correlation Versus Bandwidth for Various Scan Angles	186

CHAPTER 1

INTRODUCTION AND PRELIMINARY DESIGN DETAILS

1.1 Introduction

The design of the large Tee-shaped radio telescope array proposed for a site in southwestern Alberta [1] represents a number of challenging engineering problems. In particular, the large physical dimensions of the array, and the intention of achieving very low sidelobe levels while maintaining a high degree of flexibility in signal processing, make rather severe demands of the array feeder system. Although the results of this thesis will be specifically related to the proposed Tee configuration, it is intended that they be sufficiently general to be applied to other arrays of a similar nature.

This chapter begins with a description of the array and some of its attributes. A number of existing arrays are then examined to aid in the evaluation of the various options involved in the design of the feeder system.

1.2 Basic Configuration

The proposed array, depicted in Fig. 1.1, is an arrangement of half-wave dipole elements in the form of a Tee measuring two hundred wavelengths east-west and one hundred wavelengths north-south. The corresponding widths are two wavelengths and five wavelengths, respectively. At the nominal center frequency of 12.36 MHz, the resulting dimensions are approximately 48.5 meters by 4854 meters east-west and 121 meters by 2427 meters north-south. The dipoles filling this area are polarized east-west, with 0.625λ center-to-center spacing in this direction and 0.5λ spacing north-south. The total number of dipoles required is then 2848, of which 1248 are in the east-west array, 1568 are in the north-south array, and 32 are in the region where the two arrays overlap. A scheme is currently under investigation by which the total number of elements could be reduced to about 2000 through physical tapering, which is the modification of array response by the removal of certain elements. However, it is not certain that such a scheme will be adopted, since its performance is inferior in some respects (such as sidelobe levels) to the full Tee array.

In any case, rather severe grading of the array aperture is necessary to reduce the sidelobe responses, and this will require some electrical tapering regardless of whether physical tapering is used. The grading function planned for at present is the truncated Gaussian type, with reduction of the voltage weighting at the extreme ends of the arrays to about 6% of the weighting at the center of the Tee. No tapering across the small dimensions of the array is planned. The

overall design of the radio telescope will be such that changes in the grading functions can be made without major difficulties.

The dipole elements will likely be of folded-dipole type of construction, supported by wooden poles at a distance of 0.125λ above a plane reflecting screen ($\lambda=24.2$ meters in this and the preceding specifications).

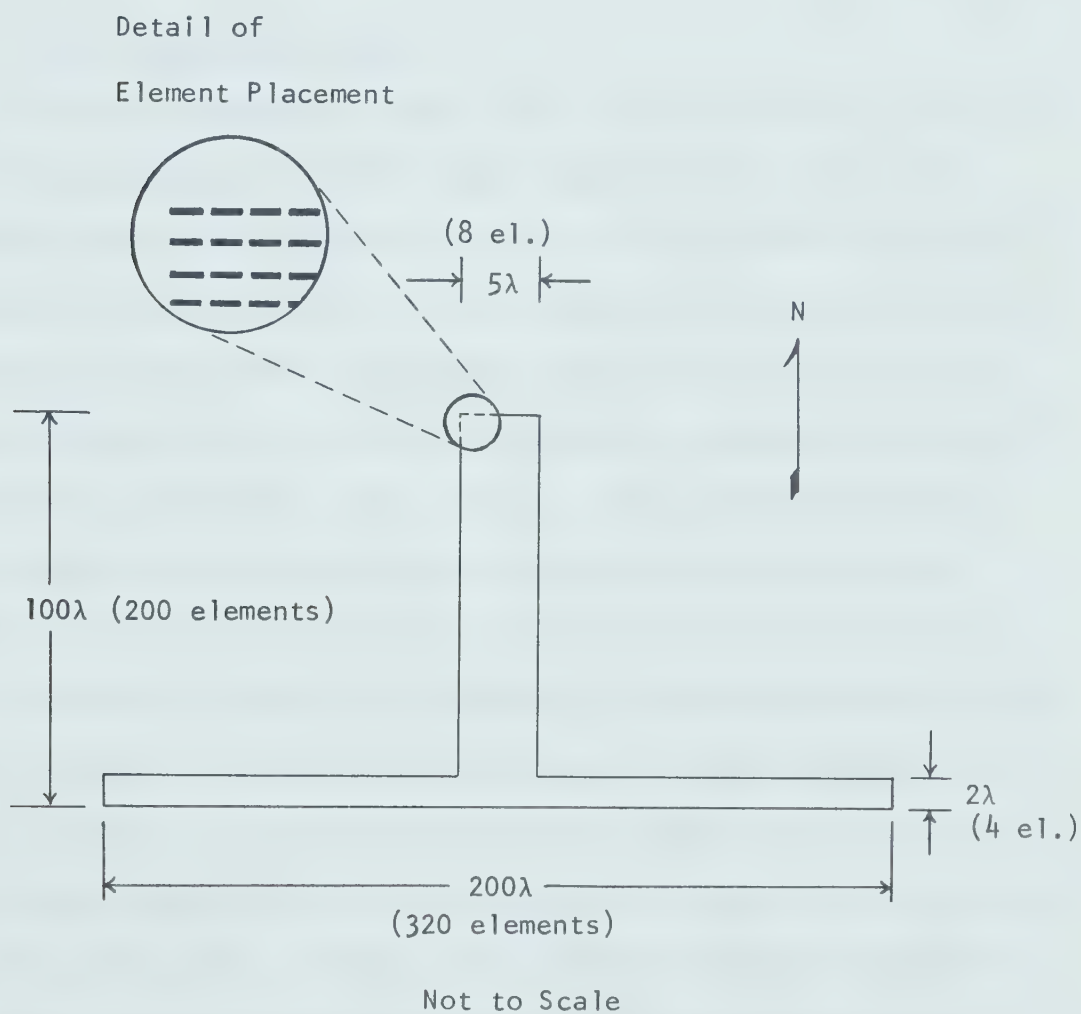


Fig. 1.1 Tee Array Configuration

1.3 Specifications and Performance Objectives

Specifications of the Tee array which affect the design of the feeder system will be introduced in this section. In most cases, the astronomical considerations leading to these specifications will be omitted or described only briefly; these topics have been dealt with in greater detail elsewhere [1],[2].

1.3.1 System Bandwidth

From the standpoint of sensitivity (defined in Sec. 2.3.1), it is desirable to have as large a system bandwidth as possible; the bandwidth, however, is subject to a number of constraints. The most serious of these is terrestrial interference. At the relatively low frequencies involved here, ionospheric "skip" propagation is a very common occurrence. The degree of interference is dependent on diurnal and seasonal variations in the ionosphere, the eleven-year sunspot cycle, solar disturbances, and numerous other factors. Although conditions which are favorable for astronomical observations tend to be unfavorable for terrestrial propagation, some interference near the center frequency is likely to be encountered in most instances. The original survey [1] which was undertaken to choose the frequency of operation disclosed that the useable bandwidths ranged from 10 to 100 KHz. The nominal center frequency of 12.36 MHz falls in a segment of the spectrum allocated to maritime ship-to-shore telephony, whose occupancy and power levels are generally lower than those of adjacent bands. The unpredictable nature of the interference makes necessary some provision for varying the system bandwidth.

Other factors which impose limitations on the bandwidth include the narrowband properties of the dipole elements, and decorrelation losses due to the differences in arrival times of the incident wavefronts at different elements. These factors are, in general, less restrictive than the interference problem; decorrelation losses, for example, can be minimized by delay compensation (Sec. 5.3). When needed in the analysis of the feeder system, the system bandwidth will be assumed to be a maximum of 100 KHz, but with allowance being made for possible extension to about 200 KHz when conditions warrant.

1.3.2 Array Pattern and Sidelobe Levels

The basic objective of the Tee array is to form a pencil-beam response by suitable phasing of the elements and cross-correlation of the outputs of the two component arrays. The beam will have a half-power beamwidth of about 30 arcmin and will be steerable in declination from 15°S to 90°N , which corresponds to zenith angles of 67° and 38° south and north of the zenith respectively. Although most large arrays of this or similar types are meridian transit instruments (i.e., they are not steerable in right ascension except by the earth's rotation), such steering is highly desirable for maximum flexibility, particularly when viewing times are severely limited by the ionosphere as they are in this case. Therefore present plans include the provision for steering the beam about 30° east or west of the zenith. The benefits of such a provision include increased sky coverage during favorable operating periods, the ability to form a number of beams simultaneously in right ascension, and the possibility of tracking sources for considerable periods of time.

The sensitivity to point sources, or that flux density which will result in a signal-to-noise ratio which is the minimum acceptable for reliable measurements, is limited by system noise (Sec. 2.3.1), confusion noise from unwanted sources in the mainbeam, and confusion noise from sources in the sidelobes. If possible, one would like to have the sidelobe levels sufficiently low that sidelobe confusion is not a significant factor in limiting the sensitivity. Such a criterion leads to the specification of a maximum r.m.s. value for the normalized power pattern excluding the mainbeam. Preliminary work in this area by Goddard [2] indicates that the necessary r.m.s. sidelobe level is of the order of 1.4×10^{-4} (-38 dB).

In addition to point source observations, it is intended that the array be useful for measurement of the brightness distribution of sources whose angular extents are greater than that of the mainbeam. An example of such a source is the background radiation originating in the interstellar plasma of our galaxy. The extended nature of these sources imposes a more severe constraint on the r.m.s. sidelobe level than does the point source criterion mentioned above. For instance, to provide 3000°K contours on the background brightness temperature distribution (an order of magnitude improvement over previous measurements near this wavelength) would call for an r.m.s. sidelobe level estimated at [2] about 2×10^{-5} (-47 dB).

The power pattern of the Tee array away from the mainbeam has rather prominent sidelobes in the array planes and relatively low levels elsewhere (Sec. 5.2). Determination of the r.m.s. sidelobe level entails numerical integration over the power pattern for the particular Tee configuration being studied. This level is affected by the array

grading, excitation errors, and the degree of element grouping into subarrays. Detailed examination of antenna patterns is not within the scope of this thesis; it is hoped, however, that the material developed, particularly in the realm of excitation errors, will aid in future studies of the field pattern of the Tee array.

1.3.3 Excitation Errors

Any deviations in phase or amplitude from the ideal voltage distribution in the array elements will, in general, result in higher sidelobe levels than for the no-error case. This will be accompanied by a reduction in gain and a beam pointing error, but these effects are usually of little concern if the errors are small. The errors are random in most instances and thus must be dealt with by statistical means.

The usefulness of this radio telescope design depends in large measure on the degree to which the excitation errors can be minimized. This subject will figure prominently in the following chapters, and relationships between errors and sidelobe levels will be examined in Sec. 5.2. It will be shown at that time that r.m.s. excitation errors no greater than about 1° in phase and 2% in amplitude are necessary for adequate sidelobe performance. Other workers (see [3], for example) have reported similar figures.

1.3.4 Multibeaming

A radio telescope operating at decametric wavelengths which formed only a single beam would be of very limited usefulness. Since observation time at these wavelengths is restricted, a number of beams are needed to obtain increased sky coverage during the opportune

periods. In addition, changes in the apparent location of a point source may occur due to ionospheric refraction; the magnitude of the change is time-dependent and may be of the same order of magnitude as the beamwidth of the proposed Tee array. Obtaining useful results from survey work in the presence of such refraction calls for the formation of several overlapping beams in declination.

There are also compelling reasons for multiple beaming in right ascension. Aside from increased sky coverage, this would offer a solution to the problem of scintillation, which refers to apparent flux density variations in a point source caused by distortion of the incident wavefronts as they encounter irregularities in the ionosphere. Multiple beams in right ascension would allow the observation of several successive transits of the source, some of which are likely to be relatively free of scintillation effects. In many cases, the results of the separate transits could be averaged, providing an increase in sensitivity. Unlike the beams in declination, these beams would be separated by several beamwidths in order to fulfill these objectives.

A further advantage of a large number of simultaneous beams is that well known sources will be encountered more often, which is very helpful for position determinations. The requirements described thus far together with other pertinent considerations have led to a proposal for a matrix of 160 simultaneous beams, comprised of 32 in declination and 5 in right ascension. Although the signal processing circuitry for this number of beams is highly complex, it can be approached in a gradual fashion, beginning with a small number in the initial phase of array development and adding more at a later date.

In addition to the main matrix of beams, it would be advantageous

to have provision for the formation of a few additional beams. One instance where such beams might be used is in the monitoring of ionospheric absorption, which could be accomplished by the simultaneous use of a section of the array to form several broad beams, one of which would be permanently aimed at the north celestial pole as a reference. The absorption data provided by measurements with these beams would help to improve the accuracy of flux density measurements made with the high resolution beams.

Another possibility for increasing the flexibility of the array is the incorporation of signal processing which would allow a cluster of beams to track a source for a considerable period of time. This type of processing, of which phased array radar is an example, would be very complex for a large array and would not likely be included in the initial installation. It is mentioned here to illustrate the need for emphasis on versatility in the design of the feeder system so that more sophisticated signal processing systems can be added in later stages of array operation.

Various techniques of multiple beam formation will be examined in the survey of arrays in Sec. 1.4. All of the beam-forming techniques can be divided into two categories: simultaneous and time-sharing. Time-sharing systems contain phase shifters which can be rapidly switched in value to steer the beam to a new direction, and the total observation time is divided equally amongst all of the beam positions. Aside from technical problems involving the switching, the basic objection to this approach lies in the inherent reduction in sensitivity which results from sharing the available integration time amongst all of the beams. The reduction factor is the square root of the number of

beams used [4]. Time-sharing systems are also less flexible than simultaneous systems, in that they do not facilitate making changes such as the addition of more beams. For these reasons, a simultaneous system of multiple beam formation is considered essential for the proposed Tee array.

1.3.5 Subarray Size

To form the maximum number of simultaneous beams possible, it would be necessary to have available at the beam-forming network the output of each individual element in the array. For a lesser number of beams this is not necessarily the case, making it possible to combine the outputs of groups of adjacent elements before the beam forming takes place. This would simplify the problem of signal transmission if the combining takes place at the elements.

Grouping of elements into subarrays results in modifications to the array field pattern, the extent of the modifications being dependent on the number of beams and the subarray size. To illustrate this, we shall consider a linear array of N isotropic sources with uniform spacing d (wavelengths). With uniform aperture illumination and excitation without phase gradients, the one-dimensional normalized field pattern may be expressed as

$$f(U) = \frac{\sin NU}{N \sin U} \quad (1.1)$$

where $U = \pi d \sin \theta$

θ = angle with respect to the broadside direction.

If we introduce additional beams with directions θ_i , the field pattern

for these beams is given by

$$f_i(U) = \frac{\sin N(U - U_i)}{N \sin (U - U_i)} \quad (1.2)$$

where $U_i = \pi d \sin \theta_i$.

Now let the array be grouped into subarrays of n elements, so that an individual subarray remains phased in the broadside direction irrespective of the beam-forming circuitry. The response is now given by the product of two terms, one of which is the subarray response, and the other the response of the "array of subarrays" phased in the direction θ_i . The first term is given simply by equation (1.1) with N replaced by n . The second term is similar to that of equation (1.2), but with the number of elements N reduced to N/n (the number of subarrays), and the spacing d increased to nd . Making these substitutions, we get:

$$\begin{aligned} f_{in}(U) &= \frac{\sin nU}{n \sin U} \cdot \frac{\sin [N\pi d(\sin \theta - \sin \theta_i)]}{(N/n) \sin [n\pi d(\sin \theta - \sin \theta_i)]} \\ &= \frac{\sin nU}{N \sin U} \cdot \frac{\sin N(U - U_i)}{\sin n(U - U_i)} \\ &= f_i(U) \cdot \left[\frac{\sin (U - U_i)}{\sin n(U - U_i)} \cdot \frac{\sin nU}{\sin U} \right] \end{aligned} \quad (1.3)$$

We see that the response with no subarrays $f_i(U)$ is now modified by a factor which is a function of θ , θ_i , and n . As one would expect, the broadside beam ($U_i = 0$) is not affected, but all other beams suffer some change in pattern. The change generally manifests itself as a decrease in mainbeam response and an increase in sidelobe levels. As a consequence, there is a tradeoff between subarray size and the number

of beams which can meet the sidelobe level criteria.

In the Tee array the picture is of course much more complex. One must now take into account the planar nature of the array and its two-dimensional field pattern, the response of the individual elements, the grading of the aperture, steering of the beam cluster off the broadside, and so forth. Studies of the effects on the performance of the east-west array due to grouping of elements into various sizes of subarrays have been carried out by D.A. Wynne [5] for the case of five beams with 1.8° angular separation. His calculations indicate that some east-west grouping may be feasible, but the sidelobe levels rise rather quickly as the subarray size increases. For example, subarrays of four elements result in an r.m.s. sidelobe level for the outer of the five beams of about one order of magnitude greater than for the central one. Because of the large number of beams desired in declination, no north-south grouping of elements is contemplated.

The decision concerning subarray size awaits further study of the antenna pattern of the Tee configuration and analysis of the tradeoffs involved. The subarray size will therefore be considered to be a variable for the present. It should be noted, however, that the introduction of subarrays would involve certain complications. Provision must be made for steering the subarray response, which means that phase shifters must be installed in the feeder system. For an N -element array with subarray size n , the minimum number of phase shifters required is $N(1 - 1/n)$ if the array is to be fully steerable. This follows from the fact that there are N/n subarrays, each of which require $(n - 1)$ phase shifters to steer the subarray response. The overall response is then steered by additional phase shifters at the

observatory. In practice, each phase shifter usually takes the form of remote-controlled multi-position switches which insert various lengths of cable into the appropriate sections of the feeder system.

The merits and drawbacks of introducing subarrays can be summarized as follows:

Advantages:

- (1) Simplification of signal transmission; less cable and/or multiplexing is needed.
- (2) Less complex beam formation; i.e., the number of inputs to the beam-forming matrix is reduced by the factor n .
- (3) Probable lower cost.

Disadvantages:

- (1) The need for remote-controlled phase shifters and their adjustment and maintenance in a rather hostile environment.
- (2) Higher sidelobe levels, especially for the outermost beams, in a simultaneous beam-forming system.
- (3) Some loss in flexibility; for example, the ability of the array to form simultaneous beams differing by more than a few beamwidths in right ascension would be compromised.

1.4 A Survey of Large Phased-Array Radio Telescopes

1.4.1 Characteristics of Selected Installations

In this section we shall examine some of the existing radio telescopes in the world, with particular emphasis on feeder design and signal transmission techniques. For convenience, some of the basic characteristics of these installations are summarized in Table 1.1. Since we are most concerned here with technical rather than astronomical parameters, such details as sensitivity, beamwidth, and collecting area have been omitted from the table. Not all of the arrays considered are of the Tee type of construction, nor are they all decametric; the common factors are large physical size and beam steering by electronic means (in addition to mechanical steering, in some cases). Some instruments have not been included because they are relatively obsolete designs; others are absent because their configuration and transmission problems differ markedly from the proposed array. Some of the radio telescopes omitted from the table will be described briefly in Sec. 1.4.2.

The following notes will clarify some of the entries in the table:

- (1) "Date" refers to the year in which the array went into full operation.
- (2) The arrangement of the elements can be deduced from the figures in parentheses under "number of elements"; if none are given, the array has one-element width.
- (3) For the arrays whose center frequency can be varied over a wide range, the element spacing is given in meters rather than wavelengths.

(4) With regard to the feeder systems, the "number" of feeders is essentially the number of array outputs independently returned to the receiver site. The "number of preamps" refers only to preamplifiers located near the array elements (i.e., outside the observatory building). For our purposes, "subarray size" will be defined as follows: in an equal-length type of feeder (see Sec. 2.1), it is the number of elements whose outputs are combined before transmission to the observatory; in a branching system, it is the number of elements whose outputs are combined before joining the binary branching network. Identifying the subarray size is more important in the equal-length case, since it affects the formation of multiple beams by simultaneous beam-forming techniques, whereas branching feeders are limited to time-sharing techniques which are limited by factors other than subarray size. In any case, the size given in the table refers to the subarray unit as it appears in the north-south array; in most cases, this is the only component array which can be electrically scanned away from the zenith.

Table 1.1a Characteristics of Some Existing Radio Telescopes: General

Name	Location Date	Reference	Array Type	Length (m)		Number of Elements		Element Spacing		Center Freq. f_o MHz	System Bandwidth (KHz)
				E-W	N-S	E-W	N-S	E-W	N-S		
DRAO 10	Penticton B.C. 1965	[6]-[8]	Tee	1242 (41.4 λ)	725 (24.5 λ)	180 (4x45)	240 (5x48)	0.9 λ	0.5 λ	10.02	8
DRAO 22	Penticton B.C. 1965	[8], [9]	Tee	1300 (96 λ)	439 (32.5 λ)	384 (4x96)	256 (4x64)	λ	0.5 λ	22.25	300
Molonglo Cross	Canberra Aust. 1967	[3], [10]-[12]	Cross	1560 (2120 λ)	1560 (2120 λ)	2816	2832	0.75 λ	0.75 λ	408.0	2500
Clark Lake Interfer.	Clark Lake Calif. 1963	[13]	Tee (Note 1)	3080 (270 λ)	1408 (123 λ)	152 (19x8)	76	38.6 λ (Note 2)	35 λ	26.3	40 (Note 4)
Clark Lake Teepee Tee	Clark Lake Calif. 1973	[14]	Tee	3000	1800	480	240	6.25 m	7.5 m	10-110 (Note 3)	3000 (Note 5)
Lebedev Cross	Lebedev Inst. USSR 1966	[15]-[18]	Cross	1008	1008	288	672	3.5 m	1.5 m	30-120	300
UTR-1	Grakovo Ukraine 1965	[19], [20]	Tee	576	600	128 (2x64)	80	9.0 m	7.5 m	10-25	3-14

Note 1: Compound interferometer; entries in this table apply to the Tee connection.

Note 2: Spacing between subarrays (19 dipoles in a linear E-W array with λ spacing between elements).

Note 3: Gain of the elements drops rapidly below 20 MHz, limiting the usefulness of the telescope here.

Note 4: Increased to 800 KHz when conditions permit. Note 5: Full bandwidth not useable at low frequencies.

Table 1.1b Characteristics of Some Existing Radio Telescopes: Feeder Systems

Name	Tran. Freq. (MHz)	Subarray Size	Cable Type	East-West Feeder			North-South Feeder			Multiple Beam Capability
				Number/Type	Length (m)	No. of Preamps	Number/Type	Length (m)	No. of Preamps	
DRAO 10	f_o	5	Coax (Foam)	4 Branched	—	0	48 Eq. Length	465	0	5 N-S Simult. (Note 7)
DRAO 22	f_o	4	Coax	4 Branched	—	4	1 Branched	—	1	5 N-S Time-Share
Molonglo Cross	11.05	16	Coax	22 Eq. Length (Note 6)	870	22	177 Eq. Length	870	177	11 N-S Simult.
Clark Lake Interfer.	f_o	19	Open Wire	1 Branched	—	0	1 Branched	—	0	None
Clark Lake Teepee Tee	f_o	15	Coax	32 Eq. Length	1600	32	16 Eq. Length	1600	16	49{ ⁷ ₇ N-S E-W Simult.
Lebedev Cross	f_o	16	Buried Coax	18 Eq. Length	465	0	42 Eq. Length	500	0	None
UTR-1	f_o	2	Coax	1 Branched	—	1	1 Branched	—	1	None

Note 6: Partially branched system; one transmission line to the observatory for each eight subarrays.

Note 7: Expandable up to 64 simultaneous beams by the addition of more receivers.

1.4.2 Other Radio Telescope Arrays

(a) The Early Mills Crosses

These instruments [21],[22] were among the first to conduct surveys of radio sources at metric and decametric wavelengths. Consisting of dipole elements coupled to a single coaxial feeder running the length of each arm, they were used in meridian transit mode with phasing in declination done by manual adjustment of the coupling points in the north-south array. Changing declination required about an hour for one man, although five adjacent declinations could be scanned using a time-sharing technique. In short, the design of these arrays was well suited to the initial systematic surveys for which they were intended, but lacked the flexibility needed to perform other tasks.

(b) The "Moving Tee" Aperture Synthesis Instruments

This type of radio telescope construction arose out of the realization that the Fourier components of the radio brightness distribution could be measured separately by sequentially providing each of the necessary antenna spacings. In the "Moving Tee" instruments [23],[24] (center frequencies of 38 MHz and 178 MHz), this took the form of a fixed east-west array similar to that of a conventional filled-aperture Tee, plus a smaller antenna movable along the north-south baseline. We shall consider here only the larger of the two "Moving Tee" arrays built, the 38 MHz array at the Mullard Observatory.

Both the fixed and movable sections of the array consisted of corner reflectors with a full-wave dipole feed. The east-west array, 1000 meters in length, used a branched feeder system with matching

transformers at each junction; these transformers also determined the array grading, which was Gaussian. The feeder system was constructed with open-wire line, which was found to be highly susceptible to moisture effects in that the velocity of propagation decreased significantly when the line became wet. This in turn caused increased phase and amplitude errors in the array excitation, particularly when the wetting was uneven. This effect was termed "the most serious practical difficulty" experienced with this array [23].

Aperture synthesis arrays of this type are, in general, unsuited for use at decametric wavelengths because they do not make efficient use of the limited observing time available. Also, they are of no use in the observation of transitory phenomena such as lunar occultations.

(c) The Culgoora Radioheliograph

The Culgoora array [25] is a rather specialized instrument which has been in operation since 1967. It consists of 96 steerable paraboloid antennas uniformly spaced around a circle of 3 km diameter, and it is specifically designed for making solar observations at 80 MHz over a bandwidth of 1 MHz.

Each antenna output is preamplified (26 dB gain) and transmitted by 1.5 km of open-wire line to the observatory located at center of the array. Here the 96 signals are down-converted to 7 MHz, at which frequency further processing such as time delay compensation is performed. Forty-eight simultaneous beams are formed in the beam-forming network, and the outputs of the 48 detectors are integrated and digitized for processing by computer.

One noteworthy aspect of the array is the rejection of coaxial

cable in favor of open-wire line in the feeder system, primarily due to the low attenuation (5 dB/km) of the latter compared with coaxial lines of similar cost. The circular configuration of the array and the moderate climatic conditions at the site mitigate to a large extent the deficiencies in the open-wire approach, such as poor shielding efficiency and the effects of moisture on propagation delay. In addition, the bounds on permissible r.m.s. excitation errors (18° in phase, 30% in amplitude) are much larger than those needed in the Tee array.

1.5 Summary of Available Options

The remainder of this chapter summarizes some of the technical details of existing radio telescopes. In some cases, immediate conclusions can be arrived at regarding the design of the proposed Tee array, but most of these topics will be examined in greater detail in the succeeding chapters.

1.5.1 Receiver Type

All of the instruments surveyed in Sec. 1.4 were found to have single-sideband receiver systems. Nevertheless, the alternative system of a double-sideband receiver may offer certain advantages. A more thorough discussion of this topic is postponed until the next chapter (Sec. 2.4.1).

1.5.2 System Bandwidth

The bandwidth figures in Table 1.1 clearly illustrate the need for relatively narrowband systems in decametric instruments. The bandwidths used at frequencies less than 30 MHz range from as little as 3 KHz up to 800 KHz, the latter being used only on an intermittent basis at a comparatively high frequency (26.3 MHz). Some of the instruments include provision for varying the bandwidth, which appears to be a valuable feature.

Even observations using very small bandwidths at low frequencies are often hampered by sporadic terrestrial interference, and a few techniques have been developed to combat this problem. One such technique is to split the signal into a number of narrow bandpass channels and select only those which are free of interference. This approach was used in the 19.7 MHz Mills Cross telescope near Sydney [22], in which the nominal 100 KHz bandwidth was divided into one fixed channel with 8.5 KHz bandwidth and four channels with 4.5 KHz bandwidth and variable center frequencies. This type of signal processing would become highly complex in a situation where large numbers of array outputs were returned to the observatory and filtered independently. A second drawback to the technique is that the interference must be monitored aurally by an operator, who then makes the appropriate adjustments; thus it is unsuitable for automatic operation and is restricted to those frequencies where the interference is relatively constant in terms of channel usage, such as commercial broadcasting.

A different method of interference reduction was used in Tasmania for observations at 10.02 MHz [26],[27]. This frequency is contained in a band allocated to aeronautical mobile stations, and thus it is subject

to highly intermittent usage. To cope with the interference, the system bandwidth was made small (2.1 KHz), and the center frequency was continuously swept across a 10 KHz band at a rate of five times per second. This caused interfering signals to appear as periodic impulses in the passband, so that they could be easily discerned from the cosmic noise and rejected by suitable "noise blanker" circuitry [28]. This method allowed unattended observations, but the small system bandwidth required made the sensitivity quite poor, and some difficulties were experienced when ionospheric scintillation was encountered.

Due to their obvious shortcomings, interference-reduction techniques such as those just described are not being planned for the new array. In any case, the need for such measures cannot be fully appreciated until some experience is had in making observations with the array.

1.5.3 Feeder Systems

There are two distinct types of feeder system used in the arrays described in Table 1.1. One is the binary branching or "Christmas tree" arrangement in which a large number of element outputs, often including all of the elements in a component array, are joined to produce a single output. A consequence of using this type of system is that beam steering and multiple beam formation must be done within the feeder system by providing variable phase shifters at the elements or, more commonly, at the junctions of the branches. Multiple beam operation is limited to time-sharing techniques in which some of the phase shifters are rapidly switched to different values. Branched feeders are often used in arrays which are permanently aimed at the zenith, as in the east-west arrays of

meridian transit instruments, a category which includes all of the radio telescopes in Table 1.1 except the "Teepee Tee" and UTR-1. The Penticton arrays provide a separate branching network for feeding each row of elements in the east-west array, allowing steering of its north-south response to improve the overall response of the antenna in declination.

A second major type of feeder consists of a number of independent feedlines of equal length. Depending on the extent to which element outputs remain separate in the feeder system, this will allow some or all of the array steering to be done at the observatory, together with the simultaneous formation of a large number of beams. This flexible but more costly system is, for obvious reasons, more often used for north-south arrays. The equal-length system also lends itself to easier measurement of excitation errors, so that it is sometimes used even in the east-west arrays of meridian transit instruments (e.g., the Lebedev and Molonglo Crosses).

A third method, little used today, consists of a single feedline along the length of each arm of the array, with the elements lightly coupled at appropriate intervals. Its simplicity and minimal cable requirements made it a reasonable choice for some of the early experimental arrays [21],[22], but it has a number of disadvantages which limit its flexibility and excitation accuracy. All three methods of feeder design will be discussed further in Sec. 2.1.

1.5.4 Signal Transmission Techniques

Almost invariably, the output signals of low frequency arrays are transmitted to the observatory without frequency conversion, usually via

coaxial cables. Down-conversion to an intermediate frequency (IF) is not generally felt to be necessary provided that the feedline losses can be kept within reasonable limits. Whether this is the case or not is largely determined by the size of the array and the cost of cable having suitably low losses. In some cases, preamplifiers are used to overcome the losses, permitting the use of less expensive cable. Open-wire line, despite having low losses, is seldom used for the main feedlines due to the problems of low shielding efficiency and phase stability mentioned previously. Because its construction facilitates coupling adjustments, however, it is often used to couple individual elements within subarrays.

1.5.5 Control of Phase Errors

Phase errors in array excitation caused by imperfections in the feeder system are a serious problem in large arrays. Few of the papers cited in Table 1.1 give detailed data on this subject, but it is apparent that shortcomings in feeder system design and construction have led to unpleasantly high sidelobe levels in some cases. Among the methods available for the reduction of phase errors are down-conversion (IF return), cable burial, and the use of special phase-stable coaxial lines. Down-conversion, such as used in the Molonglo Cross, improves the phase stability since the phase shift introduced by a given length of line is proportional to the frequency of transmission. However, this technique is complicated by the fact that a distribution system must be provided which ensures that the local oscillator signals at all of the remote mixers are in phase.

The most common approach to phase stability is the employment of more stable transmission lines and/or insulation of them from changes in

their environment. Burial of cables, where feasible, can provide an essentially constant thermal environment and thus eliminate short-term phase variations to a large extent. Even in such circumstances, however, significant long-term variations (of the order of weeks or months) may appear, necessitating regular readjustment of the lines. Such variations have been reported by Ilyasov [18], whose conjecture is that they are primarily the result of changes in the parameters of inhomogeneities in the regions where coaxial connectors were installed. Most types of coaxial cable are not suitable for direct burial and must be enclosed in some type of conduit if used in this manner. Cables designed specifically for direct burial are very expensive.

Specially designed phase-stable coaxial lines are also expensive, but they may be used in applications where the total amount of cable needed is quite small, as in a branched feeder system. In some instances, this kind of cable has been combined with regular cable to increase the overall phase stability of the feeder (e.g., the Penticton 22 MHz array). Cable using foamed polyethylene dielectric is sometimes favored since it offers lower attenuation and improved phase stability over its solid dielectric counterpart for a modest increase in cost.

1.5.6 Subarrays

All of the instruments surveyed utilize some type of grouping of elements into subarrays. Consequently, all of them, with one exception, perform at least part of their beam steering by the use of phase shifters in the feeder system. Among the types of phase shifters employed are variable-length transmission lines using switching arrangements (Lebedev Cross, Penticton 22 MHz), continuously variable helical directional

couplers (Molonglo Cross), and automatic feed point adjustment by remote-controlled diode switches (Teepee Tee). The sole exception is the Penticton 10 MHz instrument, which provides a separate return cable for each east-west row of elements throughout the array. Since it is operated in meridian transit mode, no phase shifters are needed for east-west steering.

The overriding consideration in the determination of subarray size in existing arrays has likely been the cost of transmission lines in some cases; in other, less ambitious, instruments, little would be gained from reduction of subarray size. In particular, meridian transit arrays do not suffer in performance from east-west grouping of elements, and those with single beams or time-shared multiple beams would not benefit from smaller north-south groups. The instruments most likely to benefit from smaller subarrays would be those forming simultaneous beams in the plane along which elements are grouped. The Molonglo Cross and the Teepee Tee fall into this category. In the former, the subarrays are 0.6% of the total length of either component array, and in the latter, they are 3.1% of the east-west array length. If calculations or measurements of sidelobe levels for the various beams have been carried out for these arrays, the results have apparently not been reported in the literature. Examination of existing arrays therefore sheds little light on the question of subarray size for the proposed array.

1.5.7 Multibeam Capability

Several of the radio telescopes presently in use do not form multiple beams. Soviet astronomers seem to favor wideband instruments capable of simultaneous operation on a number of widely differing

frequencies but with only a single beam direction. Others have used a time-sharing arrangement for a small number of beams (usually five), but recent designs clearly show a trend towards simultaneous formation of a relatively large number of beams.

The most sophisticated of these designs, at least in terms of beam formation, is the Teepee Tee; this is the only existing array of its type having equal beam-forming capability in either array plane. Also notable is the Penticton 10 MHz Tee, which, as noted in Table 1.1, has the ability to form up to 64 beams in declination with the addition of more receivers. This is due to the flexibility of its north-south feeder system and the lack of subarrays in the north-south array plane.

CHAPTER 2

THE FEEDER SYSTEM

2.1 Basic Types of Feeder Systems

Some basic feeder system configurations were briefly described in the preceding chapter. In this section we shall examine their characteristics more thoroughly in order to select the most suitable system for the Tee array.

2.1.1 Single-Line Feeders

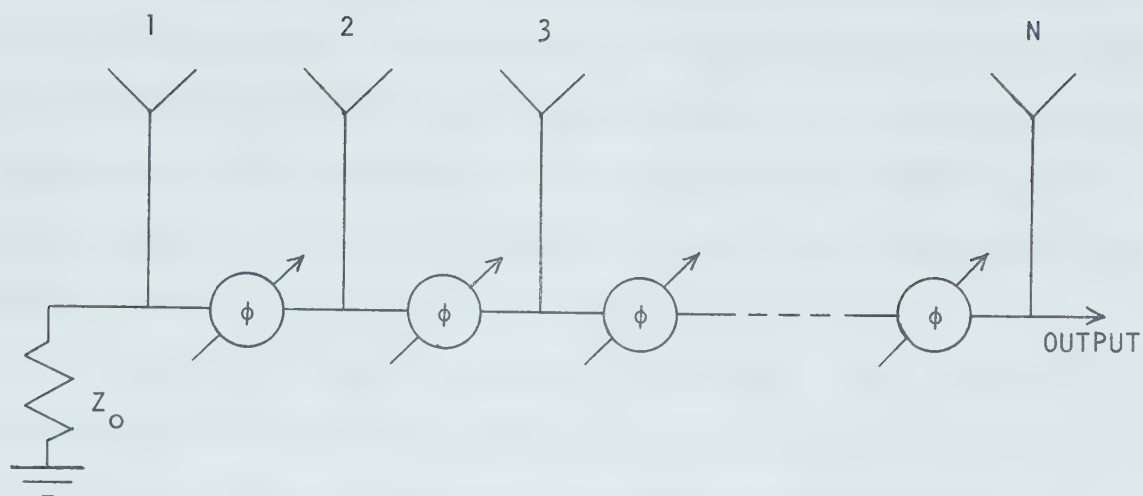
The single-line feeder, illustrated in Fig. 2.1 for a linear N-element array, consists of a single transmission line to which the elements are coupled at periodic intervals along its length. Capacitive coupling is normally employed, and the use of directional couplers is usually required to reduce interaction between the elements. The value of phase shift ϕ needed for pointing at an angle θ off the broadside is given by

$$\phi = \frac{2\pi d \sin \theta}{\lambda_0}, \quad (2.1)$$

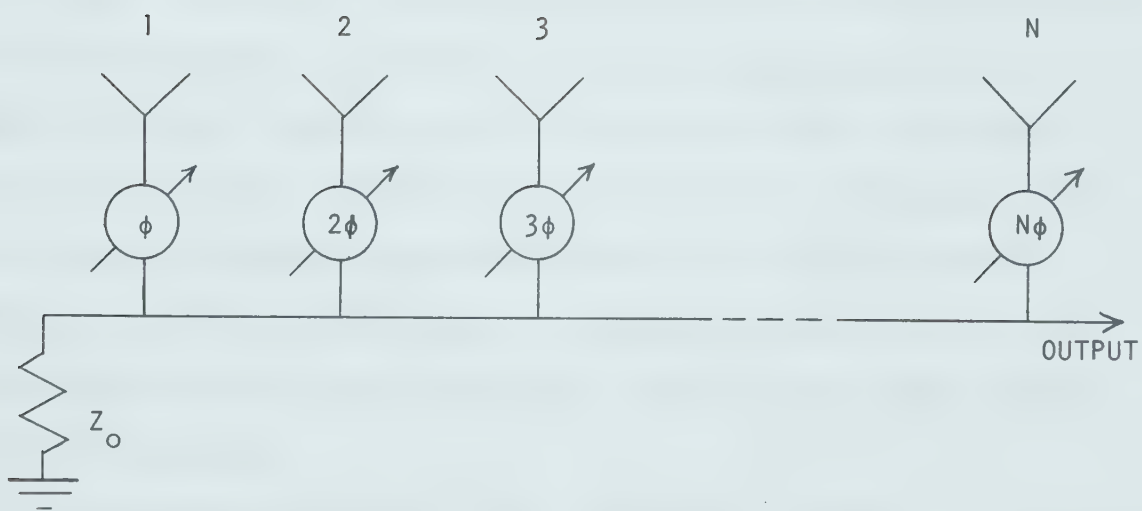
where d = the inter-element spacing

λ_0 = wavelength at the center frequency

The system of Fig. 2.1a, which may be thought of as a series connection, has the advantage that identical phase shifts are called for



(a) Series Feed



(b) Parallel Feed

Fig. 2.1 Single-Line Feeder Systems

in each phase shifter, simplifying the problem of remote control. The principle problem with this approach is the accumulation of phase errors. If a single phase shifter has an r.m.s. phase error $\Delta\phi$, then the signal from element #1 will encounter an r.m.s. phase error of $\sqrt{N-1} \Delta\phi$. This problem, together with the accumulation of amplitude errors, makes the series technique impractical for all but very short arrays.

The parallel-connected single-line feeder, shown in Fig. 2.1b, avoids the problem of error accumulation by providing each element with its own phase shifter. Control is more complex than in the series connection since the phase shifters are, in general, not set to the same value.

Both types of single-line feeder have the inherent disadvantage that the path from antenna element to observatory has a different electrical length (physical length of the transmission line divided by its velocity factor) for each element. One consequence of this fact is that differential phase errors can appear very easily; for example, a change in electrical length of the line caused by a temperature change will result in phase errors which increase with distance from the observatory. This problem could be overcome only by resorting to very expensive techniques such as the use of special phase-stable coaxial transmission lines.

A second consequence of the unequal path lengths is the restriction on the useable bandwidth imposed by decorrelation losses. As will be shown in Sec. 5.3, if a signal of bandwidth B Hz is transmitted over two paths which have identical phase shift at midband but differ in time delay by τ sec, the correlation coefficient for the two output signals is

$$\gamma(B) = \frac{\sin \pi \tau B}{\pi \tau B} = \text{sinc } \pi \tau B, \quad (2.2)$$

where $\gamma(B)$ may be thought of as the ratio of the actual output power at the receiver to the output power without decorrelation. Reduction of decorrelation losses by the installation of variable time delays in the feeder system is possible, but this is generally an unattractive proposition.

2.1.2 Binary Branching Feeders

The binary branching feeder system, depicted in Fig. 2.2, is in common use today and offers a substantial improvement in performance over single-line systems in many situations. The example shown is an 8-element array; the extension of the principle to larger arrays is obvious. As is the case for the single-line feeders, an N-element array will require N-1 phase shifters. Impedance matching is necessary at each junction, since reflections from these points will cause excitation errors. This function is usually performed by a coaxial impedance transformer. It is also necessary in most cases to decouple the elements from each other; both the isolating and matching functions can be combined in a hybrid ring or other type of directional coupler [29].

The most important characteristic of the branching feeder is that, in principle at least, all signal paths from element to receiver are identical in electrical length. This tends to minimize the excitation errors due to changes in the properties of the cable, although errors caused by differential heating and by variations in parameters from one section of cable to the next will still be present. The equal path lengths also prevent decorrelation losses when the array is pointed at

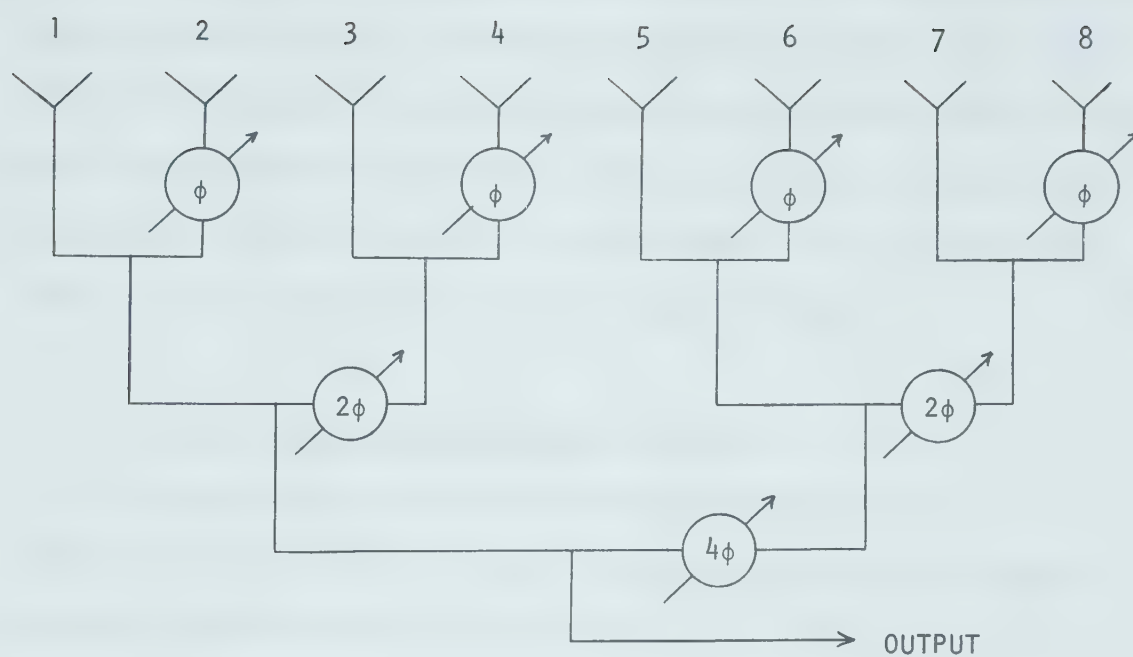


Fig. 2.2 Binary Branching Feeder System

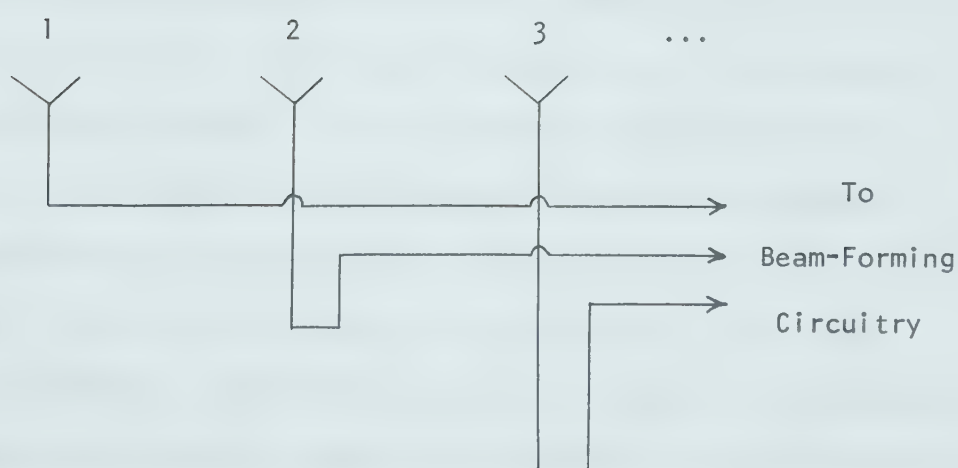


Fig. 2.3 Independent Equal-Length Feedlines

the zenith; as with any feeder system, however, it may be necessary to insert variable delays to preserve correlation at other angles. The primary difference in this regard between the branching feeder and the equal-length system to be described next is that the former must have its delays installed outdoors within the feeder system, whereas the latter can have them inside the observatory building.

2.1.3 Independent Equal-Length Feeders

The most obvious and straightforward feeder system consists simply of a separate line for each element or subarray (Fig. 2.3). To minimize the decorrelation losses and excitation errors, each line is cut to the same length, namely the distance from the observatory building to the most remote element. The amount of cable required is thus very large compared to the other feeder schemes.

Such a system does not obviate the need for phase shifters to steer the beam or time delays to prevent decorrelation losses, but it does allow these units to be located indoors at a single location adjacent to the receiver. This has important advantages in terms of ease of calibration, maintenance, and control, and the controllable environment available will result in increased phase and amplitude stability. The system also lends itself to a variety of signal processing methods; in particular, the full capability of the array to form simultaneous multiple beams can be utilized. The independence of the signal returns also means that a monitor system to automatically control the array excitation becomes a possibility (Sec. 5.1).

To offset to some extent the enormous cost of an independent-return feeder system, it becomes desirable to find methods for reducing

the total number of feedlines. There are basically two techniques which can be used singly or in combination to achieve this end. One of these, grouping of elements into subarrays, has already been described. The feeder becomes in effect a mixed system, employing one of the feeder schemes described in the preceding two sections within the subarray, together with an independent line from each subarray to the observatory. The second technique is that of multiplexing two or more signals onto each line such that they are separable at the observatory. This is equivalent to the fully independent return system and does not involve an inherent compromise in array performance as the subarray approach does; however, new considerations such as crosstalk, technical complexity, and cost will now enter the picture.

2.2 Choice of a Feeder System

It is clear that the use of single-line or branched feeder systems on a large scale would not be compatible with such performance objectives as simultaneous multiple beam formation in both array planes. Only the independent equal-length system or one of its variants can provide sufficient flexibility to allow a significant improvement over existing radio telescope designs. It is no coincidence that the most sophisticated recent designs (Molonglo Cross, Teepee Tee) make use of some type of independent-return system.

Although the decision to use an independent-return feeder in the Tee array is clear-cut, the choice of a method of implementing it is not, since there are a number of variables to consider. The remainder of this chapter will be devoted to a study of the alternatives available. One

major consideration in the evaluation will be the total amount of cable required and the attendant cost. Assuming that the observatory building is near the intersection of the Tee, and disregarding the relatively small amount of cable needed within a subarray, the total length of cable needed for the feeder of the proposed array would be

$$L = \frac{(2.5)N}{mn} \text{ km,} \quad (2.3)$$

where N = total number of elements

m = number of multiplex channels per cable

n = subarray size.

For the extreme case of no physical tapering, no subarray grouping, and no multiplexing, this amounts to a rather awesome total of 7120 km. The need for further investigation of this feeder method is evident.

2.3 Signal Transmission Without Frequency Conversion

To distinguish between the terms "transmission system" and "feeder system", we shall refer to the former as the means by which received signals are transmitted to the observatory within the framework of a given feeder system. In addition to the basic signal paths along the feeder cables, the transmission system may encompass preamplifiers, mixers, local oscillator lines, phase compensation systems, and so forth.

The most straightforward solution to the transmission problem is simply to use the basic feeder system without further embellishment, except possibly preamplification. This approach has in fact been used in

all low frequency radio telescopes constructed to date (unlike its usage in communications terminology, the term "low frequency" when referred to by radio astronomers usually means that part of the spectrum below 40 MHz). The main considerations here are cost, phase stability, and the degradation of signal-to-noise ratio caused by the attenuation of the cables.

2.3.1 Attenuation and Noise Considerations

(a) Transmission Without Preamplification

The sensitivity of a radio telescope depends on how small a change in input noise power can be detected. This is in turn a function of the r.m.s. noise fluctuations caused by the background radiation from the sky plus the noise contributions of the receiving system. The fluctuations are usually expressed as a noise temperature; the minimum detectable noise temperature is given by [30]

$$(\Delta T)_{\text{rms}} = \frac{K_s T_{\text{sys}}}{\sqrt{Bt}} \quad (^\circ\text{K}) \quad (2.4)$$

where K_s = sensitivity constant ($= \sqrt{2}$ for correlation receiver)

T_{sys} = system noise temperature referred to antenna terminals, $^\circ\text{K}$

B = predetection system bandwidth, Hz

t = postdetection integration time, sec

In the proposed array, this quantity is expected to be of the order of 2000°K .

The sensitivity is usually defined as some factor times $(\Delta T)_{\text{rms}}$, since the minimum signal detectable with confidence is considerably greater than the r.m.s. fluctuations given by equation (2.4). The

factor commonly chosen is five; if the noise is Gaussian, the probability of a random fluctuation reaching a value of $5(\Delta T)_{\text{rms}}$ is about 6×10^{-7} .

Now if we consider a single array element and its associated transmission line and receiving system, we may express the system noise temperature introduced above in the form

$$T_{\text{sys}} = T_A + T_L [(1/\epsilon) - 1] + (1/\epsilon) T_R \quad (2.5)$$

where T_A = antenna noise temperature, °K

T_L = physical temperature of the transmission line, °K

T_R = receiver noise temperature, °K

ϵ = transmission line efficiency, $0 \leq \epsilon \leq 1$

The system noise temperature is degraded both by the attenuation of the transmission line and the thermal noise generated within it; it is also degraded by noise generated in the receiver. To ensure that no significant degradation will occur, the first term of (2.5) must dominate the other two:

$$T_A \gg T_L [(1/\epsilon) - 1] + (1/\epsilon) T_R$$

or, in terms of transmission line efficiency,

$$\epsilon \gg \frac{T_R + T_L}{T_A + T_L} \quad (2.6)$$

In order to arrive at a minimum allowable value for ϵ , we must now determine some approximate values for the various noise temperatures.

At the low frequencies involved here, a receiver noise figure F_{dB}

of less than 4 dB is readily obtained (the receiver noise figure will essentially be that of the first stage of amplification). Using this figure as a worst-case value, and applying the relation

$$F_{dB} = 10 \log_{10}[1 + (T_R/290)], \quad (2.7)$$

we find that $T_R = 440^\circ\text{K}$.

The antenna temperature T_A depends on the sky brightness temperature distribution and the power pattern of the antenna. B.H. Andrew [31] has measured brightness temperatures in the range of 10 MHz to 38 MHz using dipole antennas at a latitude of 52°N , which is the same as that of the proposed array. At 13.1 MHz, the observed sky brightness varied with hour angle and had a mean value of 1.22×10^5 °K. The brightness temperature is proportional to Sf^{-2} , where S is the flux density and f is the frequency (Rayleigh-Jeans radiation law), and Andrew has determined that $S \propto f^{-0.43}$ over the stated frequency range. Thus we can interpolate to find the mean brightness temperature at 12.36 MHz, which we use as an estimate of the antenna temperature of a dipole element in the array:

$$\bar{T}_A = (1.22 \times 10^5) \left(\frac{12.36}{13.1} \right)^{-2.43} = 1.41 \times 10^5 \text{ }^\circ\text{K} \quad (2.8)$$

The interpolated minimum and maximum values are 1.01×10^5 °K and 1.87×10^5 °K respectively.

Choosing $T_L = 300^\circ\text{K}$ as the maximum temperature the cable is likely to be subjected to, and substituting all of the estimated quantities into (2.6), we find that the requirement on transmission line efficiency becomes $\epsilon \gg 5.4 \times 10^{-3}$. If we have an efficiency one

order of magnitude greater than this figure, the system noise temperature will be increased only about 10% over the antenna temperature, resulting in a minor deterioration in sensitivity. Using this criterion, the requirement becomes

$$\epsilon \geq 0.054 \quad (2.9)$$

or, in terms of cable attenuation A ,

$$A_{\max} = 10 \log_{10}(1/\epsilon) = 13 \text{ dB} \quad (2.10)$$

Although it may appear that we have made this upper bound on cable attenuation overly stringent by not striving for a very low receiver noise temperature, such is not the case. Indeed, much lower figures than 440°K are obtainable; in fact, a noise temperature of 50°K ($F_{\text{dB}} = 0.7$) is typical of a well designed low-noise 10 MHz transistor amplifier [32], [33]. However, if we set $T_R = 50^\circ\text{K}$, we find that the criterion of equation (2.10) becomes $A_{\max} = 16 \text{ dB}$, so that the cable attenuation requirement has changed relatively little. Hence there is not a great deal to gain from optimization of the receiver in terms of noise figure, and attention should instead be focussed on such parameters as gain and phase stability.

Attenuation data [34],[35] and cost for a number of common, readily available coaxial cables are given in Table 2.1. The attenuation as a function of frequency may be described as follows [36]:

$$A(f) = kL(f/f_o)^x \quad \text{dB} \quad (2.11)$$

where $\chi \approx 0.5$ (see Table 2.1 for individual values)

k = constant depending on cable construction

= attenuation in dB/m at frequency f_o

L = length of cable, m.

We shall make use of this relation again in connection with frequency conversion and multiplexing. Measurements [35],[37] on many types of coaxial cables have shown the attenuation-versus-frequency characteristic in the 1-1000 MHz range to conform very closely to that predicted by (2.11). The exponent of approximately 0.5 arises from the fact that skin-effect losses dominate the other sources of attenuation such as dielectric heating and radiation at these frequencies.

An examination of Table 2.1 reveals that most commonly-used coaxial cables have much higher attenuation than that which is called for in equation (2.10). Due to the high cost of suitable cable, the transmission system without frequency conversion or preamplification has little merit for an installation the size of the proposed array.

(b) Transmission With Preamplification

We now consider a modification of the preceding scheme, consisting of the insertion of a preamplifier having power gain G and noise temperature T_p into the remote end of each cable. Assuming that there is negligible loss in the cable which connects the antenna element to the preamplifier, the system noise temperature (referred to the antenna terminals) becomes [38]:

$$T_{sys} = T_A + T_p + \frac{(1-\epsilon)T_L + T_R}{\epsilon G} \quad (2.12)$$

Table 2.1 Characteristics of Common Coaxial Transmission Lines

Cable Type	Char. Impedance (Ohms)	α in Equation (2.11)	Attenuation (dB) at 12.36 MHz (20°C)		Approximate Cost (Dollars) (Note 2)	
			Per 100 m	2.5 km run	Per 100 m	2.5 km run
RG-58/U	53.5	0.58	4.40	110	13.5	340
FM-58 (Note 1)	50.0	0.51	3.61	90	15.1	380
RG-62A/U	93.0	0.55	3.12	78	17.7	440
RG-213/U (Formerly RG-8A/U)	50.0	0.52	2.43	61	45.9	1150
FM-8 (Note 1)	50.0	0.51	1.90	48	49.5	1240
RG-218/U (Formerly RG-17A/U)	50.0	0.55	0.85	21	221	5530

Note 1: FM-58 and FM-8 are similar to RG-58/U and RG-213/U, respectively, but have foam dielectric.

Note 2: Price based on the purchase of a 1000 foot quantity. The unit cost should be considerably lower for the large quantity required for the entire feeder system.

Except for the addition of T_p , this is the same as equation (2.5), but with the last two terms reduced by the factor G . The system noise temperature versus cable attenuation is plotted in Fig. 2.4 for various preamplifier gains. Examination of the curve for the case of no preamplification shows that 13 dB of cable attenuation corresponds to a T_{sys} of about 1.55×10^5 °K, or about 10% higher than the nominal T_A , which affirms that the criterion of equation (2.10) is reasonable. We can derive a similar criterion from equation (2.12):

$$\epsilon \gg \frac{T_L + T_R}{T_L + G(T_A - T_p)} \approx \frac{1}{G} \cdot \frac{T_L + T_R}{T_L + T_A} \quad (2.13)$$

provided that the noise figure of the preamplifier is reasonably good, say less than 10 dB. This expression clearly shows that the result of inserting the preamplifier is to compensate for an amount of cable attenuation equal to the power gain G . The new criterion for cable attenuation is therefore

$$A_{\text{max}} = 13 + 10 \log_{10} G \quad (\text{dB}) \quad (2.14)$$

This means, for example, that if a gain of about 35 dB could be realized, FM-8 type cable could be used rather than RG-218/U, which was previously the only cable of Table 2.1 which even came close to meeting the attenuation criterion. This substitution would result in a saving of about four thousand dollars per cable run, even if the preamplifiers were to cost as much as three hundred dollars apiece. The preamplified transmission system is obviously a better choice for a large array.

The principle limitations on preamplifier performance in this

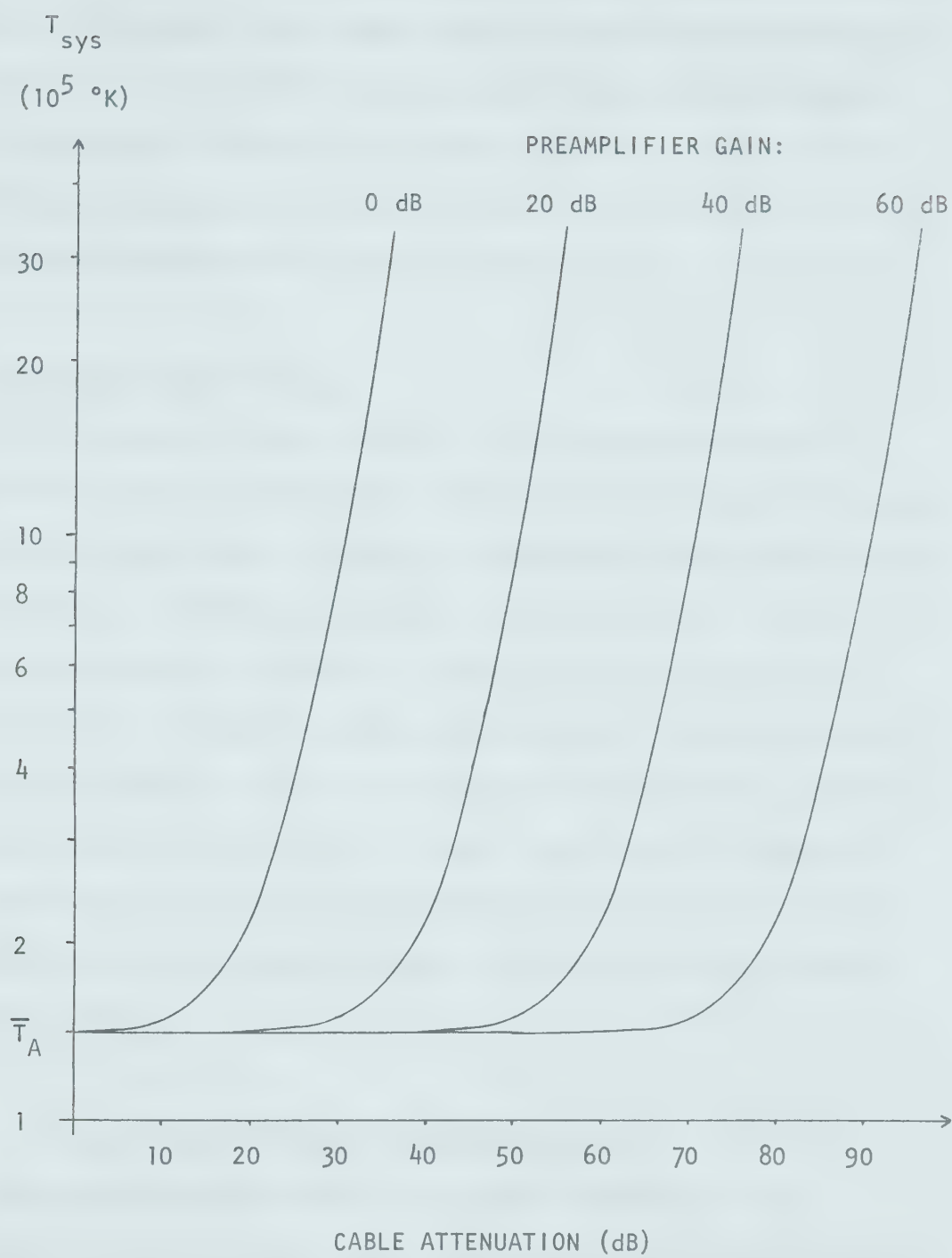


Fig. 2.4 System Noise Temperature Versus Cable Attenuation

application are stability and reproducibility. The task of producing a large number of preamplifiers whose phase and amplitude characteristics are uniform from unit to unit and stable with time is not an easy one, and it becomes more difficult as the gain required increases. In the following section, problems related to stability and uniformity of the feeder system components are explored in more detail.

2.3.2 Excitation Errors

It is rather difficult to excite a large array accurately without resorting to prohibitively expensive techniques such as the use of specially-designed cable. Although calibration of the array at some point in time is a formidable problem in itself, the most serious problems stem from the short-term and long-term variations in the properties of the transmission system which appear after calibration. Many of these problems arise from the failure of the system components to "track"; that is, they do not all react identically to changes in their environment even though they have been closely matched for one particular set of conditions. The result is inevitably an increase in excitation errors.

(a) Thermal Effects: Transmission Lines

The foremost consideration in the stabilization of the transmission system is thermal stability. Unless special measures such as burial of cables are adopted, the components of the system will be exposed to ambient temperatures ranging from about -50°C to $+30^{\circ}\text{C}$. The majority of observations will take place when the temperature is in the lower half of this range, since the ionosphere is most likely to be

transparent at 12 MHz during winter nights. Exceptions to this rule will occur, however, particularly during "quiet sun" years. Ionospheric conditions notwithstanding, there will no doubt be many serious attempts made at mapping the summer sky, so that the feeder system must be designed to deal with the full temperature range.

Coaxial cables exhibit parameter changes with temperature which are to some extent unpredictable. This is especially true of the common RG-type cables, which have not been designed for high thermal stability. Specifications on the thermal properties of these cables are usually not available from the manufacturers.

To describe the behavior of cable attenuation with temperature, one can define a coefficient of attenuation stability:

$$K_A = \frac{\Delta A \times 10^6}{A(\Delta T)} \quad \text{ppm/}^\circ\text{C} \quad (2.15)$$

where A = attenuation, dB

ΔA = increment in attenuation, dB

ΔT = small increment in temperature causing ΔA , $^\circ\text{C}$

This coefficient is positive since both the resistivity of the conductors and the dielectric losses increase with temperature. For RG-type cables with solid polyethylene dielectric, the attenuation change is quite linear with temperature, and K_A is about 615 ppm/ $^\circ\text{C}$ [34]. The coefficient is apparently quite uniform from one sample of cable to the next, so that differential effects leading to amplitude excitation errors are not expected to be a serious problem.

Unfortunately, the phase stability of most coaxial cable is not as well-behaved as the attenuation stability. A coefficient of phase

stability K_p may be defined in terms of the phase delay of the line:

$$K_p = \frac{\Delta\tau \times 10^6}{\tau(\Delta T)} \quad \text{ppm/}^\circ\text{C} \quad (2.16)$$

where τ = phase delay of the transmission line, sec

$\Delta\tau$ = increment in the delay time, sec

ΔT = small increment in temperature causing $\Delta\tau$, $^\circ\text{C}$

The change in phase shift which takes place at a given frequency f for a temperature change ΔT will be

$$\Delta\phi = 360f(\Delta\tau) = 360f\tau K_p(\Delta T) \times 10^{-6} \quad \text{degrees} \quad (2.17)$$

The changes in delay time result from changes in the dielectric constant plus changes in the physical length of the cable. This leads to a rather nonlinear delay-versus-temperature characteristic, meaning that K_p can be considered a constant only over a small range of temperatures. K_p is negative for all standard cables, and at 20°C it normally falls in the range from -100 to -250 ppm/ $^\circ\text{C}$ for solid polyethylene insulated coaxial cables and from -20 to -30 ppm/ $^\circ\text{C}$ for foamed polyethylene types [34].

The coefficient K_p increases with temperature in a manner peculiar to each individual cable type. To take an extreme example, data given by Rodriguez [39] show that for RG-58C/U, K_p is about 30 ppm/ $^\circ\text{C}$ at -20°C and increases to about 140 ppm/ $^\circ\text{C}$ at $+20^\circ\text{C}$ and 320 ppm/ $^\circ\text{C}$ at $+40^\circ\text{C}$. The changes in K_p are generally less extreme for larger-diameter cables, and such cables can often be represented by a constant K_p quite adequately over a considerable temperature range.

In considering phase excitation errors, we are concerned with differential rather than absolute changes in phase shift; if all cables in the feeder system change in exactly the same way, the relative phases will be preserved and no new phase errors will appear. Hence the critical question to be answered pertains to the variance in phase characteristics to be found in a large number of samples of a given type of cable. Unfortunately, very little data on this subject has been reported in the literature. One study reported by Kushner [40] revealed that there can be a substantial variation in phase-temperature coefficient K_p of a given cable type from one production lot to the next. Measurements of standard solid polyethylene dielectric cables in the neighborhood of 20°C showed extremes in K_p of -108 ppm/°C and -162 ppm/°C, a range of ±20% from the median. Lot extremes for a standard foam polyethylene cable were -31 ppm/°C and -63 ppm/°C, or ±33% from the median. Since the statistics other than the lot extremes from the measurements were not reported, it is difficult to predict how the variations in an actual shipment of cable might compare to these. In the absence of an assurance from the manufacturer of tighter tolerances on K_p than those given here, there is some justification for assuming them to be representative of a worst-case situation. The analysis of phase errors in the transmission lines from variations in K_p will be resumed in Sec. 2.3.3.

When a coaxial line is first cycled through a temperature range, the path followed by the curve of phase delay versus temperature will usually be found to be different for each succeeding cycle. It is only after several such cycles that the phase-temperature characteristic tends to stabilize within this range [39]. This points out the need for

allowing the feeder system cables to undergo wide variations in temperature after installation before final phase trimming and calibration is attempted.

(b) Thermal Effects: Preamplifiers

The preamplifiers in the transmission system will also be a source of excitation errors, with amplitude errors being of greater concern in this case. In some respects, thermal instability is an easier problem to cope with in the preamplifier than in the cable, since the former is a lumped circuit with highly predictable properties.

The major problem in amplifier stabilization is compensation for changes in the parameters of the active devices; compensation of the passive elements can generally be accomplished through careful circuit design and proper selection of component temperature coefficients. To compensate an active element, there are basically two approaches: one is to use negative feedback and thus reduce the effects of parameter changes in the device; the other is to constrain some device parameter to change with temperature in a certain way. The feedback technique restricts the gain available per stage to a relatively low value, but it has the advantage of being tolerant of departures from the expected values of device parameters. The second technique offers higher gain but would require greater device uniformity or the tailoring of each preamplifier individually to meet specifications.

An example of the second compensation technique has been given by Batchelor [33]; he describes the use of a thermistor in the d.c. emitter circuitry of a bipolar transistor amplifier in such a way as to keep the power gain relatively constant over a wide temperature range.

A dual-gate MOSFET can be gain-stabilized in a similar fashion by supplying the gate #2 bias from a temperature-dependent voltage divider network [41].

As far as phase stability is concerned, at the frequencies involved here the active devices will likely present a less serious problem than the associated tuned circuits.

(c) Moisture and Other Environmental Factors

Most standard coaxial cables deteriorate quite quickly in humid environments due to corrosion of the braid. The moisture enters the cable at terminations, through pin-holes in the outer jacket, or via vapor transmission through the jacket. In foam dielectric cables, moisture penetration also causes filling of the voids in the dielectric, which results in increased attenuation and poorer phase stability. The deterioration of standard cables is further accelerated by galvanic action if they are used for direct burial.

Even in above-ground use, it is desirable to provide the cable with some additional protection from rain, ice build-up, direct sunshine, rodent damage, and so forth. A system of ducts through which the cables are routed could be used for this purpose; such a system might be incorporated into the design of the ground screen. A suitable waterproof enclosure should also be provided for each preamplifier.

(d) Component Aging

As pointed out in Sec. 2.3.2(a), coaxial cable must undergo several temperature cycles before it stabilizes in a given range. In addition to these temperature-induced effects, however, the phase delay

of a cable will change with time even if it has a thermally stable environment. For example, measurements on cables in the feeder system of the Lebedev Cross [18] have shown considerable variation with time, despite the fact that they are buried at a depth of about one meter in insulated tubes. The measurements were of electrical length (phase delay times the velocity of light in free space); all lines were first trimmed to within 7 ppm of the electrical length of a standard. After a two month period, measurements revealed deviations from the standard length of 114 ppm r.m.s. The resulting excitation errors were quite noticeable in their effect on the sidelobe levels.

The probable cause of these variations was changes in the cables in the vicinity of the connectors. No doubt exposure to a wide range of temperature and humidity will accelerate this process, necessitating frequent recalibration of the feedlines. This could prove to be a highly complex and time-consuming procedure in the case of the proposed array unless an automatic system is incorporated into the feeder system to perform this task. Systems of this nature will be examined in Sec. 5.1.

Aging effects will also appear to some extent in the preamplifiers and any other electronic components present; the remedy, as with the cables, is frequent measurement and adjustment against a standard.

(e) Cable Trimming

A fundamental limitation on the attainment of small phase errors is the accuracy with which the feeder system cables can be matched in phase delay. Aside from the difficulties associated with the thermal and other variations just described, it is by no means a trivial problem to accurately match the electrical lengths of two cables at a given time.

The process consists basically of matching the phase shifts of a pair of two-port networks; it is made more difficult than usual by the large physical separation of the input and output ports.

The technique of electrical length matching which has been used almost universally in setting up large arrays was introduced by Swarup and Yang [42] in 1961. In principle, one may measure a cable's electrical length by injecting a sinusoidal signal into one end, separating from it by means of a directional coupler the signal reflected from the far end termination, and comparing the phase of the two signals. This technique results in an ambiguity in that the actual number of half-wavelengths in the cable is not determined, but this may be resolved by measurement of physical length or by pulse reflection. The method fails when the cable has appreciable attenuation, since the reflected signal will have insufficient magnitude to be distinguished from the outgoing signal, or from the other incoming signals caused by reflections from discontinuities in the cable.

Swarup and Yang proposed a modification of the reflection method involving modulation of the termination impedance, so that this reflected signal and no others becomes modulated and can be separated by a suitable detector. The original method was developed for microwave frequencies and used a gas discharge tube modulated at 1000 Hz for the reflecting device. Refinements of the method making it more suitable for low frequency measurements include the use of choppers [6] or PIN diodes [43] driven by audio-frequency square waves to replace the discharge tube.

A newer method for electrical length matching of cables [44], which is very simple and does not require modulated terminations, uses a sweep generator as the signal source. The reflected signal is separable

in this case because it differs in frequency from the outgoing signal. The method is less accurate (by approximately one order of magnitude) than that of Swarup and Yang, but it could prove useful for preliminary trimming and resolution of ambiguities.

To return to the question of accuracy, it appears that the phase shifts of the cables in the feeder system can be matched to within $\pm 0.1^\circ$. This is the figure given by Kushner [40] for accuracy attainable in the HF (3-30 MHz) range, and it is consistent with the results given by users of the Swarup and Yang technique.

There are a number of practical difficulties associated with cable trimming, not the least of which is the temperature changes which will occur during measurements. The procedure, probably consisting of the adjustment of a coaxial "line-stretcher" in each feedline entering the observatory building to make its electrical length equal to that of some standard line, would be a very time-consuming operation when repeated for each of several hundred lines. Since recalibration is likely to be needed each time the temperature changes by more than a few degrees, this operation could severely reduce the already limited observation time. This indicates a need for an automatic system of phase control which can carry out the procedure very quickly, or perhaps even continuously without interruption of observations. Such a system will be described in Sec. 5.1.

With regard to preliminary trimming of the cables, it should be noted that the electrical length of a coaxial cable is dependent to a certain extent on its physical configuration. For example, the cable's electrical length increases when it is coiled; increases of 700 ppm in the electrical length of standard flexible cables have been noted after

being coiled on an eighteen-inch diameter form [40]. In an equal-length feeder system, all cables are the same length regardless of the proximity of the antenna elements to the observatory building; this means that there will be a good deal of cable (roughly half of the total amount) which will likely remain coiled. In view of what has just been said regarding electrical lengths, it is important that the cables be installed in their permanent positions before trimming is attempted.

(f) Shielding Efficiency and Crosstalk

For most practical purposes, the shielding afforded by coaxial cables may be considered complete, in that the coupling between adjacent transmission lines is of negligible proportions. However, for a very large antenna array in which the transmission lines may run side-by-side for thousands of feet, the picture changes dramatically and no such assumption of complete shielding can be made. As we shall see, the isolation between lines in such a situation may be very poor indeed.

Before considering the possible deficiencies of the cables in regard to shielding, we shall examine the effects on the performance of a radio telescope array resulting from poor isolation between feedlines. The methods used here are similar to those used by Labrum and McAlister [45] in their analysis of the feeder system of the Culgoora Radioheliograph.

We begin by considering excitation errors caused by imperfect shielding. Suppose a given transmission line has a nominal output voltage denoted by a phasor V_o . Now due to coupling between lines, adjacent lines contribute voltage components of the form $\alpha V_o \exp(j\theta_i)$, where α is the cross-coupling or crosstalk coefficient, and the phase

angles θ_i depend on such factors as source direction and element spacing. For the purposes of this analysis, we will assume the θ_i to be random and uniformly distributed between $-\pi$ and $+\pi$ radians. The output voltage of the line is

$$V = V_o [1 + \alpha \sum_{i=1}^M \exp(j\theta_i)] \quad (2.18)$$

where M = the number of lines contributing to the crosstalk.

Using the Euler identity and assuming that $\alpha \ll 1$, this voltage may be expressed as follows, in terms of a fractional amplitude error Δ and a phase error δ (radians):

$$\begin{aligned} V &= V_o [(1 + \alpha \sum_{i=1}^M \cos\theta_i)^2 + (\alpha \sum_{i=1}^M \sin\theta_i)^2]^{1/2} \exp(j\delta) \\ &= V_o (1 + \Delta) \exp(j\delta) \end{aligned} \quad (2.19)$$

$$\text{where } \Delta \approx \alpha \sum_{i=1}^M \cos\theta_i \quad (2.20)$$

$$\begin{aligned} \delta &= \tan^{-1} \left[\frac{\alpha \sum \sin\theta_i}{1 + \alpha \sum \cos\theta_i} \right] \\ &\approx \alpha \sum_{i=1}^M \sin\theta_i \end{aligned} \quad (2.21)$$

From these last two expressions, we can derive the r.m.s. excitation errors for the ensemble of transmission lines:

$$\Delta_{\text{rms}} = (\overline{\Delta^2})^{1/2} = \alpha(M/2)^{1/2} \quad (2.22)$$

$$\delta_{\text{rms}} = (\overline{\delta^2})^{1/2} = \alpha(M/2)^{1/2} \quad (2.23)$$

To estimate the effects of inter-cable crosstalk in the proposed array, we shall assume to begin with that the cables are closely bundled together. The crosstalk introduced into a given cable will be dominated by the contributions of its nearest neighbors; we shall therefore set $M = 6$, since this is the maximum number of cables which can be in direct contact with the one under consideration.

We must digress briefly at this point to consider the magnitude of excitation errors which we are willing to accept. The sources of errors, which will be examined in Chapter 4, may be grouped into two categories; some, such as the input bandpass filter, result in errors which at some level become practically irreducible except possibly by sophisticated compensation techniques. Others, including inter-cable crosstalk, contribute errors which can be reduced to almost any desired level without recourse to special techniques. There will, however, likely be an increase in cost accompanying this reduction, so that we wish to reduce the errors in the second category only to the extent that they are dominated by those in the first category. The results of Chapter 4, summarized in Table 4.1, show that the choice of magnitudes $\Delta_{\text{rms}} = \delta_{\text{rms}} = 0.0017$ ($\delta_{\text{rms}} = 0.1^\circ$) for errors in the second category will allow this situation to prevail.

Substituting the above values into equations (2.23) and (2.24) gives a maximum crosstalk level of

$$\alpha_{\text{max}} = 10^{-3} \quad (-60 \text{ dB}) \quad (2.24)$$

In addition to causing excitation errors, inter-cable crosstalk may have a detrimental effect on the sensitivity of the radio telescope, since it causes spurious fluctuations in the system noise temperature as the beam is scanned. To determine whether this will be a problem at the crosstalk level just derived, the r.m.s. value of these fluctuations must be found. From equation (2.19), the power output from the k^{th} transmission line is proportional to

$$|V_k|^2 = |V_o|^2(1 + \Delta_k)^2 \approx |V_o|^2(1 + 2\alpha_k \sum_{i=1}^M \cos\theta_{ik}) \quad (2.25)$$

where α_k is the crosstalk coefficient of the k^{th} line. If we add the outputs of N independent transmission lines, we have, in general, N uncorrelated voltages; the total power output for a given beam direction is proportional to

$$V^2 = \sum_{k=1}^N |V_k|^2 \quad (2.26)$$

The difference between V^2 and its mean value $\overline{V^2} = N|V_o|^2$ is

$$\begin{aligned} \Delta(V^2) &= V^2 - \overline{V^2} \\ &= 2|V_o|^2 \sum_{k=1}^N (\alpha_k \sum_{i=1}^M \cos\theta_{ik}) \end{aligned} \quad (2.27)$$

Recalling the assumption concerning the random distribution of the phase angles, we can find from (2.27) the mean-square value of the power difference:

$$\begin{aligned}
\overline{[\Delta(V^2)]^2} &= 4|V_o|^4 \sum_{k=1}^N \{\alpha_k^2 (\sum_{i=1}^M \cos \theta_{ik})^2\} \\
&= 4|V_o|^4 \sum_{k=1}^N \overline{\alpha_k^2} (M/2) \\
&= 2MN|V_o|^4 (\alpha_{rms})^2
\end{aligned} \tag{2.28}$$

The r.m.s. power fluctuation is therefore proportional to

$$\begin{aligned}
\Delta(V^2)_{rms} &= \alpha_{rms} |V_o|^2 (2MN)^{1/2} \\
&= \alpha_{rms} \overline{V^2} \left(\frac{2M}{N}\right)^{1/2}
\end{aligned} \tag{2.29}$$

Finally, we can express this fluctuation in terms of a change in system noise temperature:

$$(\Delta T)_{rms} = \alpha_{rms} T_{sys} \left(\frac{2M}{N}\right)^{1/2} \tag{2.30}$$

To evaluate $(\Delta T)_{rms}$, we set $M = 6$ as before and use for T_{sys} the mean antenna temperature of 1.4×10^5 °K found in Sec. 2.3.1(a). The number of independent transmission lines N has not yet been determined, but there is little doubt that it will be of the order of several hundred. If we arbitrarily select $N = 100$ as an absolute lower bound, we find from equation (2.30) that $\alpha_{rms} < 2.9 \times 10^{-2}$ (-31 dB) will result in a value of $(\Delta T)_{rms}$ which is less than the minimum detectable change in system noise temperature (about 2000°K). This condition on maximum crosstalk level is much less stringent than that given by equation (2.24); in other words, if crosstalk is kept sufficiently small that excitation

errors are minimal, then there need be no concern that the sensitivity of the instrument will suffer.

In the analysis just concluded, the single crosstalk coefficient α was replaced by an r.m.s. value for the ensemble of all transmission lines, in recognition of the fact that the amount of crosstalk introduced into a particular line will depend on which section of the array it is feeding. The use of an r.m.s. value in (2.24) and the other expressions concerning excitation errors is equally valid and more exact than the assumption of identical crosstalk level in all lines.

We now must consider the degree to which crosstalk may be a problem when coaxial transmission lines are employed. The shielding efficiency of coaxial cables varies considerably, depending on the construction of the outer conductor(s). The types of construction commonly used, in descending order of shielding efficiency, are solid sheath, strip braid, triaxial (two independent braids), double braid (not insulated from each other), and single braid. All of the relatively inexpensive cables such as RG-213/U fall into the single braid category, and one must pay dearly for better shielding than these cables will provide. For instance, RG-214/U is a double-braided cable which is identical electrically to RG-213/U except for improved shielding efficiency, but the former costs more than three times as much as the latter.

The crosstalk between two cables depends on their shielding efficiencies plus a coupling factor which is governed by the physical separation of the cables and the grounding practices used. Unfortunately, data on coupling factors are not generally available, but it is possible to make some rough estimates. One handbook [34] gives a crosstalk figure

of -80 dB in the 1-30 MHz region for two single-braided coaxial lines laid side-by-side for a distance of twenty feet. Using an extrapolation formula given in the same publication, one arrives at a crosstalk figure of -12 dB for a one thousand foot side-by-side run. The formula is not valid for larger runs than this, but it is clear that in the proposed array feeder system with its possible side-by-side cable runs of as much as 8200 feet, close bundling of transmission lines could result in $\alpha_{\text{rms}} \approx -10$ dB. Such a high degree of crosstalk would cause excitation errors far in excess of the allowable limits.

The preceding indicates the importance of making crosstalk measurements on long cable runs before the physical configuration of the feeder system is decided upon. A certain amount of separation will have to be maintained between the cables to prevent intolerable excitation errors.

2.3.3 Summary and Evaluation

In this section the evaluation of nonconversion transmission systems will be made somewhat more precise with some further numerical estimates of excitation errors. The majority of the section will deal with the phase-temperature variations in cables introduced in Sec. 2.3.2(a), which are potentially the most serious source of errors.

To begin with, the transmission line phase errors resulting from temperature changes over the range of -50°C to +30°C will be estimated. Assuming that all cables have been carefully adjusted to the same electrical length by the techniques discussed in Sec. 2.3.2(e) at a temperature near the middle of this range, we wish to determine the extent of deterioration in excitation when the temperature approaches

the extremes of the range. Disregarding the small measurement error in the trimming process, at the temperature of calibration T_c all cables have the same phase shift:

$$\phi_c = 360f_o\tau_c \quad \text{degrees} \quad (2.31)$$

where τ_c = phase delay, μs , at $f_o = 12.36$ MHz and temperature T_c

Now at some other temperature T , a cable having phase-temperature coefficient K_p will have, from equation (2.17), a phase shift of

$$\begin{aligned} \phi(T) &= \phi_c + \Delta\phi(T) \\ &= \phi_c + 360f_o\tau_c K_p [T - T_c] \times 10^{-6} \\ &= \phi_c (1 + K_p [T - T_c] \times 10^{-6}) \end{aligned} \quad (2.32)$$

From (2.32), we can find the r.m.s. phase error:

$$\begin{aligned} \delta_{rms} &= [\phi(T) - \overline{\phi}(T)]_{rms} = \phi_c |T - T_c| [K_p - \overline{K_p}]_{rms} \times 10^{-6} \\ &= \phi_c |\Delta T| (\Delta K_p)_{rms} \times 10^{-6} \end{aligned} \quad (2.33)$$

For an estimate of $(\Delta K_p)_{rms}$, we recall from Sec. 2.3.2(a) that the value of K_p for a given type of solid dielectric coaxial cable may differ by as much as $\pm 20\%$ from the median value. Suppose we assume a Gaussian distribution about this value and arbitrarily take the $\pm 20\%$ tolerance to be the limits corresponding to 99% confidence that K_p lies

within this interval. This leads to an r.m.s. error (standard deviation of the distribution) of $(\Delta K_p)_{\text{rms}} = 0.08 |\overline{K_p}|$.

To arrive at some numerical values for phase errors, we shall continue the analysis using a representative solid-dielectric cable, RG-213/U. Data given by Rodriguez [39] shows a variation in nominal K_p for this cable of considerable magnitude, from about -130 ppm/°C at +40°C to about -80 ppm/°C at -50°C, but for our purposes the cable can be adequately represented by $\overline{K_p} = -100$ ppm/°C independent of temperature. Thus our estimate of r.m.s. deviations from the mean becomes, in this case, $(\Delta K_p)_{\text{rms}} = 8$ ppm/°C. Since the cable has a velocity factor of 0.659, the standard delay τ_c for a 2.5 km line will be

$$\tau_c = \frac{2.5 \times 10^6}{(.659)(3 \times 10^5)} = 12.65 \text{ } \mu\text{sec}$$

Using these values in equations (2.31) and (2.33), together with $f_o = 12.36$ MHz yields an r.m.s. phase error of

$$\begin{aligned} \delta_{\text{rms}} &= 360(12.36)(12.65)(8)(10^{-6})|\Delta T| \\ &= 0.45|\Delta T| \text{ degrees} \end{aligned} \quad (2.34)$$

For temperatures near the extremes of the range, this linear approximation predicts r.m.s. phase errors of about 18°.

For cables with foam dielectric, the picture is improved somewhat, since the phase-temperature coefficient is lower by a factor of about four. However, as was pointed out in Sec. 2.3.2(a), this type of cable tends to have looser tolerances on K_p , which partially

nullifies the advantage it has over solid-dielectric cable due to lower K_p . Taking as a typical figure $\overline{K_p} = 25 \text{ ppm/}^\circ\text{C}$ with a tolerance of $\pm 33\%$, and following the same procedure as before, we find that

$$\delta_{\text{rms}} = 0.18|\Delta T| \quad (2.35)$$

This results in an estimated r.m.s. error of 7.2° at the extremes of the temperature range.

The immediate conclusion one can draw from these figures is that for standard cables in a nonconversion transmission system, the phase errors will greatly exceed the tentative guideline of 1° r.m.s. set forth in Sec. 1.3.3, except within a narrow temperature range near the calibration temperature. Recalibration for excursions in temperature outside this range would be a very time-consuming process and would waste valuable observation time.

The tolerance figures used to arrive at these estimates are admittedly highly pessimistic. However, the figures would have to be in error by an order of magnitude or more before the resulting phase error estimates would come within acceptable limits. It is doubtful that any manufacturer would supply a large amount of inexpensive standard cable with a guaranteed tolerance on K_p of the order of $\pm 2\%$ or better. Furthermore, we must also consider the many other sources of excitation errors which will be present, such as the preamplifier and associated tuned circuits, the beam-forming circuitry, and so on.

Although the nonconversion approach cannot be summarily ruled out on the basis of the above estimates, it is clear that, given the importance of achieving low sidelobe levels which has been a basic

cornerstone of the new array's design, this approach may not be the best route to follow. Despite the fact that it has been used in all low frequency arrays constructed to date, transmission without frequency conversion does not appear to be compatible with the combined objectives of small excitation errors and many independent transmission lines. The alternative system examined in the following sections has inherently better excitation characteristics, and it also introduces new possibilities such as frequency-division multiplexing.

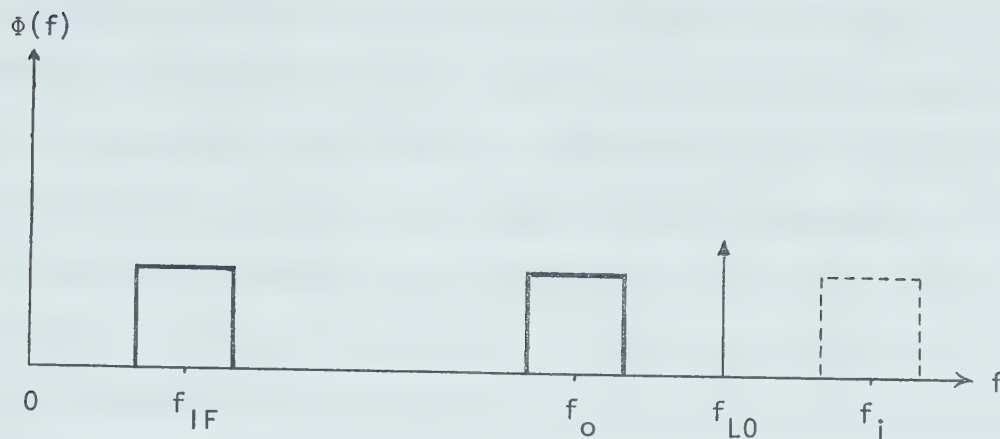
2.4 Signal Transmission With Frequency Conversion

Thus far we have confined our attention to transmission systems which operate at the center frequency of the radio telescope. We shall now examine the attributes of systems involving down-conversion of the signals at or near the array elements before transmission to the observatory. In many respects, little qualitative difference exists between the two types of system, and the results of the previous sections can be applied in a straightforward manner.

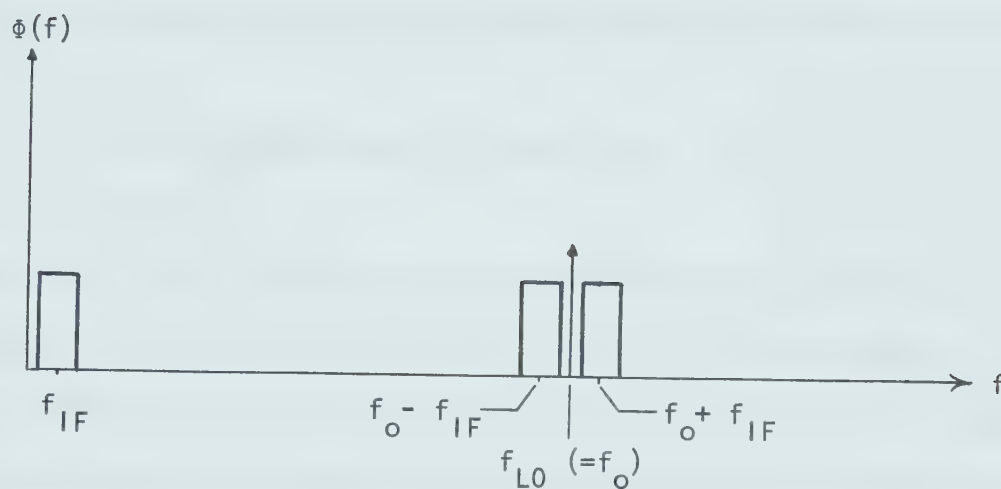
2.4.1 Receiver Type: SSB Versus DSB

The use of a frequency conversion system allows one a choice between the two options of single sideband and double sideband reception, abbreviated SSB and DSB respectively. The spectral relationships in the two methods are depicted in Fig. 2.5, the basic difference being whether signals in the band centered on the image frequency $f_i = f_{LO} + f_{IF}$ are accepted or rejected. Notice that f_{IF} is defined as the center of the resultant IF passband; $f_{IF} = f_{LO} - f_o$ only in the SSB case.

DSB reception is commonly found in two-element long-baseline



(a) SSB



(b) DSB

$\Phi(f)$ = spectral density

f_o = telescope center frequency

f_i = image frequency (rejected by input filter)

f_{IF} = intermediate frequency

f_{LO} = local oscillator frequency

Fig. 2.5 Spectral Relationships in Frequency Conversion Systems

interferometers and other types of arrays which are designed to correlate all possible pairs of element outputs. Such instruments are known as correlation arrays. Each of the $N(N-1)/2$ pairs of elements in a correlation array containing N elements forms a correlation interferometer which measures one component of the Fourier transform of the source's brightness distribution. It can be shown [46] that if the image is retained in the frequency conversion, the output of the correlator will not be affected by differential phase shifts in the intermediate-frequency channels between the mixer and the correlator. For a system bandwidth B , the correlator output is proportional to [47]:

$$B \left(\frac{\sin \pi B \Delta \tau}{\pi B \Delta \tau} \right) (\cos \omega_{IF} \Delta \tau) (\cos \omega_o \tau)$$

where $\Delta \tau = \tau - \tau_n$, the delay error caused by the time difference τ in the arrival of the wavefront from the source at the two elements, which can be reduced to any desired value by the insertion of a time delay τ_n into the appropriate channel. The $(\sin x)/x$ term is the decorrelation loss factor (see Sec. 5.3) due to the nonzero bandwidth accepted. One approaches the ideal response $B(\cos \omega_o \tau)$ by reducing $\Delta \tau$, without regard to channel phase shifts.

The proposed Tee array may be operated as a correlation array in a later phase of its development, but current plans call for the phasing of each component array to form a fan beam response, followed by cross-correlation of the two array outputs to form a pencil beam response. In this case, the immunity of the DSB system to intermediate-frequency (IF) phase errors vanishes. There may, however, still exist an advantage over the SSB system in the area of phase error reduction. Unlike the SSB

case, DSB conversion has no lower bound on the choice of f_{IF} imposed by image rejection requirements. A low IF is in fact a necessity in the DSB system if the sidebands are to be confined to the small area of spectrum available surrounding f_o . Since transmission line phase errors are proportional to f_{IF} , this is potentially an excellent method of reducing such errors.

The central problem with transmission at a very low IF is that we are now dealing with a wideband signal whose spectrum covers several octaves. This makes the problem of faithful transmission of the signal inherently more difficult; the changes in cable characteristics over the band must now be considered. One likely medium for signal transmission at a low IF is polyethylene-insulated telephone cable. The changes in some of the electrical parameters of this type of cable in the 1-50 KHz range are shown in Table 2.2 below [48]. Such changes are likely typical

Table 2.2 Properties of Standard Telephone Cable (19 AWG twisted pairs, measured at 27°C)

Frequency (KHz)	Char. Impedance (ohms)	Attenuation (dB/mile)	Propag. Velocity ($c = 3 \times 10^8$ m/sec)
1	300 - j280	1.2	0.22c
10	130 - j60	3.0	0.51c
50	110 - j20	4.5	0.60c

of other cables as well, including coaxial types. The characteristic impedance, attenuation, and velocity of propagation all vary widely with frequency, which would call for extensive use of wideband matching and equalization networks. Such networks would be complex and their characteristics difficult to reproduce.

There are several other technical problems which make the DSB approach less attractive. For example, the dual-gate MOSFET, which is probably the most suitable device for use as the first mixer, could not be used at a very low IF because of its high $1/f$ noise output in this region. DSB reception would also eliminate the possibility of multiple use of cables by frequency-division multiplexing. For these reasons, an SSB conversion system is preferred for the proposed array.

2.4.2 Image Rejection and Choice of IF

In an SSB transmission system one has considerable latitude in the choice of an IF. The need for image rejection is the primary consideration in establishing a practical lower bound on the possible choices, while the upper bound depends mainly on cable attenuation and phase errors, both of which increase with frequency. Within these bounds, one may consider such constraints as channel spacing necessary for frequency-division multiplexing, and the desirability of placing the image in a sparsely-occupied frequency band.

Image rejection may be defined by the following ratio:

$$\eta = V_{oi}/V_{oo} \quad (2.36)$$

where V_{oi} = output voltage of mixer stage due to an input signal at the

image frequency f_i

V_{oo} = output voltage of mixer stage for an input signal at the desired frequency f_o having the same field strength at the antenna element

Both outputs are at the frequency f_{IF} . The result of having the undesired signal in the output is to cause errors in excitation similar to those arising from inter-cable crosstalk, since the image signal is uncorrelated with the desired signal and can be considered a source of random errors. The mixer output voltage has the form

$$V_o = V_{oo} + V_{oi} = V_{oo}(1 + \eta e^{j\theta}) \quad (2.37)$$

where θ = random phase angle, assumed to be uniformly distributed from $-\pi$ to $+\pi$ radians

The r.m.s. amplitude and phase errors are then given by expressions analogous to (2.22) and (2.23) derived for inter-cable crosstalk:

$$\Delta_{rms} = \delta_{rms} = \eta/(2)^{1/2} \quad (2.38)$$

As in the case of crosstalk, we wish the r.m.s. error magnitudes from this source to be no greater than about 0.0017. The image rejection needed to attain this level is, from (2.38),

$$\eta = 2.4 \times 10^{-3} \quad (-52 \text{ dB}) \quad (2.39)$$

This is essentially the amount of attenuation that the input bandpass filter must provide at f_i with respect to f_o ; however, the narrowband

properties of the dipole antenna element will also aid to some extent in image rejection. The extent of the latter contribution depends on the type of construction (e.g., the thickness of the conductors), the type of impedance matching used, and the effects of mutual coupling to adjacent elements. It is not possible to evaluate all of these factors as yet, since there are a number of unknown quantities present. It will therefore be assumed that the input filter must supply the full attenuation needed at the image frequency.

Implicit in the preceding discussion is the assumption that the image signal encountered in practice will be of approximately the same magnitude as the desired signal; this assumption should be reasonably well satisfied for a low IF of the order of 1 MHz. To ensure that the image signal is minimal for a given IF, it is important that the image frequency be above rather than below the center frequency f_o . This follows both from the lower probability of encountering strong signals of terrestrial origin at the upper frequency, and from the inverse relationship between background sky brightness temperature and frequency in the region above 10 MHz.

To estimate the lower bound on IF choice imposed by the requirement of equation (2.39), it will be assumed that the amplitude characteristic of the input filter is approximately symmetric in frequency about f_o , so that the separation between f_o and f_i must be one-half of the 52 dB bandwidth of the filter. Denoting this bandwidth by B_{52} , we have

$$f_{IF}(\min) = \frac{f_i(\min) - f_o}{2} \approx \frac{B_{52}}{4} \quad (2.40)$$

This expression will be evaluated for various filter configurations in Sec. 3.3.1, in which the effect of the input filter on frequency-division multiplex systems is considered. Final specification of filter type must await consideration of the excitation errors from this source (Sec. 4.1.1).

For the sake of completeness, it should be mentioned that it is possible to design a mixer circuit which can reject the image signal without the use of filters [49]. The method uses phase shifters and a pair of balanced mixers in a circuit configuration which resembles the phase-shift method of generating an SSB signal. Owing to the complexity of the circuit and the likelihood of poor intermodulation performance, this approach has not been pursued further.

Further developments in the matter of IF selection will appear in the following pages, since such topics as attenuation of cables, phase stability, local oscillator distribution, and multiplexing are all affected by this choice.

2.4.3 Attenuation and Noise Considerations

Evaluation of system noise temperature in the case of frequency conversion is similar to the nonconversion case (Sec. 2.3.1). The only differences lie in the replacement of the preamplifier by a mixer (possibly accompanied by a stage of amplification), and the reduction of transmission line losses. Table 2.3 extends the attenuation data of Table 2.1 to the probable IF range; the entries in the table were obtained with the aid of equation (2.11). Noise figures attainable in the mixers should not differ appreciably from those used to estimate preamplifier noise temperature previously, so that the criterion of

Table 2.3 Attenuation (dB) vs Frequency for 2.5 km Cable Runs

Cable Type	Frequency (MHz)			
	0.5	1.0	2.0	4.0
RG-58/U	17	26	38	57
FM-58	18	25	35	50
RG-62A/U	14	20	29	42
RG-213/U	12	16	24	34
FM-8	9.3	13	19	27
RG-218/U	3.6	5.3	7.7	11

$A_{\max} = 13 + 10 \log_{10} G$ for the cable attenuation remains applicable, with the power gain G now including the conversion gain of the mixer. A MOSFET mixer can yield a conversion gain of the order of 20 dB, which is sufficient to obviate the need for a preamplifier or IF amplifier stage in conjunction with the mixer, and yet still permit the use of relatively inexpensive cable. For example, Table 2.3 shows that RG-58/U, which is unsuitable for any nonconversion transmission system, would satisfy the attenuation criterion for an IF up to about 2 MHz given this amount of conversion gain. This upper bound could be extended another octave to 4 MHz by switching to the use of RG-213/U cable, or by inserting an amplifier stage having about 20 dB gain.

From attenuation considerations, therefore, we can place the probable upper bound on IF selection in the region of 2 to 4 MHz.

2.4.4 Excitation Errors

All of the topics concerning excitation errors discussed in Sec. 2.3.2 remain applicable in the case of a frequency conversion system. The shielding efficiency may be slightly improved by transmission at an IF, but the difference will not be large enough to significantly affect the inter-cable crosstalk level. Similarly, there may be some advantages in the area of cable trimming (e.g., improved phase detector performance at lower frequencies), but the differences again are not expected to be substantial.

The most significant quantitative change expected is in regard to phase errors in the transmission lines resulting from disparities in phase-temperature coefficient. As we have seen from equation (2.33), the phase error δ_{rms} is directly proportional to the transmission frequency, so that it is possible to reduce this particular error by the factor f_o/f_{IF} by converting to an IF. This assumes the use of the same type of cable in both cases, however; it may well be that the phase error reduction is less than this because of the use of smaller-diameter cable in the case of IF transmission. There is a wide variation in phase-temperature stability amongst such cables, the standard representatives of which are RG-58/U (50Ω), RG-59/U (73Ω), and RG-62A/U (93Ω). Their phase stability coefficients K_p , as given by Rodriguez [39] for the range of $27^\circ\text{--}85^\circ\text{C}$, are -480 , -330 , and -60 ppm/ $^\circ\text{C}$ respectively. RG-62A/U cable has an obvious advantage in phase stability over the other types and is a notable exception to the general rule that small-diameter cables have the largest values of K_p . Reference to Tables 2.1 and 2.3 reveals that this cable also has significantly lower attenuation than RG-58/U, although the cost is roughly 30% higher for RG-62A/U.

An estimate of transmission line phase errors for the case of frequency conversion will now be made, assuming the use of RG-62A/U in the feeder system. The coefficient K_p is less temperature-dependent for RG-62A/U than for the other common RG-type cables, and it can be quite adequately represented by $\overline{K_p} = -50 \text{ ppm/}^\circ\text{C}$ over the full temperature range of -50°C to $+30^\circ\text{C}$. Making the same assumptions concerning the distribution about $\overline{K_p}$ as we did in the nonconversion case (Sec. 2.3.3), we set $(\Delta K_p)_{\text{rms}} = 4 \text{ ppm/}^\circ\text{C}$. Using equation (2.33), the r.m.s. phase error estimate becomes, for a given f_{IF} (MHz),

$$\delta_{\text{rms}} = 360(12.65)(4)(10^{-6})f_{\text{IF}}|\Delta T| = 0.018f_{\text{IF}}|\Delta T|^\circ \quad (2.41)$$

This is a considerable improvement over the nonconversion situation; even at the extremes of the temperature range, assuming the cables are trimmed for the middle of the range, the estimated r.m.s. phase error has risen to only $0.72f_{\text{IF}}^\circ$. In contrast to the nonconversion case, the possibility now exists of achieving a satisfactory sidelobe level without resorting to frequent recalibration or an automatic phase compensation system.

It would be premature to make firm design decisions at this point, but it does appear that RG-62A/U is clearly the best choice for the transmission lines. Its phase stability approaches that of the foam-dielectric cables, whereas it does not share the problem of moisture absorption into the dielectric with the latter. The attenuation in the IF range is also reasonably low for RG-62A/U.

2.4.5 Local Oscillator Distribution

In adopting a frequency conversion transmission system, one necessarily introduces the complication of distributing the local oscillator (L0) signal to the remote mixers. Since steering of the array response requires knowledge of the relative phases of the feeder outputs at the observatory, and these in turn depend on the L0 phase at each mixer, it is essential that each mixer be supplied with the same phase (or at least a known phase) of L0 signal. Departures from this ideal situation result in excitation errors, so that the L0 phase must be carefully controlled in order to fully realize the benefits of frequency conversion.

The L0 distribution system is actually a second, independent feeder system; one could visualize the problem in terms of the feeding of a broadside array with the mixers as elements and the L0 as a transmitter. Any of the basic methods described in Sec. 2.1 could be used to implement the system. The choice reduces to one between the single-line and branching types, independent lines being unnecessary and uneconomical for L0 service.

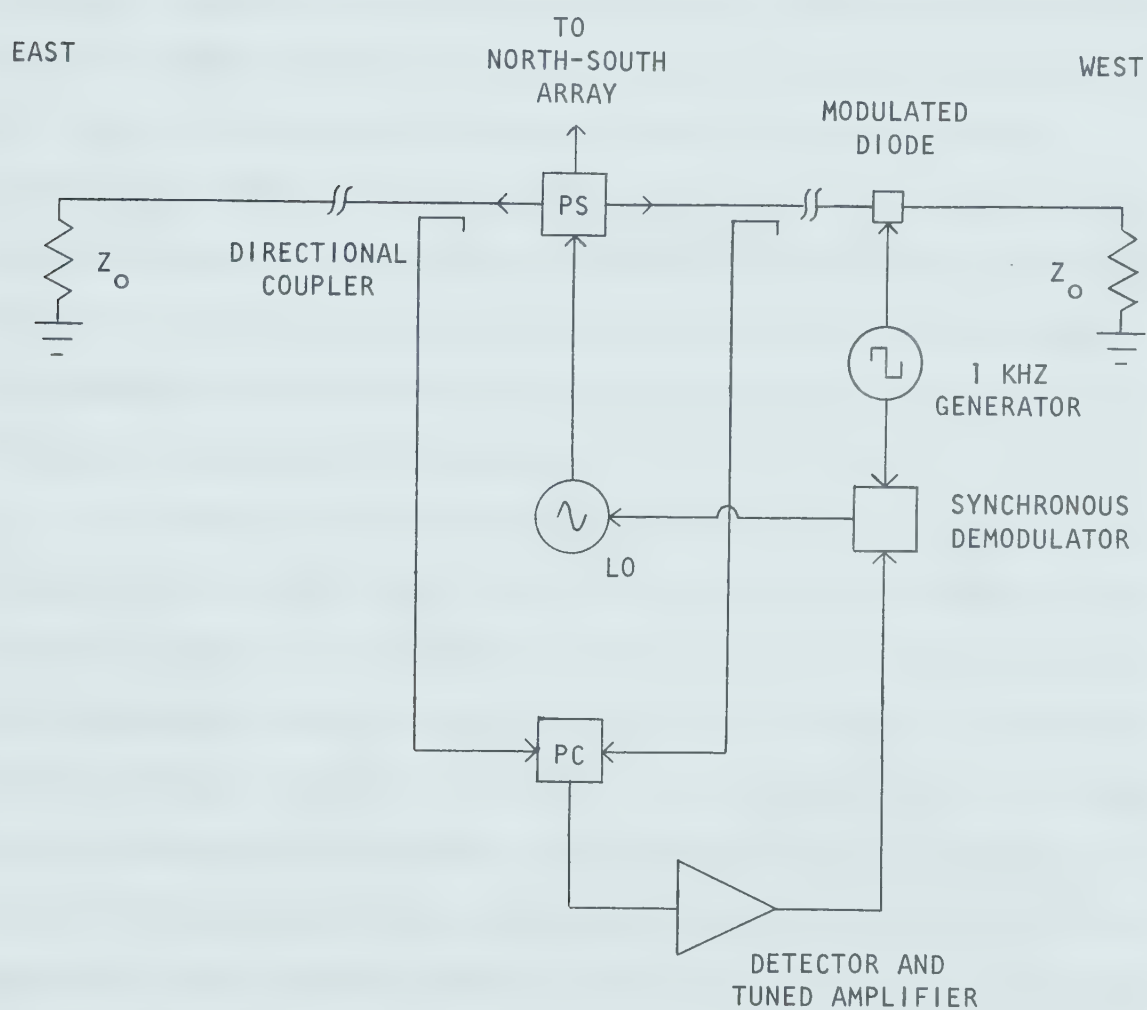
The principle attribute of the binary branching feeder is that it offers a path of equal electrical length from the oscillator to each mixer; consequently, it is self-compensating in the sense that changes in temperature, for example, will not disturb the relative phases of the outputs. The success of this compensation rests on the degree to which the changes are uniform throughout the system, and the degree to which the characteristics of the individual sections of cable are matched to each other. Since we are now dealing with a frequency greater than the center frequency, ordinary cables not designed for phase stability are

likely to have enough disparity in phase-temperature coefficient from one part of the branching system to another to result in significant phase errors.

There is a second reason why an inexpensive cable of the RG-62A/U variety may not be a good choice for the L0 system, namely the high attenuation of such cable at the L0 frequency. Although this attenuation can be overcome by the simple expedient of increasing the power output of the oscillator, it then becomes more difficult to shield the oscillator adequately to prevent radiation. A strong radiated L0 signal could cause severe crossmodulation or intermodulation problems in the mixer and preamplifier stages.

The single-line feeder system calls for a minimum of transmission line, consisting of a single line running the length of each arm of the array. It too should have low attenuation for the reason just mentioned. Depending on how critical the mixer parameters are with respect to changes in L0 injection level, attenuators may be needed at the coupling points to ensure that this level is approximately the same at all mixers. The system is not self-compensating, and phase errors will increase with distance from the oscillator when temperature or other factors change. However, due to its simplicity and low cost, the single-line technique is highly attractive if a suitable means of external compensation can be found. The basic problem is the maintenance of the electrical separation of the coupling points at integral multiples of the L0 wavelength when the velocity of propagation in the line changes. The only practical method of changing the electrical length of the line such that the change is uniformly distributed throughout the line is by adjustment of the L0 frequency. A simple method of L0 distribution based on this

concept was developed for use with the Molonglo Cross [50]; the method uses the Swarup and Yang technique (Sec. 2.3.2e) to continuously monitor the electrical length of the line and supply an error signal to the voltage-controlled local oscillator when any deviations are sensed. The distribution system is outlined in Fig. 2.6.



PS= Power Splitter

PC= Power Combiner

Fig. 2.6 Local Oscillator Distribution System

The transmission line for the single-line L0 system need not be phase-stable, but it should have uniform characteristics throughout. In this respect, the requirements are similar to those for the branching system; the difference lies in the amount of transmission line needed, which favors the single-line system in terms of cost and likelihood of achieving uniformity. To illustrate this difference, consider the problem of supplying a signal to N mixers in a linear, uniformly-spaced array of length L meters. In contrast to the L meters of line needed for the single-line system, the branching system will need at least $(L/2)(\log_2 N)$ meters of line, assuming the oscillator is located at the center of the array. The difference becomes significant for large N , and since low attenuation is needed, this difference could be quite costly. The branching system also has the additional problem of coupling and impedance matching at the junctions.

In addition to low attenuation, the construction of the L0 line should offer easy adjustment of the coupling at each point where the L0 signal is tapped off. In general, conventional coaxial lines do not meet this requirement, owing to the difficulty one would have in installing couplers. A more accessible type of line such as open-wire or air-spaced coaxial line would be preferred; such lines usually have low attenuation as well. The open-wire line would be rather susceptible to ice build-up and other forms of weather damage, so that the coaxial line would likely be the better choice. A coaxial line fabricated from iron troughs and copper tubing was used in the Molonglo L0 system [50]; such a line would have a total attenuation over a 2.5 km run of only about 3.5 dB in the neighborhood of 13 MHz. A similar type of line was used as the feeder in the original Mills Cross [21], and more recently a coaxial line

constructed from aluminum irrigation tubing was used to feed a large 7-25 MHz array designed for ionospheric studies [51].

The details of line construction and coupling arrangements remain to be worked out, but the combination of a large-diameter air-spaced coaxial line with an automatic frequency control system such as the one described earlier appears to be the best choice for L0 distribution in the Tee array. One problem arising from making the L0 frequency variable is considered in the following section.

2.4.6 Beam Pointing Error Compensation

The beam of the array is steered by the insertion of phase shifts, as given by equation (2.1); the values of phase shift needed depend on source direction, element spacing, and the telescope center frequency. Frequency conversion preserves the relative phases of the element outputs, so that the same phase shifts are needed if the beam steering is done at an IF. A shift in the L0 frequency, as required by the phase control system outlined in the preceding section, is equivalent to a shift in center frequency since the center of the IF passband (fixed at f_{IF}) no longer corresponds to f_0 . The result is a beam pointing error.

To estimate the magnitude of this error, we consider a pair of elements with spacing d ; a phase shift ϕ radians is inserted into one element output in order to point the beam in a direction θ radians off the broadside:

$$\phi = \frac{2\pi d f_0 \sin \theta}{c} \quad (2.42)$$

Now suppose that a shift Δf in L0 frequency occurs, changing the center

frequency to $f_o + \Delta f$. The phase shift ϕ now corresponds to a new beam direction $\theta + \Delta\theta$ determined by

$$\phi = \frac{2\pi d(f_o + \Delta f)\sin(\theta + \Delta\theta)}{c} \quad (2.43)$$

Equating (2.42) and (2.43), we get

$$\frac{\sin(\theta + \Delta\theta)}{\sin \theta} = \frac{f_o}{f_o + \Delta f} \quad (2.44)$$

Assuming that $\Delta f \ll f_o$ and $\Delta\theta \ll 1$, (2.44) can be simplified to

$$1 + \Delta\theta(\cot \theta) \approx \frac{f_o}{f_o + \Delta f}$$

$$\text{or,} \quad \Delta\theta \approx \frac{-\Delta f(\tan \theta)}{f_o + \Delta f} \approx \frac{-\Delta f(\tan \theta)}{f_o} \quad (2.45)$$

The beamwidth of the north-south array of the Tee for a zenith angle θ will be approximately $\theta_{BW} = 30(\sec \theta)$ arcmin. If we wish the pointing error to be small, say an order of magnitude less than the beamwidth, then we must have $|\Delta\theta| < \theta_{BW}/10$. Inserting this expression into (2.45), with θ_{BW} expressed in radians, we have:

$$\frac{|\Delta f(\tan \theta)|}{f_o} < \frac{\pi(\sec \theta)}{3600}$$

$$\text{or,} \quad |\Delta f| < \frac{f_o |\csc \theta|}{1146} \quad (2.46)$$

The pointing error is worst at large zenith angles, for which $|\csc \theta| \approx 1$. Using this approximation and $f_o = 12.36$ MHz in (2.46), the requirement on the L0 frequency shift becomes

$$|\Delta f| < 11 \text{ KHz} \quad (2.47)$$

A frequency shift of this magnitude would indicate a change from the nominal electrical length of the L0 line of about 820 ppm, for an IF of 1 MHz. It is quite probable that changes in the length of coaxial lines of the type described in the preceding section could approach this value. The changes at the Molonglo L0 installation amounted to about 180 ppm from the nominal length [50], but the range of temperatures encountered at the Alberta site would be considerably greater than at the Australian site.

Rather than attempt to design the L0 line to minimize Δf , a more satisfactory solution to the problem of pointing errors is to perform a second frequency conversion (after transmission to the observatory) in which the second L0 frequency is derived from that of the first in such a way as to keep the center frequency constant. This concept will be incorporated into the frequency-division multiplex systems discussed in the next chapter.

2.5 Protection from Lightning

Regardless of which feeder/transmission system configuration is decided upon, protection of the array from damage by lightning strikes must be considered as an integral part of its design. A direct hit on

the array could have catastrophic consequences; widespread destruction of cable and electronic systems would be almost inevitable if steps were not taken to protect them.

There are two basic approaches one can follow to secure protection from lightning, with the most effective system involving a combination of the two. The first involves shielding of the protected area by the use of masts and overhead lines. Extensive data on determining the efficacy of a particular shielding configuration has been given by McRae and Hromass [52]. Good grounding practices [53] are essential in shielding installations to prevent flashover to protected components.

The second facet of lightning protection is more passive, concentrating on preventing the electronic systems from being damaged by the surge voltages induced by nearby lightning strokes. The protective device usually consists of a circuit element at the input to the electronic circuit which breaks down at a given voltage and provides a low impedance path to ground for the surge current. One protective device which has proven effective in telemetry applications [54] combines several such elements, including a zener diode, a fuse, and a carbon-block lightning arrestor similar to those used in telephone work.

It is likely that operation of the array would be suspended in the presence of thunderstorm activity. The surge protectors could then consist of shorting switches, to be activated at all times that the array is not in use. The topic of lightning protection is obviously one which requires further study.

CHAPTER 3

MULTIPLEXING IN THE FEEDER SYSTEM

3.1 Multiplexing: An Overview

As we have seen, one of the fundamental prerequisites for versatility in the Tee array is the independent return to the receiver site of a large number of array outputs. The cost of cable acquisition and installation, and the physical problems involved in cable placement with tolerably low crosstalk levels, make this a difficult proposition. It is desirable, therefore, to investigate the feasibility of multiplexing several of these signals onto each transmission line.

Multiplexing is achieved by arranging that the signals be distinguishable by virtue of their differences in time, frequency, or phase. Leaving aside the special case of phase-quadrature multiplexing, which when used alone is limited to only two signals, the basic time and frequency multiplexing systems are similar as far as their limitations are concerned. In both cases, the degree to which multiplexing can be utilized in a given situation is determined by the two fundamental considerations of bandwidth and crosstalk. The manner in which these factors arise and the technical differences in implementation will determine which system, if any, is most suitable.

3.2 Time-Division Multiplexing

Time-division multiplexing (TDM) can be implemented in a number of ways, depending on how the information to be transmitted is encoded; we shall first consider one of the simplest implementations, pulse-amplitude modulation (PAM). A PAM modulator consists of a sampling gate which is commutated periodically amongst all of the signals to be multiplexed. It also includes provision for the generation of synchronizing pulses which are distinguishable in some way from the samples. The demodulator performs the inverse operation to separate the sampled signals, followed by filters to recover the original signals from the sampled spectra.

The sampling rate required at the modulator depends on the bandwidth of the input signal, which in turn is a function of the input filtering and the spectral density of the signal delivered by the antenna. It will be assumed that the bandwidth is sufficiently small that the spectral density of the input signal can be considered to be flat. The signal bandwidth at the output of the first bandpass filter is then essentially that of the filter itself. If the filter has bandwidth B such that signals outside the frequency range $f_1 \leq f \leq f_1 + B$ are attenuated to a negligible level, the sampling theorem for bandpass signals [55] states that the minimum sampling frequency needed for distortionless reproduction is given by

$$f_s(\text{min}) = 2B(1 + \frac{k}{M+1}) \quad (3.1)$$

where $M = [f_1/B]$; i.e., the greatest integer in f_1/B

and $k = (f_1/B) - M$

When f_1 is considerably larger than B , as will be the case in the proposed array, equation (3.1) can be simplified to

$$f_s(\min) \approx 2B \quad (3.2)$$

A section of the output spectrum resulting from sampling at the minimum rate is depicted in Fig. 3.1 below. We are concerned with the recovery of the signals in a narrow band centered on f_o in the input

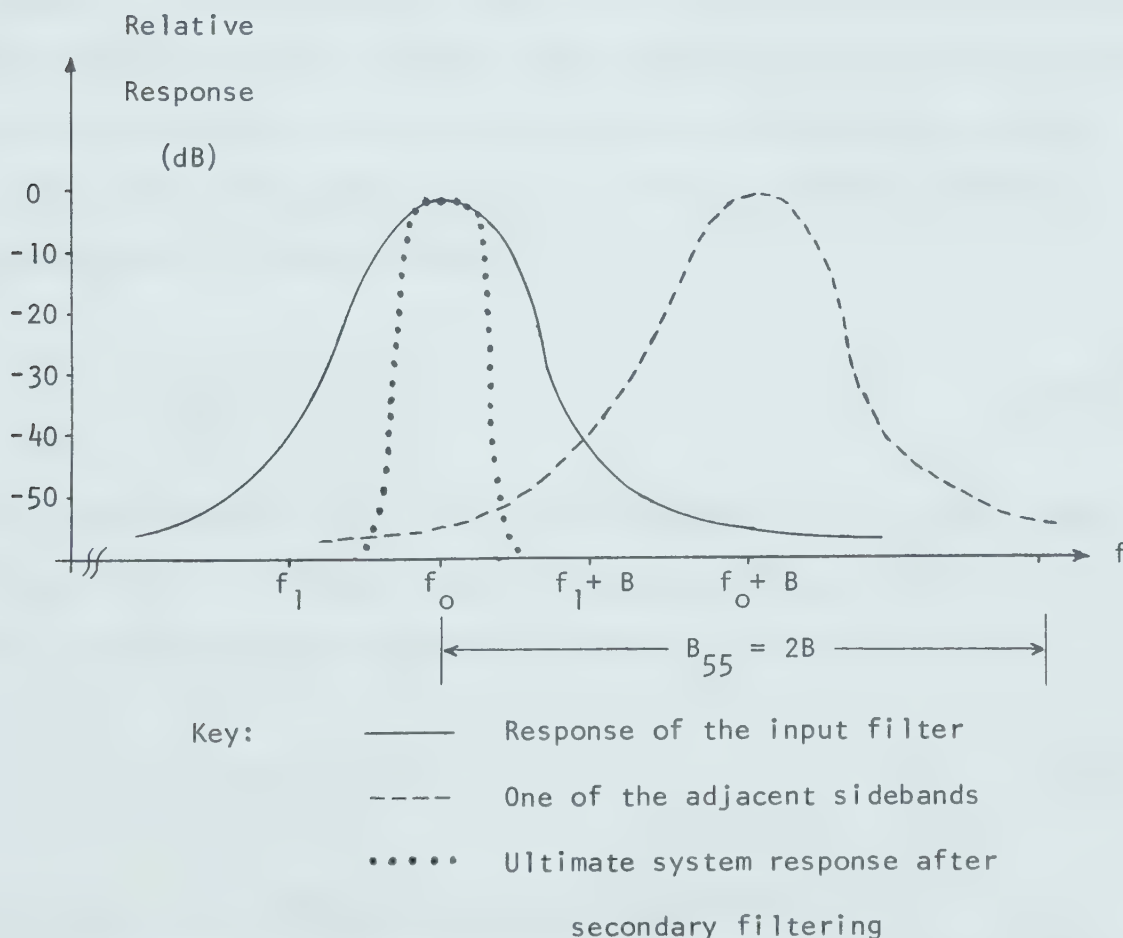


Fig. 3.1 Section of Sampled Signal Output Spectrum

spectrum, but we must also accept some unwanted signals due to the sidebands generated by the sampling process. The interference from these sidebands, only one of which is shown in the figure, may be considered a form of crosstalk. Assuming that the input filter response is approximately symmetric with respect to f_o , the crosstalk level α will be numerically equal to the attenuation of the filter for a bandwidth of $2B$ (i.e., we are assuming that the points $f_o \pm B$ have the same attenuation). This assumption is valid provided that B is sufficiently small that $[(f_o+B)(f_o-B)]^{1/2} \approx f_o$, or, in other words, $f_o \gg B$.

Since the interfering signals are uncorrelated with the desired signals, the analysis of this crosstalk can follow the methods used for inter-cable crosstalk, which was considered in Sec. 2.3.2(f). The r.m.s. excitation errors are found from equations (2.22) and (2.23), taking account of the fact that only the two adjacent sidebands contribute significantly to the crosstalk:

$$\Delta_{\text{rms}} = \delta_{\text{rms}} = \alpha \quad (3.3)$$

As in the previous cases of reducible excitation errors, we set 0.0017 ($\delta_{\text{rms}} = 0.1^\circ$) as an upper limit. To achieve $\alpha = 0.0017$ (-55 dB), the sampling rate must be, according to (3.2),

$$f_s(\text{min}) \approx 2B \approx B_{55} \quad (3.4)$$

where B_{55} = the 55 dB bandwidth of the input filter

Let us assume, for the sake of obtaining some numerical results, that the input filter consists of one or more double-tuned, critically-

coupled stages (this choice will be reconsidered in Chapter 4 in the light of excitation errors caused by the filter). The bandwidth B_α corresponding to a given attenuation α for such a filter is [56]:

$$B_\alpha \approx \frac{\sqrt{2} f_o [\alpha^{-(2/q)} - 1]^{1/4}}{Q} \quad (3.5)$$

where q = number of stages

Q = geometric mean of the primary and secondary loaded quality factors

When we set $f_o = 12.36$ MHz, and choose Q such that the 3 dB bandwidth is 200 KHz so as not to restrict the possible system bandwidth to less than this figure, we find from (3.5) the following 55 dB bandwidths:

$$\begin{aligned} q = 1 : B_{55} &\approx 4.8 \text{ MHz} \\ q = 2 : B_{55} &\approx 1.2 \text{ MHz} \end{aligned} \quad (3.6)$$

Larger numbers of stages would make uniformity very difficult to achieve, and the excitation errors from this source would quickly exceed those due to crosstalk which we are attempting to reduce (see Sec. 4.1.1).

Having the necessary sampling rate for our PAM system, it remains to determine what difficulties lie in the transmission of a series of pulses over a distance of 2.5 km. If we are to multiplex m channels onto one line, then the pulse repetition rate becomes mf_s , so that each pulse is allotted a "window" of $(mf_s)^{-1}$ sec. In practice the pulse rate must be greater than this, since we must also allot one or more channels to a synchronizing pulse which is readily distinguished from the sample

pulses; we accordingly set the pulse rate at $(m + 1)f_s$. The size of the window is then 42 ns for $q = 1$ and 167 ns for $q = 2$ when we set $m = 4$. Even in this example of only four multiplexed channels, it will become evident that the transmission of the pulses without crosstalk is not easily accomplished. The source of the crosstalk is the non-ideal attenuation-versus-frequency characteristic of the cable, which results in distortion of the pulse such that it has not fully decayed when the next one appears.

Pulse distortion on coaxial lines has been analyzed by Wigington and Nahman [57] under the assumption that the distortion is solely due to skin effect. This means that the attenuation must follow the half-power law (see Sec. 2.3.1) closely in the frequency range of interest; this proves to be the case for most common coaxial cables in the 1-100 MHz region. The output waveforms were found corresponding to input pulses with risetime t_r (assumed to be a linear ramp), and the results are applied to a particular cable type by multiplication by a normalization factor k_A :

$$k_A = \frac{[0.115A(f)]^2}{4\pi f} \text{ sec} \quad (3.7)$$

where $A(f)$ = total attenuation of the cable, dB, measured at f Hz
This factor, evaluated at 10 MHz for a 2.5 km length, is given for some common coaxial cables in Table 3.1.

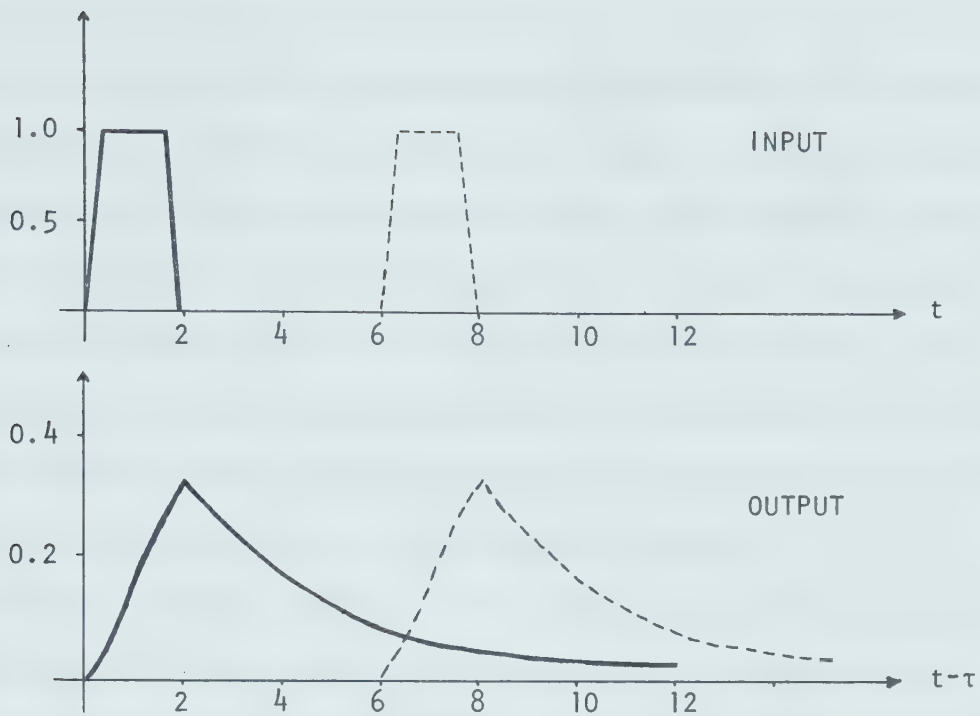
The results of Wigington and Nahman show that if the input rise time t_r is of the same order of magnitude or less than k_A , the output waveform has rise time (no longer linear) of the order of $100k_A$. However, in the present case it is not necessary that the output reach

Table 3.1 Normalization Factor for Cables

Cable Type	k_A (ns)
RG-58/U	1000
RG-62A/U	580
RG-213/U	310
RG-218/U	38

the peak value of the input, since some attenuation can be tolerated; if we permit 13 dB loss (see Sec. 2.3.1a), the output pulse need only rise to $\log^{-1}(-13/20) = 0.22$ of the peak value. For this to take place, one must have a time interval of about $2k_A$. Inspection of the figures in Table 3.1 reveals that of the cables listed, only RG-218/U has a sufficiently small value of k_A that a pulse of duration $2k_A$ can be accommodated in the 167 ns window for $q = 2$.

Figure 3.2 shows the calculated response of 2.5 km of RG-218/U to a series of pulses with $2k_A$ width (76 ns), rise and fall times of a few nanoseconds, and unity amplitude. Only two pulses are shown for clarity, and their amplitudes are the same, although this will not generally be the case in a PAM system. Two effects are immediately evident from the figure: severe distortion of the shape of a given pulse, and crosstalk caused by the slow decay of the previous pulses. The pulse distortion alters the shape of the sampled spectrum, but this



Time t in units of $k_A = 38$ ns

τ = propagation delay of the cable (2.5 km length)

Fig. 3.2 Normalized Pulse Response of RG-218/U Cable

problem can be overcome by a suitable choice of filter transfer function in the demodulation process [58]. It is the interchannel crosstalk which poses the more difficult problem, since it cannot easily be dealt with after the fact. From Fig. 3.2 we see that at the time at which the response to the second pulse attains its peak value of 0.32, the response to the preceding pulse has only decayed to 0.05; the addition of the two results in a 15% amplitude error in the sample represented by the second pulse. Earlier pulses will also contribute some crosstalk. Despite the use of a two-stage input filter and rather expensive cable, the PAM-TDM

transmission system is inadequate even for the case of only four channels.

A possible solution to the crosstalk problem lies in the use of pulse-code modulation (PCM) to transmit the signals in digital form. The modulator could consist of a PAM modulator plus an analog-to-digital (A/D) converter which converts each sample into a binary word, which is then transmitted serially as a stream of bits. Since one is now only concerned with differentiating between two possible states in the incoming series of pulses at the demodulator, a relatively large amount of pulse distortion can occur without causing crosstalk.

The number of bits needed in each word depends on the number of quantization levels used, which in turn depends on the amount of quantization noise which can be tolerated. This noise is an expression of the error in the reconstructed waveform due to quantization; it is a zero-mean random fluctuation similar in character to thermal noise. It can be shown [59] that for P levels of quantization, the signal-to-quantization noise power ratio approaches P^2 for $P \gg 1$. We wish to reduce this noise power to the point that the fluctuations are not detectable at the receiver. Recalling from Sec. 2.3.1 that the expected r.m.s. system noise temperature fluctuation is about 2000°K and the maximum system noise temperature about $2 \times 10^5^\circ\text{K}$, we must have

$$P^2 > \frac{T_{\text{sys}}}{(\Delta T)_{\text{rms}}} = 100$$

$$\text{or,} \quad P > 10 \quad (3.8)$$

For negligible deterioration in sensitivity, the quantization noise

temperature should be about one-fifth of $(\Delta T)_{\text{rms}}$, which would call for $P = 22$; however, it will be assumed in this evaluation that $P = 16$ is adequate. This means that each sample is represented by a 4-bit word.

The pulse repetition rate needed for this PCM-TDM system is $4mf_s$. Taking $m = 4$ and $f_s = 1.2$ MHz as in the PAM system, the rate becomes 19.2 MHz, corresponding to a window of $t_w = 52$ ns per pulse. Again referring to [57], it can be shown that if a cable has $k_A > t_w$, a pulse generated within one window will decay only slightly during the period of the following window. This gives rise to the possibility of errors in the identification of the value of a bit. RG-218/U is again the only cable listed in Table 3.1 which is useable, but unlike the PAM case, it can provide a PCM system which is free of crosstalk caused by pulse distortion. Less expensive cables could be used in conjunction with regenerative repeaters [60], but the net cost would likely not be reduced appreciably, and timing errors would increase.

The A/D converters in the PCM system must have 4-bit resolution and a conversion rate of mf_s MHz. For the particular case under consideration, the conversion rate needed is 4.8 MHz, which is well within the state of the art; 4-bit converters featuring speeds up to 100 MHz are presently on the market. The major stumbling block in implementing the system would occur in attempting to condition the signals to match the input voltage range, typically ± 5 volts, required by the A/D converters. The signal voltages involved would be very much smaller than this range. The available power from an antenna element is $kT_A B$, and the mean-square voltage output, after filtering, is

$$\overline{v^2} = kT_A R_O B \quad (3.9)$$

where k = Boltzmann's constant (1.38×10^{-23} joules/°K)

T_A = antenna noise temperature, °K

R_O = radiation resistance of antenna, ohms

B = equivalent noise bandwidth of the input filter, Hz

We shall assume that $T_A = 2 \times 10^5$ °K and $R_O = 300\Omega$ (approximate radiation resistance of a folded dipole element); B will be approximated by the 3 dB bandwidth, 200 KHz. Using these quantities in equation (3.9) gives $\overline{v^2} = 1.66 \times 10^{-10}$ V², or an r.m.s. voltage of 13 μ V. This is about five orders of magnitude smaller than the input levels required by the A/D converters. Some increase in voltage will occur as a result of impedance matching to the multiplexer circuitry, but an amplifier with at least 80 dB voltage gain will also be needed. This is an unpleasant prospect, since achieving stability over the wide temperature range plus good unit-to-unit uniformity in phase and amplitude characteristics would be extremely difficult.

The PCM system requires a fairly complex demodulator to correctly sort out the incoming data. In addition to bit synchronization, which tells the detector when to decide the value of an individual bit, there must be provision for determining the start of a word and the start of an m-word multiplex frame. Synchronizing the clock generators at all of the multiplexers is a problem comparable to LO distribution in an analog transmission system. Another complication would arise from the need to compensate for the relative phase shifts between the channels introduced by the serial nature of the signal transmission.

Considering the numerous shortcomings mentioned above, it is difficult to find merit in a TDM scheme for the feeder system of a large array such as the proposed Tee.

3.3 Frequency-Division Multiplexing

3.3.1 Basic System Design

A second possibility for the sharing of transmission lines is frequency-division multiplexing (FDM). A simple two-channel FDM system is illustrated in Fig. 3.3, in which adjacent array outputs are converted to different IF channels before addition of the signals in a power combiner. At the output end of the transmission line, the channels are separated by bandpass filters and the original frequency is restored by a second conversion. A practical system would likely differ from that shown in several respects. For example, the outputs of the second conversion could be at some appropriate second IF rather than at f_o , and the bandpass filtering might be deferred until after the second conversion, making all of the filters identical. These possibilities will be discussed after the preliminaries have been considered.

As in TDM, it is the bandwidth of the input filter which is the basic determining factor in the extent to which FDM can be implemented. The bandwidth governs the frequency separation needed between channels in order to maintain the inter-channel crosstalk below a given level. The situation is similar to that depicted in Fig. 3.1 if we now consider the responses shown to be those of two neighboring IF channels. As far as bandwidths and crosstalk levels are concerned, the relationships are the same as those discussed in Sec. 3.2; if we adopt the same criterion concerning excitation errors as before, the crosstalk level must again be held to -55 dB, as given by equation (3.3). We assume here, for simplicity, that each of the m channels receives equal crosstalk interference from two adjacent channels, with all other contributions

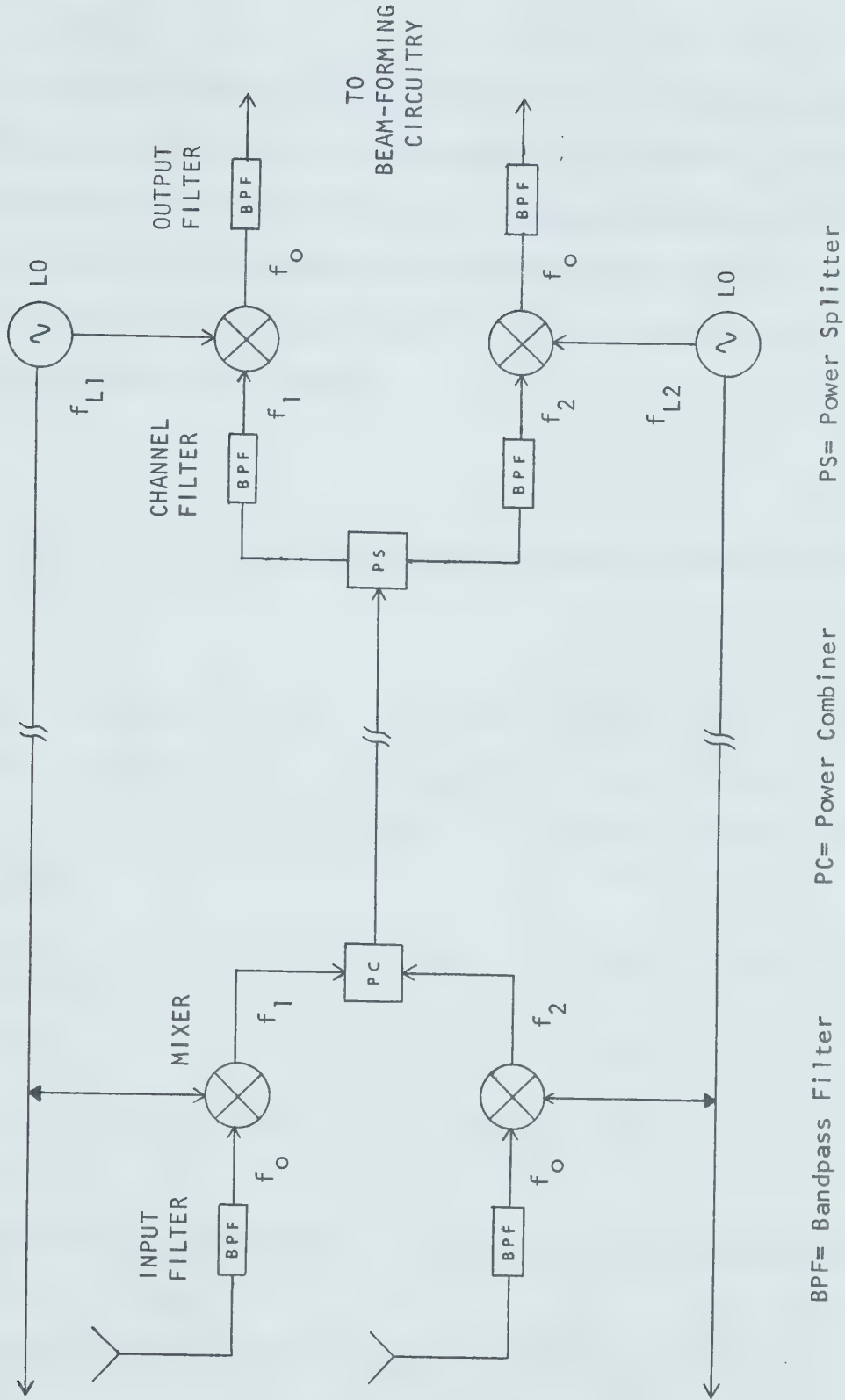


Fig. 3.3 Basic Two-Channel Frequency-Division Multiplex System

being negligible.

To meet the criterion of -55 dB inter-channel crosstalk levels, the channel separation must be approximately $B_{55}/2$, where B_{55} is the 55 dB bandwidth of the input filter as introduced previously. This and other pertinent data are summarized in Table 3.2 for a variety of possible input filter configurations [56],[61]. In each case, the 3 dB bandwidth has been set to 200 KHz.

Table 3.2 FDM System Parameters for Various Input Filters

Type of Filter	Number of Stages	Trans. Funct. Order	Bandwidth (MHz)			Minimum Channel Spacing $\approx B_{55}/2$	$f_{IF}(\text{min})$ (Note 1) $\approx B_{55}/4$	Possible Channels (Note 2) $m(\text{max})$
			B_3	B_{40}	B_{55}			
Double-Tuned (crit. coup.)	1	3	0.2	2.0	4.8	2.4	1.2	1 (1)
Double-Tuned (crit. coup.)	2	6	0.2	0.78	1.2	0.6	0.3	5 (3)
Butterworth	3	6	0.2	0.93	1.7	0.85	0.43	3 (3)
Butterworth	4	8	0.2	0.63	0.98	0.49	0.25	6 (4)

Note 1: From equation (2.40), $f_{IF}(\text{min}) \approx B_{52}/4$. Here we assume that

$$B_{55} \approx B_{52}.$$

Note 2: $m(\text{max}) = \text{greatest integer in } \frac{f_{IF}(\text{max}) - f_{IF}(\text{min})}{B_{55}/2} + 1.$

$f_{IF}(\text{max}) = 2.7 \text{ MHz}$, assuming 20 dB mixer conversion gain and the use of RG-62A/U cable. Figure in brackets is for a minimum IF of 1 MHz.

In the case of the one-stage double-tuned filter, the necessary channel separation exceeds the available range of $f_{IF}(\text{max}) - f_{IF}(\text{min})$, so that no multiplexing is possible if the crosstalk criterion is to be met. Adding a second double-tuned stage improves the picture markedly, as there is now sufficient frequency range to accommodate five channels; however, this would mean placement of the lowest-frequency channel in the vicinity of 300 KHz. At an IF this low, one is faced with the problem of transmitting a wideband (about two octaves) channel, leading to dispersion in the cables and other obstacles mentioned previously in Sec. 2.4.1. To reduce the problems related to wideband transmission, a lower bound of about 1 MHz will be placed on f_{IF} ; the results of doing so are shown in the table. The approximate upper bound of 2.7 MHz could be increased by adding preamplifier stages to the mixers if the added cost is warranted by the improvement in multiplexing capability. For example, an additional gain of 20 dB would raise the upper bound to about 5.5 MHz.

Having found that it is possible, in principle, to transmit several FDM channels on one transmission line, let us now examine in more detail some of the technical aspects of implementing such a system. Figure 3.4 shows a two-channel FDM system which differs in two respects from that shown in Fig. 3.3. One change is that all outputs of the second conversion are at some new frequency f_{iO} rather than the center frequency f_o . The reasoning behind this change lies in the presumption that a lower frequency output will facilitate further signal processing such as beam-forming; it may well be, however, that f_o would be a satisfactory choice. In any case, the additional hardware required for conversion to f_{iO} is quite small, consisting of a stable oscillator at

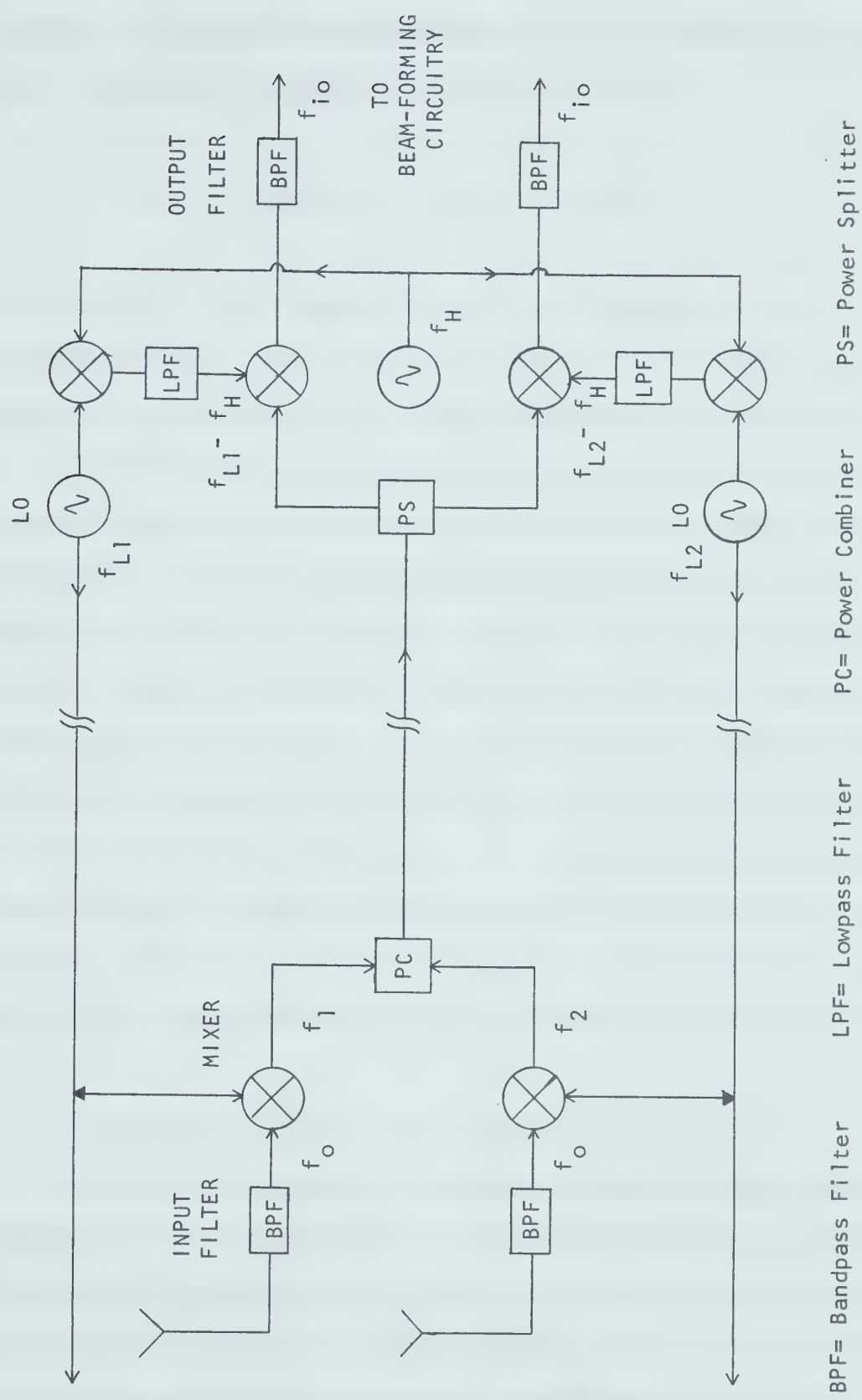


Fig. 3.4 Modified Two-Channel Frequency-Division Multiplex System

frequency f_H plus m mixers and lowpass filters for the entire array. The output frequency is determined by the relationship

$$f_{io} = (f_{LO} - f_H) - f_{IF} = f_o - f_H \quad (3.10)$$

The frequency of the heterodyne oscillator is therefore $f_H = f_o - f_{io}$, independent of f_{IF} . The second $L0$ is derived from the first such that changes in f_{L0} will not result in pointing errors (Sec. 2.4.6).

The second change appearing in Fig. 3.4 is the removal of the bandpass filters preceding the second conversion (hereafter referred to as channel filters to distinguish them from the input and output filters shown in the figure) which normally appear in an FDM system. The output bandpass filters then perform the dual function of demultiplexing and setting the system bandwidth. Since these filters are needed in any event, this implementation of FDM does not call for the addition of any new filters compared to the case of no multiplexing. Elimination of the channel filters is highly desirable because they are designed for m different center frequencies, which makes it particularly difficult to match their phase and amplitude characteristics from one channel to another.

To determine whether this is indeed a viable system of multiplexing, it is necessary to examine carefully the implications of allowing all of the IF channels to reach the second mixers undiminished in strength. The danger in allowing this to take place is that the intermodulation products generated in these mixers will result in severe crosstalk and hence excitation errors. This possibility will be considered in the next section.

In considering the second frequency conversion, one must again be aware of the need for image rejection. In converting a given IF channel to f_{iO} from f_{IF} , we also convert to f_{iO} any signal present at the image frequency $f_{IF} + 2f_{iO}$. According to the criterion for image rejection derived in Sec. 2.4.2, the signal level at this frequency should be down at least 52 dB relative to the level at f_{IF} . For convenience, we shall instead use -55 dB so that the figures compiled in Table 3.2 can be used in this evaluation. If the channels are closely spaced at less than twice the minimum allowable spacing of $B_{55}/2$, then the lowest image frequency meeting the requirement is approximately given by the upper -55 dB point of the highest-frequency channel. To make the relation more general, consider an m -channel FDM system with channels at center frequencies of f_1, f_2, \dots, f_m in ascending order of frequency. The minimum allowable value of f_{iO} is that which provides adequate image rejection in the conversion of f_1 to f_{iO} :

$$f_1 + 2f_{iO}(\text{min}) = f_m + \frac{1}{2} B_{55}$$

$$\text{or,} \quad f_{iO}(\text{min}) = \frac{1}{2} (f_m - f_1 + \frac{1}{2} B_{55}) \quad (3.11)$$

3.3.2 Crosstalk from Intermodulation Distortion

Our examination of TDM revealed that crosstalk will result from insufficient sampling rates and from variations in the amplitude-versus-frequency characteristic of the transmission medium. The second source proved to be much more difficult to handle than the first. Not surprisingly, the situation with FDM is analogous; one source of crosstalk, as we have seen in the previous section, is insufficient

channel spacing. A far more troublesome source of crosstalk is nonlinearity in the transmission medium.

The transfer characteristic of a device in the transmission path of the multiplexed signals can be expressed as a power series expansion of the output voltage V_o in terms of the input voltage V_i :

$$V_o = a_o + a_1 V_i + a_2 V_i^2 + a_3 V_i^3 \quad (3.12)$$

Nonlinearities of higher than third order seldom contribute significantly to the output if the operating region of the device being modeled is suitably chosen; the series is accordingly truncated at this point. In the present case, the DC term a_o is not of concern. Of the other terms, one generally wishes to minimize all but a_1 in an amplifier or passive element, and all but a_2 in a mixer.

Intermodulation (IM) distortion refers to all of the undesired outputs resulting from the nonlinear terms in equation (3.12). The IM products have frequencies and amplitudes bearing definite relationships to those of the input signals. The only devices in the FDM system which would be likely to have sufficient nonlinearity to cause IM problems are the second mixers, and it is the IM levels which will determine the feasibility of eliminating the channel filters which would normally precede these mixers. The question to be answered may be stated as follows: if the entire FDM spectrum is allowed to reach the mixer, can an IF output frequency f_{io} be found which is sufficiently free of IM products that tolerable crosstalk levels are not exceeded? The answer depends on the number and the placement of the channels, and on the properties of the mixer (i.e., the coefficients a_1, a_2, a_3).

In principle, given the spectral density of the input signal plus these coefficients, one can use the transfer function of (3.12) to determine the spectral density of the output. In practice, this is very difficult to do, except in the case where the input consists of a few discrete frequencies. In the classical treatment of IM distortion by Bennett [62], results for discrete frequencies are extended to continuous FDM channels by making certain assumptions such as considering each channel to have a rectangular spectrum. Other assumptions appropriate to telephone work such as intermittent channel usage are included, and the analysis does not consider mixers.

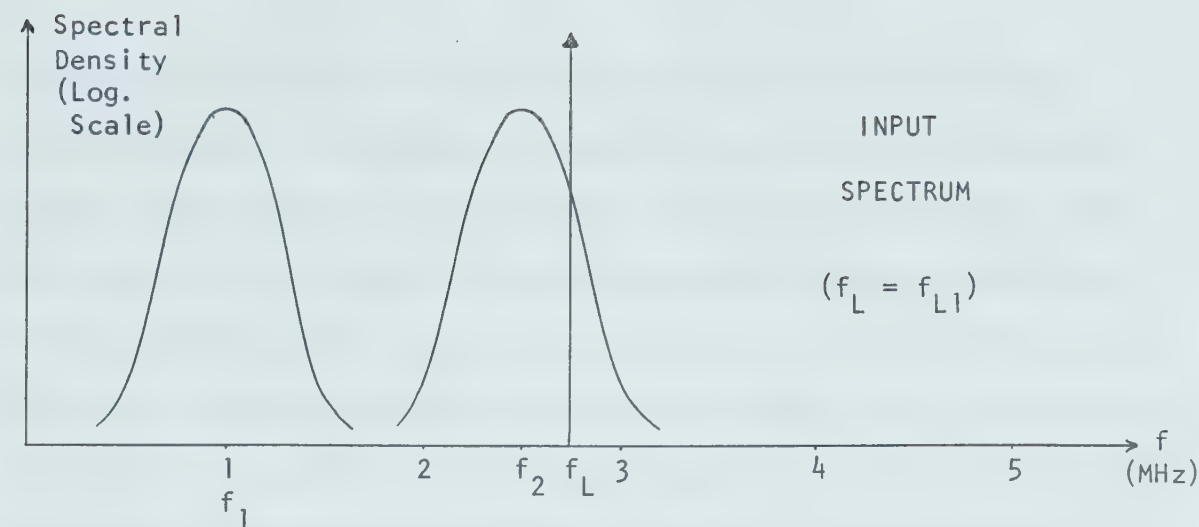
To illustrate the nature of the spectrum which one would find at the output of a second mixer when no channel filters are used, a simple two-channel case is depicted in Fig. 3.5. To keep the picture from becoming hopelessly cluttered, it is assumed that a two-stage double-tuned input filter precedes the first mixer, and that the IF channels centered on f_1 and f_2 are well separated in frequency. The channel frequencies are arbitrarily chosen, within the constraints discussed in the preceding section, to be $f_1 = 1$ MHz and $f_2 = 2.5$ MHz, and the IF output is set to $f_{i0} = 1.75$ MHz to avoid the first-order responses in the output. The LO is placed at $f_{L1} = f_1 + f_{i0} = 2.75$ MHz, as required for the demodulation of channel #1; a similar spectrum would exist in the other channel, where the LO needed is at $f_{L2} = 4.25$ MHz. The vertical extent of the spectra in Fig. 3.5 are roughly indicative of their relative spectral densities, but no attempt has been made to scale them accurately.

The figure clearly shows which IM products may be troublesome for this choice of frequencies, the significant responses being the second-

order ones at $f_2 - f_1$ (1.5 MHz) and $2f_1$ (2 MHz), and the third-order ones at $f_{L1} + f_1 - f_2$ (1.25 MHz) and $f_1 + f_2 - f_{L1}$ (1.5 MHz). None of the peaks fall within 250 KHz of f_{i0} , but the nearby responses are not greatly attenuated at this frequency. It is not difficult to visualize, using Fig. 3.5, the results of adjusting one or more of the variables; for example, if one were to shift f_1 and f_{L1} 250 KHz higher in frequency, f_{i0} would remain at 1.75 MHz but the second-order responses at $f_2 - f_1$ and $2f_1$ would shift to 1.25 MHz and 2.5 MHz respectively. This would greatly reduce the second-order interference, but at the expense of making the third-order interference from the products at $2f_2 - f_{L1}$ and $f_{L1} + f_1 - f_2$ worse. The net effect would likely be beneficial since the third-order products would be much weaker than the second-order products in a well-designed mixer.

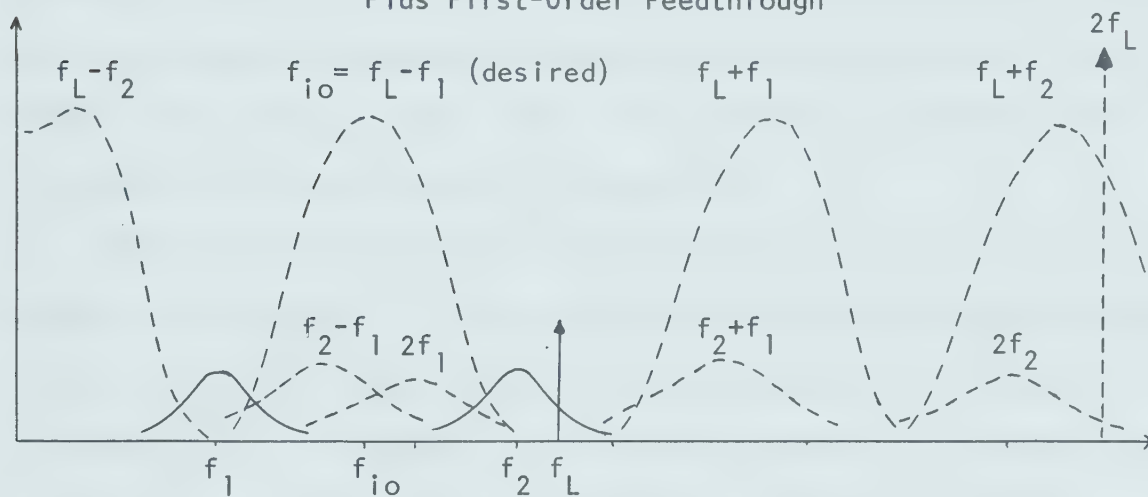
It should be noted that the IM situation may be quite different for the demodulation of channel #2. In this case we have a higher LO frequency; the second-order interference does not change appreciably from the previous case, but the troublesome third-order products at 1.25 MHz and 1.5 MHz are now removed to 2.75 MHz and 0.75 MHz respectively, and no new products appear near f_{i0} . The IM interference level will therefore be somewhat less in this channel.

The preceding example illustrates the difficulties inherent in an analytical approach to optimizing the choice of channel and output frequencies for minimum crosstalk. The picture worsens rapidly as the number of channels m increases; for large m , the total number of second-order products becomes proportional to $(m + 1)^2$ and the total number of third-order products to $(m + 1)^3$ [63]. As a result of this complexity, it is felt that an empirical approach involving simulation of the FDM



OUTPUT SPECTRUM: ALL FIRST- AND SECOND-ORDER PRODUCTS

Plus First-Order Feedthrough



OUTPUT SPECTRUM: ALL THIRD-ORDER PRODUCTS BELOW 5 MHz

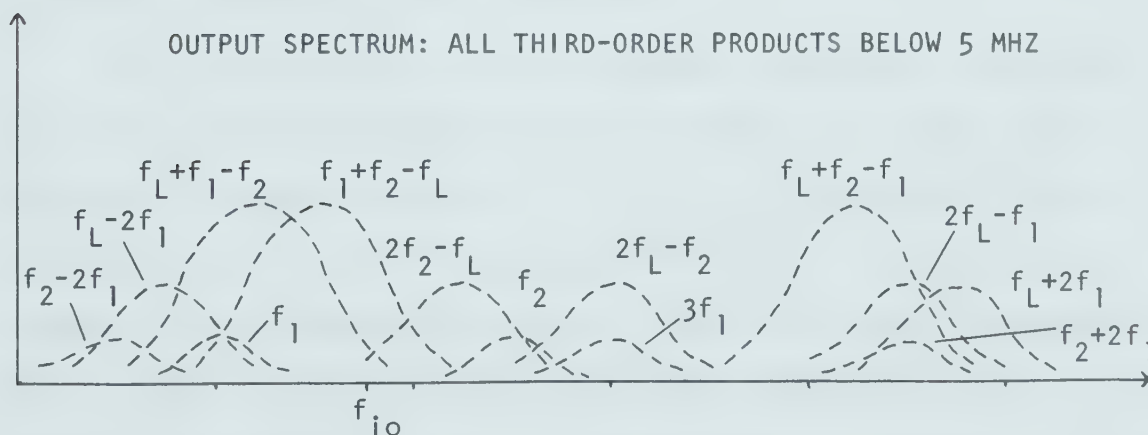


Fig. 3.5 Intermodulation Products of a Mixer

system is the best way to evaluate the IM interference levels. A possible method of simulation is shown in Fig. 3.6 for a two-channel system; the extension to larger numbers of channels is obvious. The noise generator and shaping filter simulate the output of the dipole antenna element, while the remainder of the test set-up resembles the actual FDM system. Replacement of the transmission line by an attenuator reflects the assumption that amplitude equalization will be included in the actual transmission system (see Sec. 3.3.5). The variables f_1 , f_2 , and f_L can be adjusted while the output spectrum is examined; it will be necessary to make provision for temporarily removing the signals in the undesired channels to observe the effect on the desired output. A channel filter can be inserted after the attenuator to determine the improvement in crosstalk that it can provide.

The measurement procedure described above is itself rather complex, since we have $m + 1$ variables to adjust, and the demodulation of each channel must be examined in turn for each choice of these variables (i.e., the channels are allocated, and then f_L is adjusted to produce the desired f_{i0} in each case). One can simplify the task somewhat by following certain guidelines:

(1) The frequencies can be selected to minimize interference from second-order IM products. Since in choosing f_{i0} we must avoid the first-order outputs centered on f_1, f_2, \dots, f_m which result from both the V_i and the V_i^3 terms of the transfer function, it would be helpful to arrange that the second-order products also fall on these frequencies. One can accomplish this by assigning channel frequencies which are harmonically related to that of the lowest-frequency channel (f_1). This will insure that all second-order products will appear at multiples of

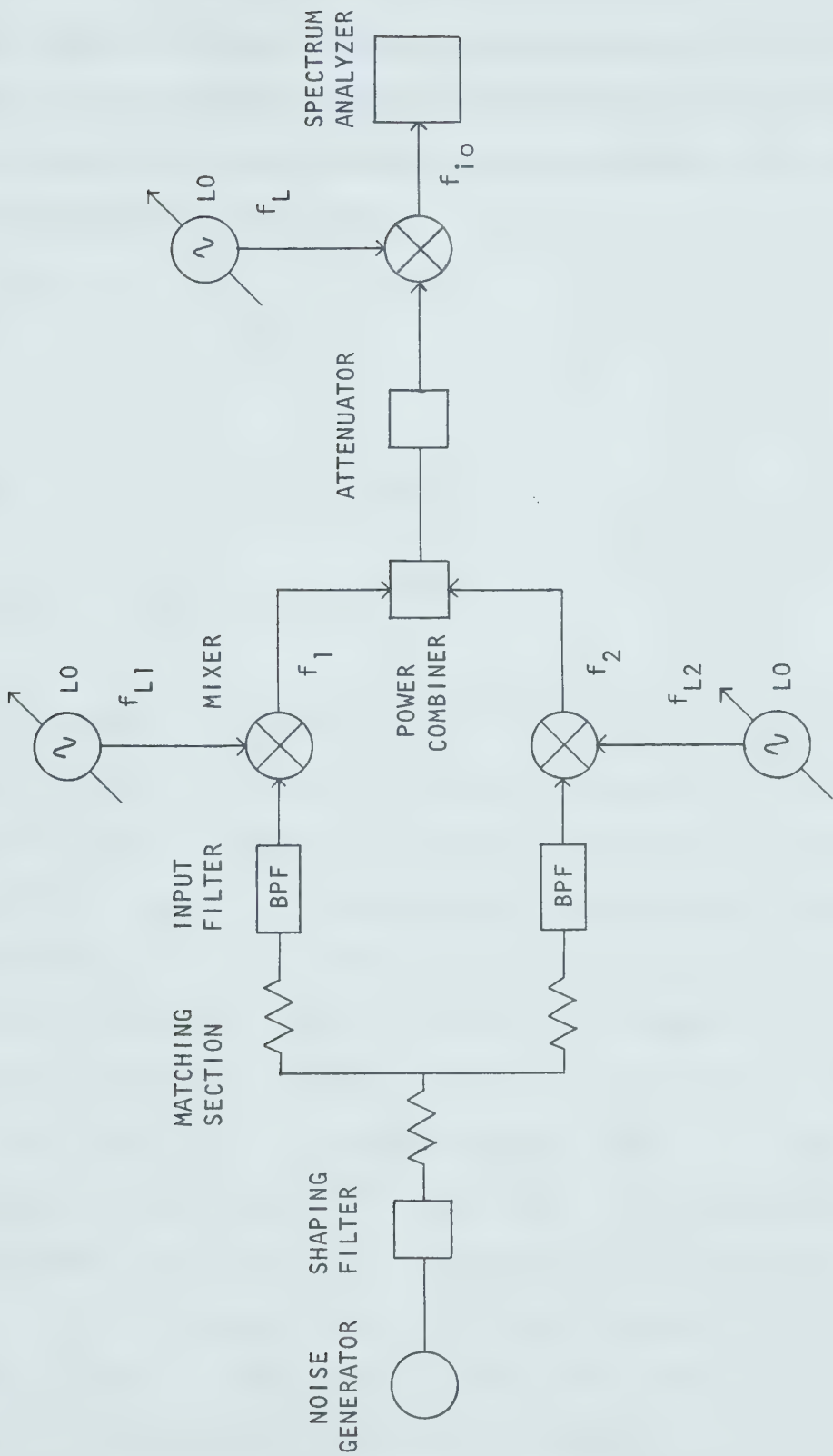


Fig. 3.6 Test Set-Up for Intermodulation Measurements

f_1 , leaving the inter-channel spaces relatively free of IM products other than third order. Assuming the assignment of $f_j = jf_1$ is adopted, the testing procedure is greatly simplified, since f_1 must be at least as large as the minimum channel spacing and there will be less latitude for adjustment of frequencies:

$$f_1 \geq \frac{B_{55}}{2}$$

and
$$f_m = mf_1 \leq f_{IF}(\text{max})$$

hence
$$\frac{B_{55}}{2} \leq f_1 \leq \frac{f_{IF}(\text{max})}{m} \quad (3.13)$$

If, for example, we take the case of $m = 4$ and a two-stage double-tuned input filter, we find from (3.13) that the bounds on f_1 are 600 KHz and 650 KHz under the assumptions upon which the figures in Table 3.2 were based. The testing is thus essentially reduced to the selection of f_{i0} for minimum IM crosstalk. The most serious drawback to this scheme of channel allocation is that it may call for placement of f_1 at a lower frequency than one would want from consideration of the problems involved in the transmission of a wideband channel. Even if it is not rigidly adhered to, the principle of harmonically relating the channel frequency assignments may prove useful in reducing the IM interference.

(2) The demodulation of the lowest channel at f_1 will tend to be the worst case in terms of IM crosstalk. The reason for this tendency is that this case involves the lowest LO frequency $f_{L1} = f_1 + f_{i0}$, which tends to concentrate the third-order products involving f_{L1} in the lower

part of the spectrum where we wish to place f_{i0} . Thus the crosstalk for this choice of f_L should be examined first, as it will likely be the best indicator of whether a given choice of f_{i0} is suitable.

Up to this point we have tacitly assumed that f_{i0} should be as low as possible, since the final bandpass filtering and (unless a third frequency conversion is performed) all other signal processing must be done at this frequency. It has not yet been established, however, what the optimum value of f_{i0} might be. Moderately high frequencies have been used for processing in other installations; in some, no frequency conversion is used (10 MHz and 22 MHz arrays at Penticton), and in others the final IF is quite high (5.5 MHz in the Molonglo Cross, 5 MHz in the Clark Lake Teepee Tee). In one sense, a high frequency is desirable since it results in a more narrowband signal; on the other hand, if one wishes to use active filter configurations and devices such as integrated operational amplifiers for the signal processing, a low frequency is essential.

The use of a high f_{i0} greatly increases the likelihood that channel filters can be dispensed with. It becomes much easier to avoid IM crosstalk because the majority of IM products are clustered around the original channel frequencies. If the choice of f_{i0} is restricted to frequencies above $3f_m$, which is highest-frequency IM product not involving f_L , then all first- and second-order products plus all third-order inter-channel products can be disregarded. In the spectrum between $3f_m$ and f_L there appear, in addition to the desired output at f_{i0} , only third-order products of the form $f_L - 2f_j$ and $f_L \pm f_j \pm f_k$; a census of these products shows that there are exactly m^2 such products in this range. For $m = 2$, the relevant products are $f_L - 2f_1$, $f_L - 2f_2$,

$f_L + f_1 - f_2$, and $f_L - f_1 - f_2$; by the simple expedient of setting $f_2 = 3f_1$, one can insure that the peaks of no IM products will fall within the range $f_{i0} \pm f_1$. The IM products are less easy to avoid for larger values of m , but one can see that the levels of IM interference are generally diminished for the higher-frequency choices of f_{i0} . One possible choice for f_{i0} is the center frequency f_0 ; in this case the same LO can perform both conversions, as was shown in Fig. 3.3. In view of its simplicity, this choice should be investigated first, followed by attempts to improve the IM crosstalk situation by selecting other frequencies for f_{i0} . The final choice will probably be influenced by decisions regarding the beam-forming techniques to be used.

3.3.3 Local Oscillator Distribution and Phase Equalization

A suitable LO distribution system for single-channel IF transmission was described in Sec. 2.4.5. The most obvious system for LO distribution in the FDM system is obtained by simply duplicating the single-channel arrangement for each additional channel. Other possible methods include the distribution of a single signal from which all of the necessary LO signals can be derived, or the transmission of all of the LO signals over the same line, to be separated by filters. The latter two methods call for the addition of a good deal of electronics in connection with the remote mixers, making excitation errors more difficult to control and, in general, making the transmission system unnecessarily complex. In the following work, the use of m independent distribution systems will be assumed.

Recalling that the basis of the single-channel distribution scheme was a feedback control system which adjusted the LO frequency to

keep the phase shift of the transmission line constant, we must now examine the consequences of having such frequency changes in the FDM system. Consider a signal at f_o which is down-converted to f_{IF} and transmitted by cable to the observatory; this signal will undergo a phase shift of

$$\phi(f, \tau) = 360f_{IF}\tau \quad \text{degrees} \quad (3.14)$$

where τ is the phase delay of the cable, which is generally a function of frequency (dispersion). As we have seen previously, we need not be concerned with the value of ϕ itself, since phase excitation errors result only from differential errors; that is, we are concerned with deviations from the mean value of ϕ over the ensemble of all IF channels.

In a single-channel system, changes in L0 frequency will have little effect on the differential phase errors. The input signal at f_o will be converted to some new value of f_{IF} , but the change is the same for all channels. Now consider two FDM channels with nominal center frequencies of f_j and f_k transmitted over the same cable as before; each will encounter a phase shift as given by (3.14), in which we assume for the moment that τ is independent of frequency. This means that if the two signals are initially in phase, after the second conversion they will be restored to the same frequency but with a relative phase shift:

$$\begin{aligned} \Phi(f_j, f_k) &= \phi(f_j) - \phi(f_k) \\ &= 360(f_j - f_k)\tau \end{aligned} \quad (3.15)$$

This phase shift must either be removed at some point or taken into account in the beam-forming circuitry. In either case, the process is complicated by the fact f_j and f_k are independent, and to a large extent unpredictable, functions of time. However, the difference $f_j - f_k$ is the same as the difference in the corresponding L0 frequencies, which are accessible for measurement. From equation (3.15) it can be seen that a differential phase error of 0.1° between the two channels will result from an error in measurement of $f_j - f_k$ of about 22 Hz, assuming a constant phase delay of 12.65 μsec for 2.5 km of coaxial line. Frequency measurement with errors of less than 1 Hz can be readily achieved using digital techniques, so that this aspect of compensating for the phase shifts would not present a serious problem.

Estimation of the phase delay poses a more difficult problem due to the limitations on measurement accuracy involved. The quantity we seek is the mean phase delay $\bar{\tau}$ taken over all of the transmission lines; phase errors caused by departures from this value in individual cables have been considered separately (Sec. 2.4.4) and are not of concern here. At the calibration temperature, $\bar{\tau}$ would be the phase delay of the reference cable against which all of the others are trimmed. At other temperatures, it would be necessary to find the mean delay by making a sizeable number of measurements. The phase shift of a length of cable can be measured on an absolute basis with an accuracy of about $\pm 0.3^\circ$ in the 1-10 MHz range [40]. In the light of what has just been discussed, this would be a reasonable estimate of the limits of accuracy with which one can determine the differential phase shift given by (3.15). In practice, dispersion in the cable must also be taken into consideration. This will be done in the following section.

Investigation of this matter of phase equalization between channels is of particular importance because the excitation errors which result from this source are systematic rather than random in nature. For example, the distribution of phase errors for the elements whose outputs are transmitted at f_j will be displaced from the distribution for elements using the channel at f_k by an amount which depends on the success of the equalization. The periodicity of this error pattern throughout the array could give rise to serious grating sidelobes rather than just an increase in overall sidelobe level. This effect could be reduced by randomly assigning the channel numbers within each group of array outputs to be multiplexed, which would tend to break up the regular error patterns resulting from an orderly channel assignment.

3.3.4 Dispersion in the Transmission Lines

The phase velocity in the transmission lines, which determines the phase delay τ , has thus far been considered to be independent of frequency. This is a reasonable assumption over the narrow bandwidth of a single channel, but it may not be safe to make this assumption when considering widely-separated FDM channels.

The velocity of propagation in a coaxial cable is, in fact, a slowly increasing function of frequency [64]. This effect, called anomalous dispersion, extends up to microwave frequencies for most cables and results in a decrease in phase delay with frequency. Extrapolation of measurements at higher frequencies [37] indicates that the phase delay of RG-213/U may vary about 1% between 1 MHz and 3 MHz. There is considerable uncertainty about the exact values, but even dispersion an order of magnitude smaller than this could not be ignored.

Equation (3.15) must therefore be revised to include the effect of dispersion on the differential phase shift:

$$\Phi(f_j, f_k) = 360[f_j\tau(f_j) - f_k\tau(f_k)] \quad (3.16)$$

To retain accuracy of phase equalization of the order mentioned in the previous section, it will probably be necessary to measure the mean phase delay separately for each channel. Since the equalization must adapt to changing conditions such as temperature, it is essential that it be automatically controlled. If the beam-forming circuitry is controlled by a digital computer (this is highly probable in view of the complexity of the proposed array), real-time measurements of phase delays and LO frequencies could be included as inputs to the program which determines the settings of the phase shifters for a given source direction. Another possibility for automatic equalization would be a phase error compensation system which works within the feeder system; this will be investigated in Sec. 5.1.

3.3.5 Amplitude Equalization

In addition to the differential phase shifts encountered in the FDM system, one must also be prepared to compensate for the differences in cable attenuation at the different channel frequencies. The problem is more complicated than it appears at first glance, since the attenuation change over each channel's bandwidth must be taken into account. In single-channel operation the response of the cable, although not flat, is the same for each transmission path, so that the relative amplitudes of the element excitations are preserved over the bandwidth.

However, when we have an FDM transmission system, the slope of the attenuation characteristic is different for each channel. This means that simply equalizing the center-of-channel attenuations may not be sufficient.

To illustrate the nature of the equalization problem, consider two channels with 200 KHz bandwidth centered on 1 MHz and 2.5 MHz. The attenuation of a 2.5 km run of RG-62A/U cable for these frequencies is given in Table 3.3. There is a difference of 11.6 dB in the attenuation at the channel centers, but if we attempt to equalize the channels by inserting 11.6 dB of attenuation into the 1 MHz channel, there remains a discrepancy of 0.4 dB at the band edges. Of course, the error becomes less nearer the channel centers, and most channels in the FDM system will not be separated in frequency as much as these two hypothetical ones are. The r.m.s. amplitude error caused by the discrepancies would likely be about 0.1 dB in practice. Errors of this magnitude might be

Table 3.3 Cable Attenuation (dB) for Two Typical IF Channels

Channel	Frequency (MHz)		
	$f_{IF} - 0.1$	f_{IF}	$f_{IF} + 0.1$
Channel #1 ($f_{IF} = 1$ MHz)	19.0	20.0	21.0
Channel #2 ($f_{IF} = 2.5$ MHz)	31.0	31.6	32.2
Channel #1 after band-center equalization	30.6	31.6	32.6

tolerable, but they are quite large compared to most of the other errors present in the transmission system, and it would be preferable to reduce them if it is at all possible to do so. Like the differential phase errors discussed in Sec. 3.3.3, these amplitude errors are systematic in nature and could lead to more serious sidelobe problems than if they were randomly distributed.

Rather than attempt to design separate equalizers for each channel, it is likely best to equalize the cables over the full FDM spectrum to produce a flat attenuation characteristic. A method of cable equalization using networks (RC) having alternating poles and zeros on the negative real axis of the complex frequency plane has been described by Mackay [36]. These equalizers are designed around transistor amplifier stages in order to produce gain which exactly balances the cable attenuation, but in the present case it is not desirable to have active devices in the FDM transmission medium because of possible IM distortion problems. Instead, we require a passive equalizer at the output of each transmission line to bring the attenuation up to the same level for all channels; in other words, a highpass filter must be created such that when it is placed in cascade with the cable, an allpass characteristic over the FDM spectrum results.

The number of pole-zero pairs needed in the equalizer is a function of the extent of the frequency range covered and the maximum cable attenuation within the range, and of the amount of amplitude ripple permissible in the equalized characteristic. For example, a cable having 10 dB attenuation at f MHz can be equalized over the decade from $0.1f$ to f with a maximum ripple of about 0.005 dB if two correctly chosen pole-zero pairs are used. Since ripple in the attenuation

characteristic between the channels is of no concern, the choice of pole and zero locations could probably be further optimized for a particular allocation of channels. The equalizer as described here would not adapt to changes in cable attenuation such as those caused by temperature variations (Sec. 2.3.2a). The possibility of automatically compensating for such changes will be considered in Sec. 5.1.

3.3.6 Summary

The FDM approach has been shown to be a more practicable form of multiple use of transmission lines than TDM for this particular array design. The number of channels possible depends on a number of variables, including the 55 dB bandwidth of the input filter, the power gain of the pre-transmission electronics, the type of cable used, the IM performance of the second mixer, and the cost of implementation. Most of these factors have not yet been firmly ascertained.

Phase and amplitude equalization is a vital part of the FDM system, and the viability of the system rests to a large extent on whether adequate equalization can be provided at reasonable cost. Equalization will be discussed further in the remaining chapters.

Before leaving the topic of FDM systems, it should be noted that the nearly square-law transfer characteristic of the field-effect transistor yields considerably lower IM product levels in mixer service than does the exponential characteristic of the bipolar transistor [65]. The performance of dual-gate MOSFET devices [66] is particularly good in this regard, and they offer additional advantages such as isolation of the local oscillator from the signal channel.

3.4 Quadrature Multiplexing

3.4.1 Basic System Design

A third possibility for multiplexing in the feeder system is quadrature multiplexing (QM), also known as quadrature-carrier or phase-division multiplexing. The system is illustrated in Fig. 3.7; it may be used alone as a two-channel system, or in conjunction with an m -channel FDM system to provide $2m$ channels. The QM technique is not widely used, but it has found application in telemetry [67],[68] and color television transmission.

The principle behind QM is that two signals which overlap in the time and frequency domains may still be transmitted over the same medium without crosstalk if they are first processed by means of multiplication by orthogonal signals. In the case of Fig. 3.7, the transformation is applied by inserting a 90° phase shift in the L_0 line to one of the first converters. If the input signals to these converters are $s_1(t)$ and $s_2(t)$, the composite signal entering the transmission line may be expressed in the form

$$S(t) = s_1(t) \cos \omega_{L_0} t + s_2(t) \sin \omega_{L_0} t \quad (3.17)$$

This signal, after being delayed by an amount τ in the transmission line, is demodulated in the cosine channel by multiplication by a second L_0 signal of $\cos \omega_{L_0}(t-\tau)$. The output signal $S(t-\tau) \cos \omega_{L_0}(t-\tau)$ contains only $s_1(t-\tau)$ plus terms in $2\omega_{L_0}$ which are removed by filtering; similarly, the sine channel has an output of $s_2(t-\tau)$.

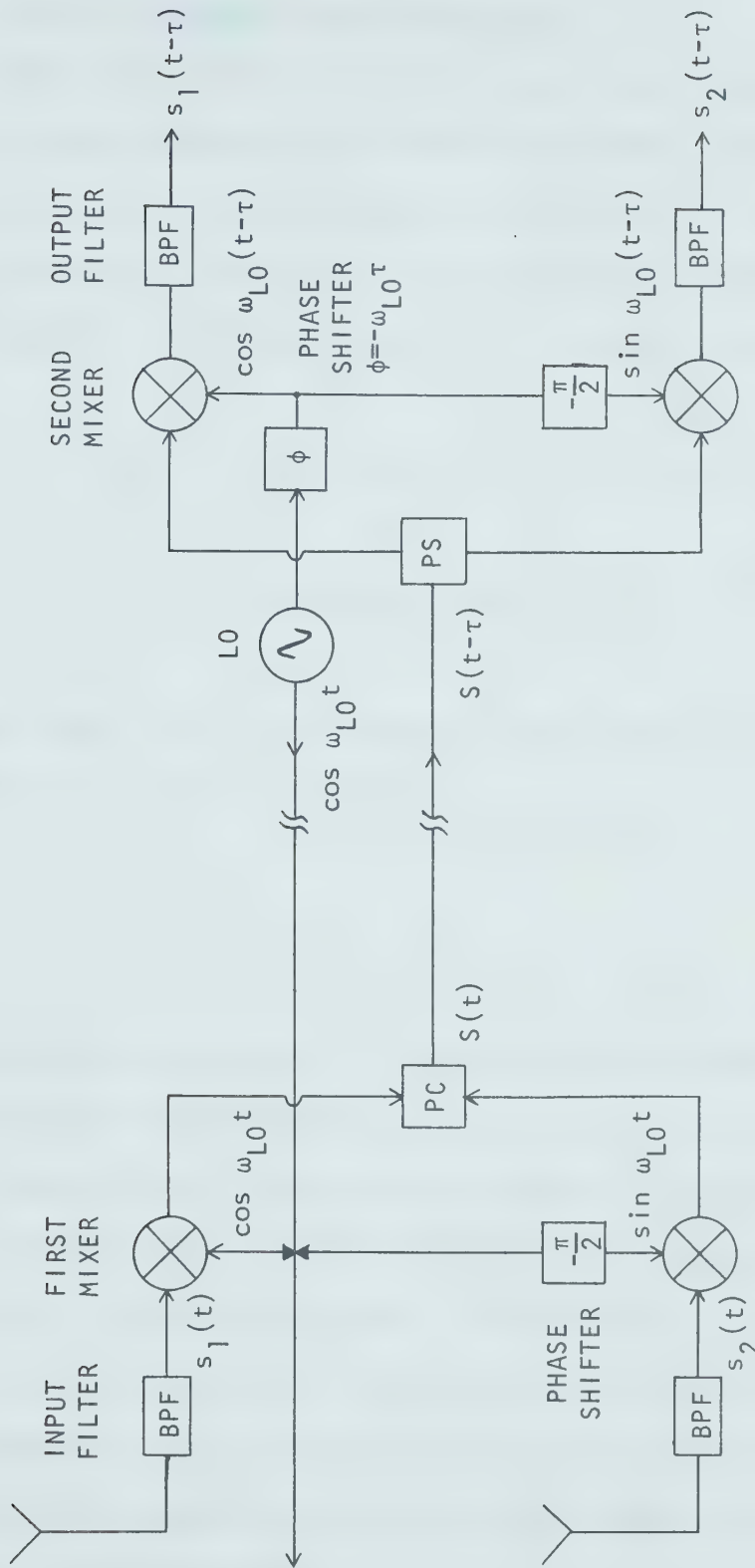


Fig. 3.7 Quadrature Multiplexing System

3.4.2 Crosstalk from Phase Errors

Departures from the ideal QM system just described will occur in practice, and crosstalk is the inevitable result. Suppose that in the demodulation of the cosine channel the L0 signal is now given by $\cos[\omega_{L0}(t-\tau) + \phi_e]$, where ϕ_e is the phase error in radians. The channel output $S_o(t) = S(t-\tau) \cos[\omega_{L0}(t-\tau) + \phi_e]$ becomes, after filtering,

$$\begin{aligned} S_o(t) &= s_1(t-\tau) \cos \phi_e + s_2(t-\tau) \sin \phi_e \\ &\approx s_1(t-\tau) + \phi_e s_2(t-\tau) \end{aligned} \quad (3.18)$$

provided that $\phi_e \ll 1$. The crosstalk coefficient α_p is therefore numerically equal to the phase error:

$$\alpha_p \approx |\phi_e| \quad (3.19)$$

This expression also holds for the sine channel; however, the phase error ϕ_e , which results from errors in the L0 distribution system or in the 90° phase shifters, may differ between the two channels.

The phase errors must clearly be tightly controlled, since they lead directly to excitation errors. To evaluate the latter, we let $s_1(t) = V_o \cos \omega_o t$ and $s_2(t) = V_o \cos(\omega_o t + \xi)$, where ξ is a phase factor which depends on the source direction and the spacing between the elements whose outputs we are multiplexing. The output of the cosine channel is then proportional to

$$S_o(t) = V_o \cos \omega_o(t-\tau) + \phi_e V_o \cos[\omega_o(t-\tau) + \xi] \quad (3.20)$$

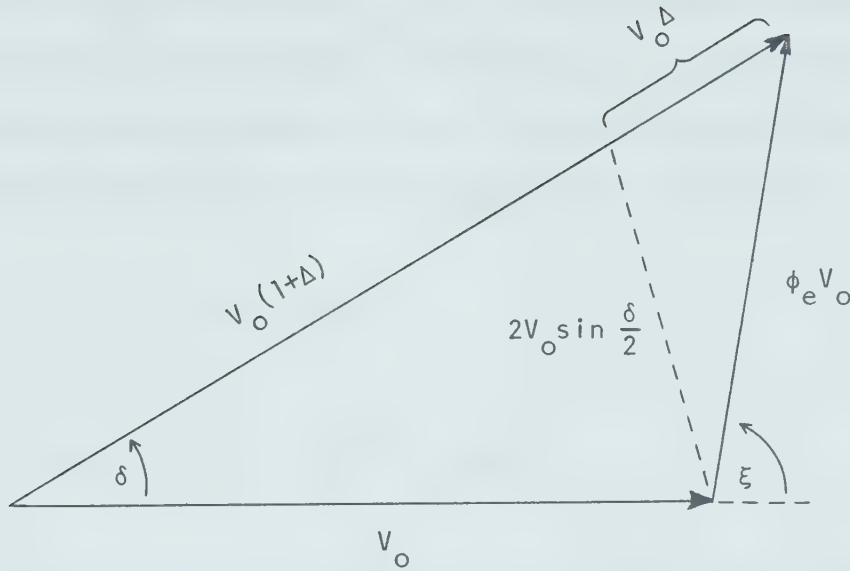


Fig. 3.8 Phasor Representation of QM Crosstalk

A phasor representation of equation (3.20) is shown in Fig. 3.8, with the error in the output signal expressed in terms of a phase error δ and a fractional amplitude error Δ . If $\phi_e \ll 1$, then $\delta \ll 1$ and

$$\begin{aligned}
 (\phi_e V_o)^2 &\approx (V_o \Delta)^2 + (2V_o \sin \frac{\delta}{2})^2 \\
 &= V_o^2 (\Delta^2 + \delta^2)
 \end{aligned}
 \tag{3.21}$$

From (3.21) we can determine that the sum of the mean-square amplitude and phase errors is

$$\overline{\Delta^2} + \overline{\delta^2} = \overline{(\phi_e)^2}
 \tag{3.22}$$

In Sec. 1.3.3 it was stated that overall r.m.s. excitation errors of the order of $\Delta_{\text{rms}} = 0.02$ and $\delta_{\text{rms}} = 1^\circ$ (0.017 radians) would be needed to ensure adequate sidelobe performance in the array. The sum of the mean-square errors is then 7.1×10^{-4} ; we must require that the contribution given by (3.22) is much smaller than this maximum value:

$$\overline{(\phi_e)^2} \ll 7.1 \times 10^{-4}$$

$$\text{or, } (\phi_e)_{\text{rms}} \ll 2.7 \times 10^{-2} \quad (1.5^\circ) \quad (3.23)$$

This is a fairly stringent requirement, but it could likely could be met without great difficulty if the L0 distribution system outlined in Sec. 2.4.5 is used.

3.4.3 Crosstalk from Amplitude Errors

In the preceding analysis of the QM system, the amplitude characteristic of the transmission medium was not considered. A thorough analysis of the system must take cognizance of the fact that signals of the form $s_1(t) \cos \omega_{L0}t$ and $s_2(t) \sin \omega_{L0}t$ are composed of sum and difference terms, and these signals will lose their orthogonality if the terms are attenuated unequally. To show this, we again let the input signals be $s_1(t) = V_o \cos \omega_o t$ and $s_2(t) = V_o \cos(\omega_o t + \xi)$; substituting into equation (3.17), we have

$$\begin{aligned} 2S(t) = & V_o \{ \cos(\omega_{L0} - \omega_o)t + \cos(\omega_{L0} + \omega_o)t \} \\ & + V_o \{ \sin[(\omega_{L0} - \omega_o)t - \xi] + \sin[(\omega_{L0} + \omega_o)t + \xi] \} \end{aligned} \quad (3.24)$$

Now suppose that the terms in $(\omega_{L0} - \omega_o)$ are attenuated in transmission by a factor A_d , with the terms in $(\omega_{L0} + \omega_o)$ attenuated by a different factor A_s . Assuming the transmission line is dispersionless and has propagation delay τ , the cosine channel can be demodulated without phase errors by using the L0 signal $\cos \omega_{L0}(t-\tau)$. The result, after filtering, is

$$4S_o(t) = V_o \{ (A_d + A_s) \cos[\omega_o(t-\tau)] - (A_d - A_s) \sin[\omega_o(t-\tau) + \xi] \} \quad (3.25)$$

We can again evaluate the crosstalk by using a phasor representation of the output signal similar to that of Fig. 3.8, and deriving an expression analogous to (3.21). Taking the magnitudes of the desired output and of the crosstalk term from equation (3.25), we find that the excitation errors, provided that they are small, are approximately given by

$$\overline{\Delta^2} + \overline{\delta^2} = \overline{(\alpha_A)^2} \quad (3.26)$$

where α_A is an amplitude crosstalk coefficient given by

$$\alpha_A = \left| \frac{A_d - A_s}{A_d + A_s} \right| \quad (3.27)$$

To gauge the effect of attenuation imbalance on crosstalk, we shall determine the amount of imbalance which will result in errors in a particular channel being equal to the level given in Sec. 1.3.3 as a guideline for overall r.m.s. error. Setting the left-hand side of equation (3.26) to 7.1×10^{-4} in accordance with this guideline, and

making use of (3.27), we have:

$$A_d/A_s = 1.06 \quad (0.5 \text{ dB}) \quad (3.28)$$

assuming that the attenuation is greater at the sum frequency than at the difference frequency.

It is apparent from (3.28) that the attenuation of the transmission line must differ by no more than a fraction of a decibel at the sum and difference frequencies. Since these frequencies are separated by $2\omega_o$ or $2\omega_{L0}$ (whichever is the smaller), the QM technique is best suited to situations in which ω_o is small (e.g., audio signals), or in which a high IF comparable to ω_o can be used. Unfortunately, neither situation pertains in the present case.

To relate this result more directly to the application of multiplexing in the feeder system, we consider as an example the conversion to a typical IF of 1 MHz; the L0 will be at (12.36 ± 1) MHz, the upper value being preferred for reasons of image rejection. The sum terms will thus be centered on 25.72 MHz. For a 2.5 km run of RG-62A/U cable, the attenuation at 1 MHz would be about 21 dB; at 25 MHz it would be about 124 dB. Such a large disparity would result in negligible separation between the two channels.

Although equalization of the attenuation characteristic of the cable is possible and is widely used in communication systems, it would not be feasible to equalize differences of the order of 100 dB, particularly when most of the equalization must take place before transmission (due to noise problems). We must accordingly reject QM as a possible adjunct to FDM in a multiplexed feeder system.

CHAPTER 4

ASSESSMENT OF ARRAY EXCITATION ERRORS

In the following sections, the various components of the signal transmission and processing systems will be examined from the point of view of excitation errors. Individual error estimates will be compiled and used to estimate the overall excitation errors for the proposed array. These data will then be used in Chapter 5 in the investigation of compensation systems and the effect of the errors on the sidelobe levels.

4.1 The Remote Electronic Components

The electronic components at the remote ends of the transmission lines are of particular concern with regard to excitation errors, since they will be exposed to large variations in environment. Provision of suitable enclosures should minimize moisture effects, but it does not appear to be feasible to stabilize the ambient temperature of each unit. Arrangements similar to the thermostatically-controlled ovens used to stabilize crystal oscillators may be worth investigating, however.

4.1.1 The Input Bandpass Filter

Some of the characteristics of possible input bandpass filters were summarized in Table 3.2. Ideally, we would like to have a filter with a very sharp cut-off characteristic beyond the 200 KHz passband; this would prevent cross-modulation from out-of-band signals and would

permit the closest spacing of FDM channels. This requirement runs counter to the one for low excitation error levels, which calls for simple, easily duplicated filters with gentle phase slopes.

The double-tuned filter configuration suggests itself as an effective compromise between the conflicting requirements just mentioned. In Sec 3.3.1 we saw that one double-tuned stage would be inadequate for FDM purposes, but that the two-stage filter offered considerably improved performance. One drawback to this design is the need to place a stage of amplification between the two filter stages for isolation, since each resonant circuit must be coupled to only one other. Having only one stage of filtering ahead of it, this preamplifier will be quite susceptible to cross-modulation problems. The other major shortcoming of the double-tuned filter is the difficulty in controlling the coefficient of coupling. Small discrepancies in the coupling may cause a pair of filter units to appear identical in amplitude response in spite of considerable differences in phase response. It was for this reason that this type of filter was rejected in favor of the Butterworth filter (sixth-order) for use in the Molonglo Cross array [69].

The Butterworth configuration has the advantage of a flat amplitude response in the passband, and it would probably be one of the easiest filter characteristics to reproduce accurately amongst a large number of units. Its principle shortcoming, compared to the double-tuned filter, would likely be a greater insertion loss. Since its 3 dB bandwidth is only 1.6% of its center frequency, the 200 KHz bandwidth filter under consideration here is a rather narrowband case, and the components must therefore have very high Q factors if insertion losses are to be held within reasonable limits. Inductors with sufficiently

high Q to reduce the insertion loss to negligible proportions are not available. Measurements made by the author on various types of air-core inductors at 12 MHz revealed unloaded Q factors that were generally in the range from 200 to 300; to restrict the insertion loss to less than 1 dB, on the other hand, would require Q factors greater than 1200 for the sixth-order Butterworth filter [70]. If $Q_u = 250$ is chosen as a realizable unloaded Q factor in this instance, the insertion loss becomes about 6.4 dB for the sixth-order Butterworth and 10.6 dB for the eighth-order Butterworth. This loss must be taken into account in the system noise calculations and the criterion for maximum cable attenuation given by equation (2.14) modified accordingly by subtraction of the insertion loss.

Exact specification of the input filter must await further study of the transmission system; in particular, an experimental mock-up of a multiplex group is needed to simulate and investigate the feasibility of the FDM system proposed in the last chapter. Anticipating a favorable outcome of the FDM system study, we shall tentatively specify an eighth-order Butterworth input filter, which would allow inter-channel spacing of about 0.5 MHz. In view of the insertion loss estimated above, the allowable cable attenuation at the highest-frequency channel would then be approximately given by

$$A_{\max} \approx G_p + G_c \quad (\text{dB}) \quad (4.1)$$

where G_p = power gain of the preamplifier stage (if any), dB

G_c = conversion power gain of the first mixer, dB

This sets the value of $f_{IF}(\max)$.

In addition to the FDM study, another factor which could influence the choice of filter type is the possible implementation of a phase compensation system, as described in Sec. 5.1. Substitution of a filter having a linear phase (flat group delay) characteristic for the Butterworth filter might permit more accurate phase compensation over the full bandwidth. Such a substitution, assuming that the order of the filter remains the same, would result in a poorer attenuation figure for a given bandwidth but lower insertion loss. For example, if the eighth-order Butterworth filter is replaced by a maximally flat delay (Bessel) filter of the same order, B_{55} is increased by about 50% but the insertion loss drops from 10.6 dB to 4.9 dB [70].

Having made a tentative specification of an eighth-order Butterworth input filter, we must now ask how large the phase and amplitude errors arising from this filter might be. Since the filter contains four resonant circuits, it is evident that considerable effort will have to be expended to minimize these errors. All inductors should be air-core, since the permeability of most other core materials is quite sensitive to temperature; the use of commercial coil stock would insure good uniformity amongst the inductors. The capacitors would likely be a combination of air-spaced trimmers and NPO (zero temperature coefficient) ceramic types. One filter should be chosen as a standard and all of the others matched as closely as possible to it in phase and amplitude characteristics. For this and other test procedures, the remote electronics should be assembled as a unit, with suitable terminations provided.

The question of how closely the individual filter characteristics can be matched is not an easy one to answer. As a starting point, we

shall consider the accuracies obtainable at a single frequency in the passband when the filters are initially tested. Since a relative, rather than absolute, measurement is needed, the accuracies obtainable are generally very good.

The classical method of gain or loss measurement consists of supplying the same sinusoidal input signal to the reference network and to the network being adjusted, and observing their relative outputs with a suitable detector such as an oscilloscope with differential inputs. When performed carefully, measurements made in this fashion can routinely achieve amplitude matching to within ± 0.01 dB ($\pm 0.14\%$ in voltage gain) [71].

Accurate phase measurement is not so easily realized; instruments such as oscilloscopes and vector voltmeters typically have accuracies of about $\pm 1^\circ$ when used for this purpose. However, phase comparators have been designed [72],[73] which can measure relative phase with an accuracy of $\pm 0.01^\circ$. In one such instrument [73], the signals to be compared are down-converted to a frequency in the audio range and then applied to zero-crossing detectors. The time interval between the zero crossings is measured using an electronic counter with multi-period averaging, and the result is then converted into phase difference.

In practice, the matching of filter characteristics must include the entire passband rather than just a single frequency, and the overall accuracies obtainable will inevitably be considerably less than those given above. Some method of sweep testing by which the phase and amplitude characteristics over the full bandwidth could be examined would be preferred to the single-frequency measurements; this might take the form of a network analyzer which alternately displays the

response of the reference filter and of the filter being compared to it.

In addition to the difficulties associated with initially duplicating the response of the reference filter, one must consider the increase in errors which will take place after the filters are put into service. The causes of this increase include imperfect temperature compensation, component aging, and differences in the impedances of the array elements due to mutual coupling (see Sec. 4.7.2). The r.m.s. excitation error estimates must therefore be much larger than the single-frequency measurement errors. The following estimates should be sufficient to include all sources of error in the input filters:

$$\Delta_{\text{rms}} = 0.01 \quad (0.086 \text{ dB departure from nominal value})$$

$$\delta_{\text{rms}} = 0.5^\circ \quad (4.2)$$

4.1.2 The Preamplifier/Mixer and Local Oscillator

The first mixer and any associated preamplifier stages will be considered here as a unit. Due to its high input impedance and good mixer characteristics, the MOSFET appears to be the most suitable device available for use in these stages. The gain of the MOSFET stages, including the conversion gain of the mixer, depends on the device transconductance, which must be stabilized against temperature changes. The transconductance of a typical dual-gate MOSFET designed for mixer service, the 3N141, exhibits a nearly linear change with temperature of about $-40 \mu\text{mho}/^\circ\text{C}$. As pointed out in Sec. 2.3.2(b), this variation can be virtually eliminated by deriving the gate #2 bias from a suitably chosen resistor network containing a thermistor [41].

The problem remains of compensating for variations in the transconductance from one device to the next; the range from maximum to minimum encountered in inexpensive devices such as the 3N141 may be as much as three-to-one. Some selection of devices would be necessary to reduce this range to more manageable proportions, with further matching accomplished by trimming the gain of the preamplifier stages or adjusting an attenuator at the output of the mixer. The matching operation would proceed as described for the input filter in the previous section; it may in fact be possible to consider all of the remote electronics as a unit for matching purposes. Certainly a comparison of the entire unit to a standard should constitute a final test, if not the full matching procedure.

Phase shift introduced by the preamp/mixer due to a reactive component in the transconductance of the MOSFETs will be quite small (of the order of 10° at 12 MHz, judging from device data sheets). It is not known whether this parameter varies significantly with temperature or manufacturing variations. The latter can be compensated for in the matching operation, but we must make some allowance, say 0.1° , for temperature variations and component aging. The gain of each preamp/mixer can be trimmed to within 0.01 dB of that of the standard, but the r.m.s. error will be estimated as 0.05 dB to allow for these same factors:

$$\Delta_{\text{rms}} = 5.8 \times 10^{-3} \quad (0.05 \text{ dB})$$

$$\delta_{\text{rms}} = 0.1^\circ \quad (4.3)$$

Phase and amplitude errors in the mixer stage can also result from another, independent, source: the L0 system. As discussed in Sec. 2.4.5, supplying each mixer with exactly the same phase and amplitude of L0 signal is quite difficult when the mixers are separated by large distances. The magnitude of phase errors in the L0 distribution system should be approximately the same as those resulting from measurement errors in the main transmission lines (see the following section), since both systems will likely be set up using some variant of the Swarup and Yang technique. The estimate for phase errors from this source is consequently set to

$$\delta_{\text{rms}} = 0.1^{\circ} \quad (4.4)$$

This value is to be maintained after the initial adjustment by the feedback scheme described in Sec. 2.4.5.

Since the conversion gain of the mixer is proportional to the L0 injection voltage, this voltage must be the same at each mixer and must be stabilized against temperature variations. In the proposed L0 distribution system, the attenuation suffered by the L0 signal varies from one mixer to the next, and the differences must be equalized at each mixer by an attenuator. The temperature coefficient of the attenuators must match that of the L0 line if equalization is to be maintained over the temperature range. With care, one should be able to reduce the r.m.s. variation in L0 voltages to the order of 0.05 dB. The same figure will apply to the amplitude excitation error:

$$\Delta_{\text{rms}} = 5.8 \times 10^{-3} \quad (0.05 \text{ dB}) \quad (4.5)$$

assuming that the mixer conversion gain is directly proportional to LO voltage [65].

4.2 The Transmission Lines

4.2.1 Measurement Errors

Limitations in the accuracy of measurement techniques establish the lower bound on phase and amplitude errors arising in the transmission lines. As pointed out in Sec. 2.3.2(e) on cable trimming, the Swarup and Yang technique can be used to match the phase shift of a cable (in the 3-30 MHz range) to within $\pm 0.1^\circ$ of that of another cable chosen as the standard. After completion of phase trimming, one would expect to find the phase shifts of the transmission lines to be normally distributed about the phase shift of the standard. If 0.1° is taken as the standard deviation of the distribution, this becomes the estimate of r.m.s. phase error:

$$\delta_{\text{rms}} = 0.1^\circ \quad (4.6)$$

As far as amplitude errors are concerned, we are faced with equalization of small differences in attenuation from one cable to another, plus larger differences between FDM channels. The methods used to achieve this would probably be similar to those used in the LO distribution system, and we shall accordingly adopt the same estimate for amplitude errors, namely

$$\Delta_{\text{rms}} = 5.8 \times 10^{-3} \quad (0.05 \text{ dB}) \quad (4.7)$$

4.2.2 Phase and Amplitude Stability

Variance in phase-temperature coefficients, which was discussed extensively in Chapter 2, is likely to be the major source of excitation errors caused by deficiencies in the transmission lines. We shall proceed under the assumption that RG-62A/U cable will be used, since this type offers the best combination of low attenuation and good phase stability amongst the available low-cost coaxial cables. It was estimated in Sec. 2.4.4 that the worst-case r.m.s. phase error resulting from temperature effects would be, for a feeder system using RG-62A/U,

$$\delta_{\text{rms}} = 0.72f_{\text{IF}} \quad (\text{degrees}) \quad (4.8)$$

where f_{IF} is in MegaHertz. For an FDM system, the phase errors thus depend on the channel frequencies.

The derivation of (4.8) was admittedly based on pessimistic assumptions; the temperature is presumed to be near the extremes of the range (-50°C to $+30^{\circ}\text{C}$) which may be encountered in the operation of the array, and a fairly loose tolerance on phase-temperature coefficients is assumed. Operation near the temperature extremes is certainly a reasonable assumption for a worst-case estimate, but the latter assumption concerning temperature coefficients may prove to be overly pessimistic if the cables are all drawn from the same production lot. On the other hand, an estimate of δ_{rms} which is on the high side will help to make allowance for other error sources of an unpredictable nature, such as cable aging and temperature gradients (caused, for example, by cloud shadows) in the feeder system.

Differences in the attenuation-temperature coefficient amongst

the cables is expected to be quite small, since this coefficient is primarily a function of the resistivity of the conductors. It will be assumed that temperature changes will not cause a significant increase in the amplitude error estimated in equation (4.7). Occasional readjustment of the amplitude equalization will be needed to compensate for aging effects.

4.2.3 Inter-Cable Crosstalk

Crosstalk between transmission lines was studied in Sec. 2.3.2(f). It was concluded that standard single-braid coaxial cables cannot be run side-by-side for distances greater than a few hundred feet without causing serious crosstalk levels. Until field tests are carried out, it is difficult to predict the extent to which this type of crosstalk can be reduced before further physical rearrangement becomes impractical. Following Sec. 2.3.2(f), we shall set as a minimum requirement an r.m.s. crosstalk level of $\alpha_{\text{rms}} = 10^{-3}$ (-60 dB), which corresponds to excitation errors of

$$\Delta_{\text{rms}} = 1.7 \times 10^{-3} \quad (0.015 \text{ dB})$$

$$\delta_{\text{rms}} = 0.1^\circ \quad (4.9)$$

4.2.4 Impedance Mismatches and Inhomogeneities

In addition to the desired signal arriving at the output of each transmission line, there will exist signals caused by multiple reflections in the line, which will result in phase and amplitude errors in a manner similar to crosstalk. One source of such errors is that part

of the desired signal which is reflected from the output termination back to the input termination, where it undergoes a second reflection and returns to the output as an interfering signal. If the reflection coefficients at the input and output terminations are ρ_i and ρ_o , respectively, and the one-way attenuation factor is a_{io} (related by $A = -10(\log a_{io})$ to the attenuation A as introduced in Sec. 2.3.1), then the interfering signal will have magnitude $\beta = \rho_i \rho_o (a_{io})^2$ relative to that of the desired signal. It should not be difficult to match the feedline at each end such that $\rho_i = \rho_o = 0.1$ (VSWR of 1.21), and from Table 2.3 we find that $a_{io} = 0.1$ ($A = 20$ dB) for 2.5 km of RG-62A/U at 1 MHz. The relative magnitude of the interfering signal is therefore about 10^{-4} , and the resulting phase and amplitude errors are negligible compared to those discussed in the previous sections.

A second source of interference is impedance discontinuities caused by inhomogeneities in the cable. Such a discontinuity with reflection coefficient ρ_d will result in interfering signals of relative magnitude

$$\beta = \rho_d \rho_x (a_{dx})^2 \quad (4.10)$$

where ρ_x is the coefficient of reflection at input, output, or some other discontinuity, and a_{dx} is the attenuation factor between the two points. This situation is potentially very serious, since a_{dx} may be close to unity; for example, a discontinuity near the input end of the cable will cause interference with a relative magnitude of about $\rho_d \rho_i$, which may be appreciable if ρ_d is larger than about 0.01. The resultant interfering signal at the output due to all of the internal reflections

may be expressed in the form

$$\beta_{\Sigma} = \left[\sum_k (\beta_k)^2 \right]^{1/2} \quad (4.11)$$

where the β_k are the relative magnitudes of the significant interfering signals as given by (4.10); these signals add randomly since they are uncorrelated. The excitation error levels are calculated in the same manner as for crosstalk, as outlined in Sec. 2.3.2(f). Each cable is characterized by a particular interference level β_{Σ} ; if the r.m.s. value of this interference level over the ensemble of all cables is denoted by β_{rms} , then the excitation errors will be given by

$$\Delta_{rms} = \frac{\beta_{rms}}{\sqrt{2}}$$

$$\delta_{rms} = 40\beta_{rms} \quad (\text{degrees}) \quad (4.12)$$

Since these errors could become quite large, it will be necessary to minimize β_{rms} by carefully matching the impedances at both ends of each transmission line, and by testing each line for significant discontinuities by means of time domain reflectometry [74]. If ρ_i and ρ_o are no greater than 0.1 in each cable, and inhomogeneities with $\rho_d > 0.01$ are removed, then it should be possible to achieve a β_{rms} of the order of 5×10^{-3} . In this case, using the relations of (4.12), the estimated excitation errors are

$$\Delta_{rms} = 3.5 \times 10^{-3} \quad (0.03 \text{ dB})$$

$$\delta_{rms} = 0.2^\circ \quad (4.13)$$

4.3 The Multiplexing System

4.3.1 Inter-Channel Crosstalk

In considering inter-channel crosstalk in the discussion of FDM systems (Sec. 3.3.1), the figure of -55 dB was adopted as a compromise between excitation errors and the maximum number of channels permissible. The corresponding excitation error levels were

$$\Delta_{\text{rms}} = 1.7 \times 10^{-3} \quad (0.015 \text{ dB})$$

$$\delta_{\text{rms}} = 0.1^\circ \quad (4.14)$$

from equation (3.3). This appears to be a reasonable allowance for errors from this source; however, the trade-off involved should be re-examined after further study of the FDM system. If the error budget could absorb a six-fold increase over the levels given in (4.14), then the crosstalk criterion could be lowered to -40 dB. This would allow the reduction of spacing between channels to about 0.31 MHz from 0.5 MHz, assuming the use of an eighth-order Butterworth input filter (data from Table 3.2). The estimates of (4.14) will be used for the purposes of the present assessment.

4.3.2 Intermodulation Crosstalk

Crosstalk from IM products was discussed in a general way in Sec. 3.3.2, with no attempt being made to determine the magnitudes involved pending actual measurements on the FDM system components. Lacking such data on IM crosstalk levels, we shall set as an objective

the familiar figure of -55 dB.

As has been pointed out, channel filters may be necessary in the demodulation process, and they would be themselves a source of excitation errors. These errors would tend to increase as the filter response approaches the ideal rectangular bandpass function, whereas the errors from IM crosstalk would decrease. Therefore one would expect that there would exist an optimum filter response which minimizes the combined error magnitudes. It is possible, however, that no distinct minimum exists and that channel filters would not significantly improve the overall excitation error performance. In view of this possibility, one must take heed of the fact that -55 dB crosstalk levels with corresponding error levels as given by (4.14) may not be obtainable without channel filters, in which case the errors in the filters must be included in the assessment or the crosstalk criterion lowered accordingly. Emphasis must be placed on excellent IM performance in the second mixer, together with careful placement of channel frequencies, in order to approach this criterion as closely as possible.

4.3.3 Equalization

The importance of phase and amplitude equalization in the FDM transmission system was discussed in Sections 3.3.3 through 3.3.5. Consideration was given in Sec. 4.2.1 to equalization of cable losses for single-channel operation by the use of attenuators at the output of each line. The same concept applies to an FDM system, but in addition to an attenuator, each cable must have an additional amplitude equalizer. As explained in Sec. 3.3.5, this equalizer will ensure that the $f^{1/2}$ attenuation characteristic of the cable will not cause a significant rise

in amplitude errors. Since it will have a very moderate phase slope compared to the bandpass filters, the equalizer is not likely to be a significant source of phase errors. Allowance was made in Sec. 4.2.1 for errors in amplitude of the cable plus attenuator combination. It will be assumed that multi-channel operation does not entail larger errors, since the number of attenuators, and the number of measurements required to set them, are unchanged.

Phase equalization, as indicated in Sec. 3.3.4, would probably be incorporated into the beam-forming circuitry; excitation errors in this area will be considered in Sec. 4.5.2. The possibility of automatic equalization in the transmission system and the resulting effect on the errors will be examined in Sec. 5.1.

4.4 The Second Mixer

The second mixers would likely be similar in design to those in the remote stages of the transmission system. In the case of the second mixers we have a more stable thermal environment, nearby L0 signal sources, and easy access to the mixers for adjustment of their parameters, so that phase and amplitude errors are generally easier to control. The overall excitation errors, considering both the mixer itself plus L0 errors, should be little more than the errors which are inherent in the measurement process. It is assumed that the measurements and adjustments will be repeated sufficiently often that no significant long-term variations due to component aging will appear; however, the following estimates do allow for short-term variations such as small changes in temperature in the observatory building:

$$\Delta_{\text{rms}} = 5.8 \times 10^{-3} \quad (0.05 \text{ dB})$$

$$\delta_{\text{rms}} = 0.1^\circ \quad (4.15)$$

4.5 Signal Processing After the Second Mixer

After the array outputs emerge from the second mixers, they must be filtered, phase shifted, weighted, and correlated to form the desired response. Excitation errors arising in this section of the radio telescope will now be briefly examined.

4.5.1 The Output Bandpass Filter and IF Amplifier

The bandpass filter which immediately follows the second mixer completes the demultiplexing process and sets the system bandwidth. In conjunction with this filter will be one or more stages of amplification to compensate for losses in the filter and phase shifters, and to increase the signal level to that required by the correlators.

In these stages and in the following circuitry, few firm specifications have been made, and the evaluation of excitation errors must be based to a large extent on conjecture. In the first stage of array development, the bandpass filter is likely to be quite simple, with the effective system bandwidth being fixed at some value in the 50 to 100 KHz range. Like the input filter, this filter would have an easily-reproduced transfer function such as the Butterworth function. Provision for changing the bandwidth is highly desirable; in the case of conventional passive filters, this would require insertion of a different filter for each bandwidth.

A later phase in array development might include the replacement of the conventional filters by digital filters, which would allow precise duplication of filter characteristics plus programmable center frequency and bandwidth. For the purposes of the present accounting, the use of conventional passive filters will be assumed. The filter and IF amplifier stages can be considered as a single unit, to be matched as closely as possible to a standard unit in gain and phase characteristics. The filter would likely be divided into several interstage filter elements between the amplifier stages.

As discussed in Sec. 4.1.1, measurement techniques are available by which gain matching to within 0.01 dB and phase matching to within 0.01° can be achieved at a single frequency in the passband. The degree to which this accuracy can be approached over the full system bandwidth depends mainly on the amount of time and effort expended in the matching procedure. The output filter/amplifier unit is more complex than the input filter, but the latter will be exposed to much larger temperature variations; on the whole, the errors from the output unit would probably turn out to be somewhat smaller. The following estimates are consequently about one-half as large as those previously given for the input filter:

$$\Delta_{\text{rms}} = 0.005 \quad (0.04 \text{ dB})$$

$$\delta_{\text{rms}} = 0.2^\circ \quad (4.16)$$

4.5.2 Beam Formation and Other Signal Processing

Although general conclusions concerning the formation of multiple beams have been reached, the choice of a particular method of beam formation remains a matter for further study. The design of the feeder system has proceeded along lines which will allow a high degree of flexibility in making the initial choice, and in modifying or replacing it at a later date. The beam-forming matrix consists essentially of a systematic network of variable phase shifters which supply the phase shifts necessary to form the fan-beam responses of the component arrays. The outputs of the network are then cross-correlated to form the pencil-beam response patterns. At some point prior to correlation and the summing of element outputs which precedes it, these outputs must be properly weighted to achieve the desired aperture illumination.

Among the options available for accomplishing the fan-beam formation are networks of analog phase shifters, an excellent example of which is the Molonglo Cross system, and digital phase shifters using shift registers, as employed in the Clark Lake Teepee Tee. The digital approach would appear to have an advantage in areas such as reproducibility and programmability. Digital signal processing in general seems very promising as a means of realizing the full capability of the array and minimizing the excitation errors. Another possibility in the signal processing area is electrooptical processing [75]. In this case, the array would be operated as a correlation array (see Sec. 2.4.1) and no phase shifters would be needed for beam forming.

From the foregoing, it can be seen that no definite statements concerning excitation errors in the final stages of signal processing can be made at this time. This being the case, it is wise to budget for

errors fairly generously here. Work with the Molonglo Cross indicates that r.m.s. errors encountered in the beam-forming system were of the order of 0.1 dB in amplitude and 0.5° in phase [12]. These figures can likely be improved upon, but we shall adopt them pending further design work in this area:

$$\Delta_{\text{rms}} = 0.012 \quad (0.1 \text{ dB})$$

$$\delta_{\text{rms}} = 0.5^\circ \quad (4.17)$$

These estimates do not seem pessimistic when it is recalled that they must also include errors in setting the array grading (amplitude weighting of the elements), and in equalizing the differential phase shifts arising from multiplexing (Sec. 4.3.3).

4.6 Summation of Excitation Errors

The error estimates arrived at in the preceding sections are summarized in Table 4.1. The entry for transmission line phase errors due to temperature changes assumes that the temperature is near an extreme value, and was determined as follows: The r.m.s. phase error for signals transmitted on an IF channel centered at f_k MHz is $0.72f_k^\circ$, as given by equation (4.8). The r.m.s. phase error for the ensemble of m FDM channels is then

$$\delta_{\text{rms}} = \left[\frac{1}{m} \sum_{k=1}^m (0.72f_k)^2 \right]^{1/2} = 0.72(f_{\text{IF}})_{\text{rms}} \quad (4.18)$$

Table 4.1 Summary of Error Estimates

Source of Errors	Estimated RMS Excitation Errors	
	Phase (Degrees)	Fractional Amplitude ($\times 10^{-3}$)
Input Bandpass Filter	0.5	10
First Mixer/Preamp	0.1	5.8
First Mixer: LO Errors	0.1	5.8
Transmission Lines:		
Measurement	0.1	5.8
Temperature (see text)	1.3	—
Crosstalk	0.1	1.7
Impedance Mismatch	0.2	3.5
Multiplexing:		
Inter-channel Crosstalk	0.1	1.7
IM Crosstalk	0.1	1.7
Second Mixer (incl. LO Errors)	0.1	5.8
Output Bandpass Filter and IF Amplifiers	0.2	5.0
Beam-Forming Circuitry	0.5	12
Estimated Overall	1.5	20.6
RMS Errors	(0.026 rad)	(2.1%)

The number of channels m and the frequency allocations f_k are not yet known. For this estimate, we shall assume that $m = 4$, with channels at 1.0, 1.5, 2.0, and 2.5 MHz. Substituting these values for f_k into (4.18) yields $\delta_{\text{rms}} = 1.3^\circ$.

The overall error estimates of Table 4.1 were arrived at by making the usual assumption that the individual error sources are independent, so that the total r.m.s. errors are simply the square root of the sum of the individual mean-square values.

4.7 Other Sources of Error

In spite of the large number of error sources just considered, we have not yet exhausted the possibilities. One such source is delay errors, which lead to a loss of correlation for nonzero system bandwidth even when the phasing is perfect. These errors, which are considered in Sec. 5.3, are similar in some respects to the amplitude errors discussed in this chapter, but they do not arise in a random fashion and hence are more controllable than random amplitude errors. A few more effects which tend to raise the array sidelobe levels above those of the no-error pattern are briefly examined below.

4.7.1 Positional Errors

Any imperfections in positioning the array elements will tend to cause a rise in sidelobe levels. Positional errors may in fact play a larger role in sidelobe level deterioration than phase and amplitude errors unless adequate care is taken in the physical construction of the array.

The effects of both positional and electrical errors in two-dimensional scanned dipole arrays have been studied by Elliott [76]. He makes use of a rectangular coordinate system and distinguishes between translational errors in the placement of the dipole centers, and errors in angular orientation with respect to their desired axes. The dipoles are intended to lie parallel to the x-axis; the orientation errors are defined in terms of the angles between the x-axis and the projections on the x-y and x-z planes of the actual dipole axis.

Assuming that the translational errors are normally distributed with the same standard deviation σ_1 (in wavelengths) in all three coordinates, it can then be shown that such errors have roughly the same effect on sidelobe levels as an r.m.s. amplitude error given by

$$\Delta_{\text{rms}} = \frac{k_o \sigma_1}{\sqrt{2}} \quad (4.19)$$

where $k_o = \text{wave number} = \frac{2\pi}{\lambda_o}$

$\lambda_o = \text{design wavelength of the array}$

Similarly, errors in orientation as defined above, with standard deviation σ_2 , have the same effect as an r.m.s. phase error of the same magnitude:

$$\delta_{\text{rms}} = \sigma_2 \quad (4.20)$$

We shall now determine the bounds on σ_1 and σ_2 which will limit the effect of these errors to an equivalent of no more than a 10% increase in the overall r.m.s. amplitude and phase errors, respectively, estimated in Table 4.1. For amplitude errors, we arrived at an estimate

of 2.06×10^{-2} ; assuming that the positional errors are independent of the electrical errors, we require that

$$[(2.06 \times 10^{-2})^2 + (\frac{k_o \sigma_1}{\sqrt{2}})^2]^{1/2} \leq (1.1)(2.06 \times 10^{-2})$$

$$\text{or,} \quad \sigma_1 \leq (2.1 \times 10^{-3})\lambda_o \quad (4.21)$$

At the design wavelength of the Tee array, $\lambda_o = 24.2$ m, this becomes

$$\sigma_1 \leq 5.1 \text{ cm} \quad (4.22)$$

For the phase excitation errors, we had $\delta_{\text{rms}} = 1.5^\circ$, so that the criterion for orientation errors is, using (4.20),

$$[(1.5)^2 + (\sigma_2)^2]^{1/2} \leq (1.1)(1.5)$$

$$\text{or,} \quad \sigma_2 \leq 0.7^\circ \quad (4.23)$$

The figures in (4.22) and (4.23) are indicative of the tolerances which must be placed on element positions if severe sidelobe degradation from this source is to be avoided. It is clear that accurate surveying and construction practices which emphasize physical stability will be necessary. Positional errors will assume even greater significance if the electrical errors are reduced by means of the compensation methods outlined in Sec. 5.1.

4.7.2 Mutual Coupling of the Array Elements

The dipole elements of the Tee array have thus far been considered to be ideal in the sense that their properties remain identical and invariant when they are placed into the array environment. Unfortunately, this ideal situation cannot exist in practice. Due to mutual coupling, the elements will not all have the same impedance; furthermore, their impedances will change with scan angle [77]. The resulting impedance mismatches in the feeder can cause a marked change in the properties of the array.

The most serious effect in most cases is a decrease in gain of the array due to reflection of power at the mismatch. Another effect, which is of greater concern in the context of this investigation, is the altering of the excitation distribution of the array. If the array were infinite in extent, all elements would change identically and only the first effect would appear (barring indirect effects on the excitation resulting from changes in the feeder system). For finite arrays, edge effects assume an importance which depends largely on the dimensions of the particular array under consideration.

In the case of the Tee configuration, the array is virtually infinite in extent along the long dimensions as far as the vast majority of elements is concerned, and the mutual coupling will have only a slight effect on the component array patterns in their respective array planes (excepting gain reduction). However, edge effects are much more prominent across the narrow widths of the arrays, and some changes in the broad dimensions of the fan beams will occur [7]. The effect on the Tee pattern would likely be a rise in relative sidelobe levels, particularly near the array planes, as the beam is scanned from the

zenith. Due to the close north-south element spacing and the narrow width of the east-west array, the changes in pattern should be most noticeable in the north-south array plane.

In addition to the effects just mentioned, the changes in element impedances with scan angle may have an indirect effect on excitation errors. Since the antenna element provides the input termination (through a matching device) for the input bandpass filter, a change in element impedance will undoubtedly alter in some fashion the phase and amplitude characteristics of the filter. Here again the edge effects are most important, since they lead to disparities in the impedances seen by different filters. This fact was recognized when the r.m.s. errors in the filters were estimated in Sec. 4.1.1, but it is not certain that the allowances made were sufficient.

A detailed study of mutual coupling is beyond the scope of this thesis. The importance of conducting such a study, and of relating the results to the changes in array excitation to be expected, is clear from the preceding comments. If the effects are found to be significant compared to those of the other excitation errors discussed in this chapter, it may be necessary to develop some means of reducing the element impedance variations. One of the most successful techniques of improving the impedance matching for variations in scan angle has been to interconnect adjacent elements with lossless passive networks containing distributed or lumped components [78].

4.7.3 Miscellaneous Error Sources

Certain of the feeder system components are not explicitly accounted for in the excitation error estimates of Table 4.1. In some

cases these components can be considered, for the purposes of measurement and adjustment, to be an integral part of some other component which is listed in the table. For example, the power combiner and power splitter which terminate each transmission line have not been distinguished from the line itself. Similarly, baluns or other antenna matching devices needed have been included as part of the input filter.

Since the remote electronic stages will be located in close proximity to the antenna elements, excitation errors arising in the cables which link the two should be relatively insignificant. However, it must be kept in mind that if the elements are grouped into subarrays, then remote-controlled variable phase shifters (usually switched lengths of cable) are required at this point in the feeder system. These phase shifters are actually part of the beam-forming circuitry, for which error allowances have been made, but the excitation errors are likely to be somewhat greater than in the case where all beam formation is done at the observatory.

In general, overlooking a few sources of small errors will have a negligible effect on the overall estimates. For instance, if an additional r.m.s. phase error of 0.2° from an independent source were included in the estimates of Table 4.1, the overall r.m.s. phase error estimate would increase by less than one per cent.

CHAPTER 5

ERROR COMPENSATION SYSTEMS AND SIDELOBE CALCULATIONS

In this chapter, possible methods of dealing with phase, amplitude, and delay errors are examined and evaluated. In particular, techniques for reducing certain of the excitation errors assessed in the previous chapter are investigated. An attempt is made to determine how the sidelobes of the array pattern will be affected by excitation errors.

5.1 Reduction of Excitation Errors

The basic approach to error reduction in feeding the array consists of refinement of the measurement processes, accompanied by an increase in the stability of component parameters and/or a decrease in the time interval between measurements. The frequent periods during which the ionospheric conditions are unfavorable for astronomical observations can be profitably used to carry out these measurements and the accompanying adjustments. Some of the error reduction procedures, however, would be extremely complex and time-consuming, especially where the feeder system is concerned. It is therefore worthwhile to investigate the possibility of developing an automatic or semi-automatic system which maintains a low level of excitation error. Such a system may be categorized according to whether it can operate continuously, coexisting with regular array operation, or whether it must interrupt array operation periodically in order to make adjustments.

5.1.1 Continuous Phase Error Compensation

In general, an automatic calibration system consists of the injection of a test signal of known phase and amplitude at some point in each channel or multiplex group, recovery of the signal at some later point for comparison to a reference signal derived from the original test signal, and use of the result of the comparison to match the channel's phase and amplitude characteristics to that of the reference channel. The phase shift of the reference channel need not be accurately known or extremely stable, since we are only concerned with differential errors.

If operation of the system is to be continuous, the test signal clearly must be situated at a frequency outside of the passband of the receiver. For this reason, the scheme is not useful for matching the bandpass filter characteristics; this is essentially a transmission line compensator only. One possible method of implementing the system is outlined in Fig. 5.1 for the case of two-channel FDM. The test signal in this case is the difference between the two L0 frequencies, but there are numerous other possibilities for synthesizing a suitable signal. A separate distribution system for the test signal would be somewhat more accurate than the use of L0 signals for synthesis. At the output end of the line, the test signal is picked off and compared in a phase detector to the reference signal, which was in phase with the original test signal before undergoing a time delay τ_s . The phase detector output controls the value of the variable delay $\Delta\tau$, adjusting it to produce zero phase difference at the detector, at which point the transmission line delay becomes τ_s . The action of the system is similar to that of a phase-locked loop.

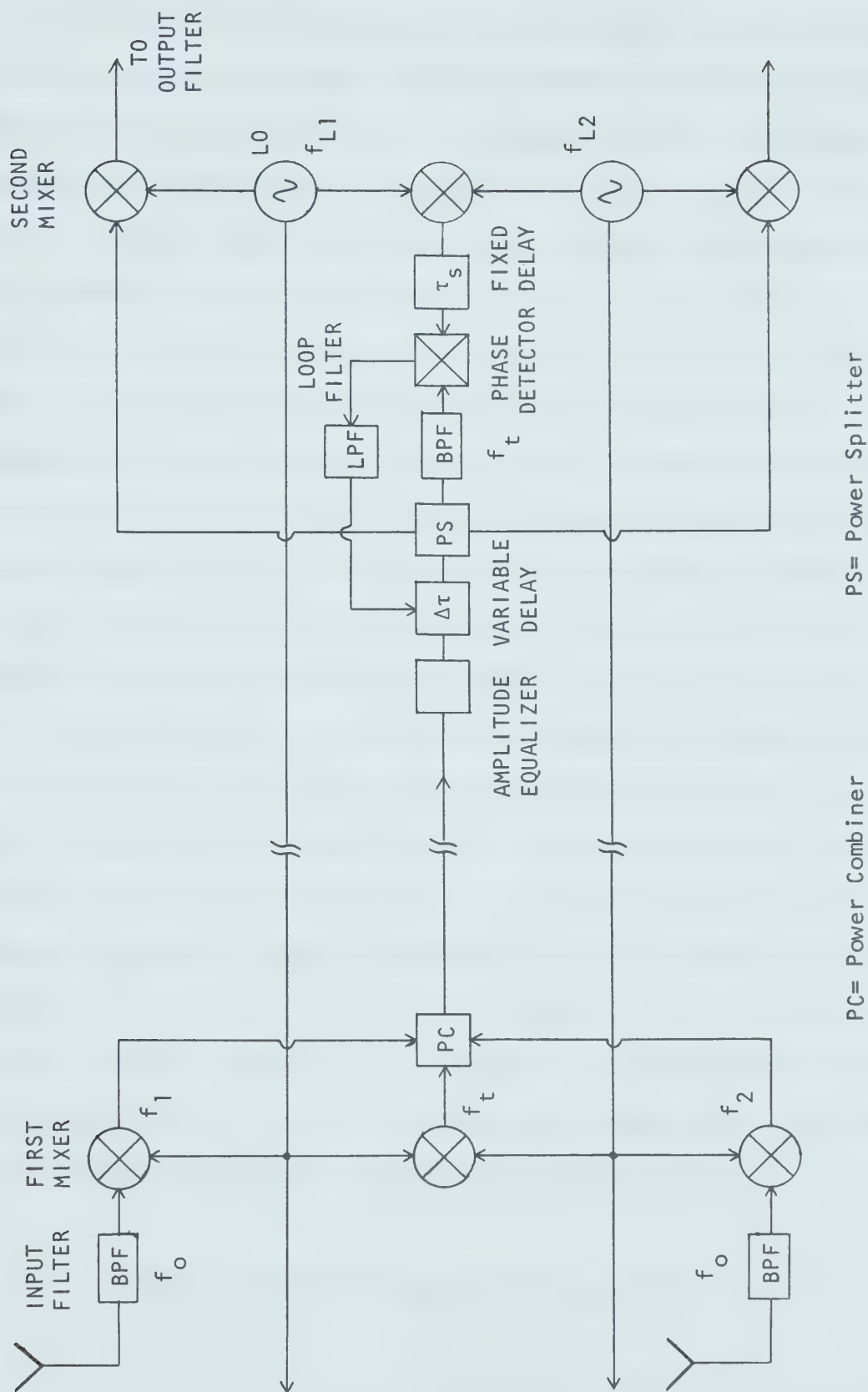


Fig. 5.1 FDM System With Transmission Line Phase Compensation

The most critical component of the compensator is the time delay $\Delta\tau$, which must be continuously variable and have a sufficiently large bandwidth to encompass all of the FDM channels plus the test signal. To determine the range of delay needed, we begin by assuming that all cables are trimmed after installation such that their time delays are fairly closely matched to some value τ_c (within 1 ns or so) at a temperature T_c near the center of the range of -50°C to $+30^\circ\text{C}$. The value of τ_c will be about 12.65 μs for 2.5 km of solid polyethylene dielectric coaxial cable at -10°C . Trimming of the cables to this accuracy can be done by the swept-frequency method [44], which does not require special far-end terminations or feedback schemes. Accuracy in this process is not essential to the operation of the system; it serves only to reduce the range of variable delay needed.

Figure 5.2 depicts the delay-versus-temperature characteristics of the two cables in the transmission system which have the extreme values of phase stability coefficient K_p , as defined in Sec. 2.3.2(a). The value specified for RG-62A/U (Sec. 2.4.4) was $-50 \text{ ppm}/^\circ\text{C}$, with a standard deviation of 4 $\text{ppm}/^\circ\text{C}$ determined from the assumption of $\pm 20\%$ tolerance on K_p . The extreme values corresponding to this tolerance are $K_p(\text{min}) = -40 \text{ ppm}/^\circ\text{C}$ and $K_p(\text{max}) = -60 \text{ ppm}/^\circ\text{C}$. We first assume the use of a standard delay τ_{s1} which is independent of temperature; the range of variable delay needed to compensate all cables is then

$$\begin{aligned}\Delta\tau(\text{max}) - \Delta\tau(\text{min}) &= \tau_{-50}(\text{max}) - \tau_{30}(\text{min}) \\ &\approx -80\tau_c K_p(\text{max}) \times 10^{-6} = 61 \text{ ns} \quad (5.1)\end{aligned}$$

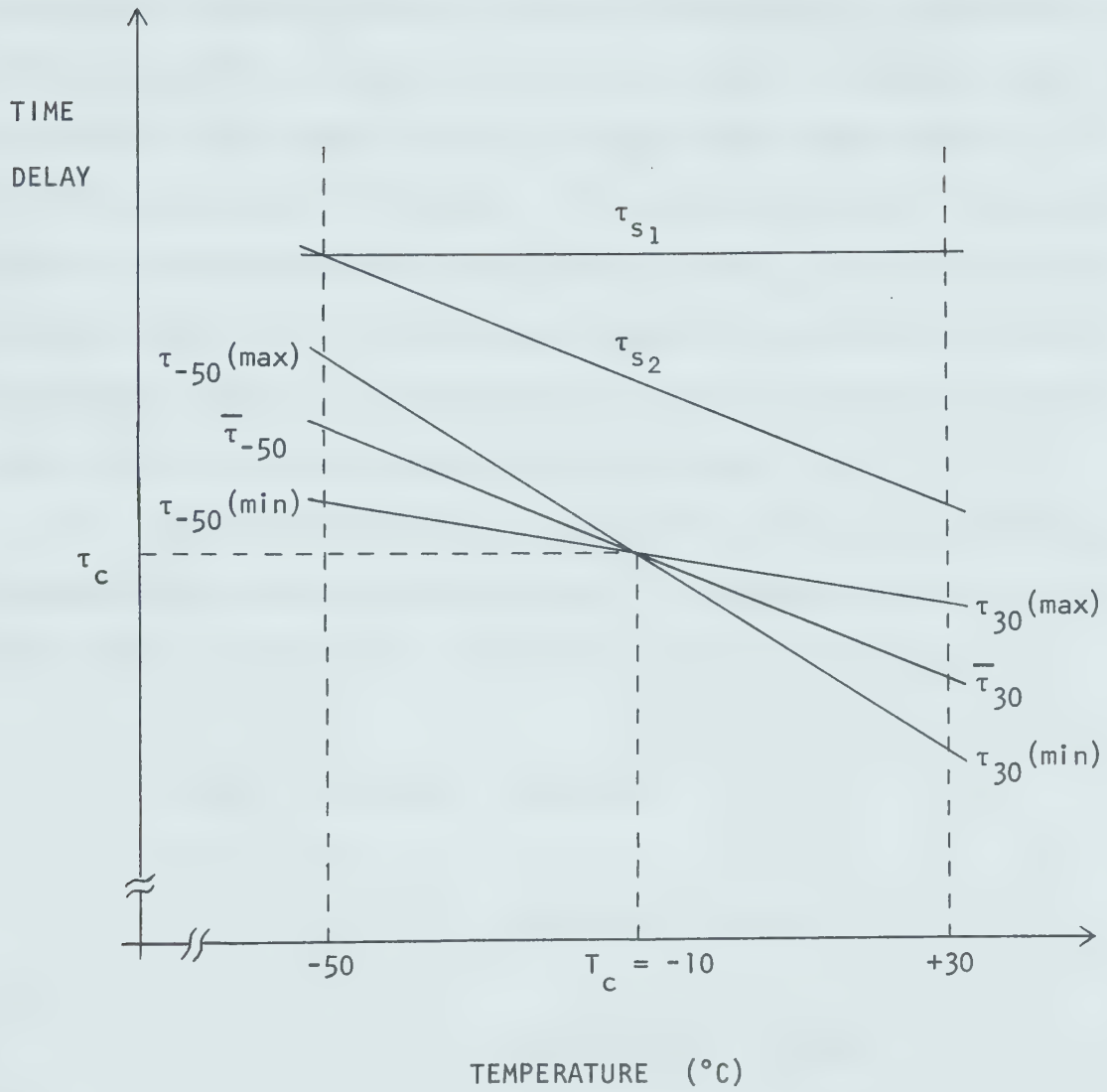


Fig. 5.2 Temperature Characteristics of Cable Delays

This expression is only an approximation since the delay-versus-temperature characteristic of the cable will not be linear over such a large temperature range; however, in the case of RG-62A/U the expression is reasonably accurate. The nonlinearity is caused by K_p increasing with temperature, which will result in the actual values of τ_{-50} and τ_{30} being smaller than those found by using the linear approximation, but the difference between the two can still be determined quite accurately using the approximate method. The standard delay τ_{s_1} can be set to any convenient value that is larger than $\tau_{-50}(\text{max})$ by a reasonable margin; for example, setting $\tau_{s_1} = 12.85 \mu\text{s}$ would call for a delay $\Delta\tau$ which is variable over the range of about 170 ns to 230 ns.

The range of delay needed can be further reduced by making the standard delay temperature-dependent, as illustrated by the τ_{s_2} characteristic of Fig. 5.2. In this case, the delay range needed is

$$\begin{aligned}
 \Delta\tau(\text{max}) - \Delta\tau(\text{min}) &= \tau_{-50}(\text{max}) - \tau_{-50}(\text{min}) \\
 &= \tau_{30}(\text{max}) - \tau_{30}(\text{min}) \\
 &\approx 40\tau_c [K_p(\text{min}) - K_p(\text{max})] \\
 &= 12 \text{ ns} \qquad (5.2)
 \end{aligned}$$

This result holds only if the standard delay has a temperature coefficient near the mean value $\overline{K_p}$ for RG-62A/U, a logical choice for τ_{s_2} being a suitable length of this cable.

There are a number of ways in which a voltage-variable delay for

$\Delta\tau$ might be implemented. One possibility is a lumped-constant delay line with voltage-dependent components, such as a cascade of LC filter sections containing varicap diodes. Hannan et al [79] have described a delay line of this type which is variable from 150 ns to 250 ns and maintains a phase linearity of $\pm 2.5\%$ over a bandwidth of 16 MHz. This exceeds the requirements for $\Delta\tau$ by a considerable margin in both delay and bandwidth.

The phase linearity of the delay line is an important parameter, since the success of the compensation system rests on the accuracy with which phase shifts set at the test frequency are translated into the phase shifts needed to equalize the delay of each IF channel to the standard delay (this should not be confused with equalization of the phase differences between channels which are inherent in the FDM system; we are concerned here only with equalizing the phase differences at a given IF between different cables). The effect of phase nonlinearity in the delay line will now be evaluated.

Consider a transmission line having phase delay τ (no dispersion) without the compensation system. The phase error for a channel at f_{IF} transmitted on this line is given by

$$\delta = 2\pi f_{IF}(\tau - \bar{\tau}) \quad (\text{radians}) \quad (5.3)$$

where $\bar{\tau}$ is the ensemble average of the phase delays of the transmission lines. The r.m.s. phase error over all of the lines is

$$\delta_{\text{rms}} = 2\pi f_{IF} [(\tau_{\text{rms}})^2 - (\bar{\tau})^2]^{1/2} \quad (5.4)$$

We now include in each transmission line the phase compensator of Fig. 5.1, with the test signal at frequency f_t . In the line with uncompensated delay τ , the test signal will undergo an additional phase shift in the delay $\Delta\tau$ given by

$$\phi_d(f_t) = 2\pi f_t(\Delta\tau) = 2\pi f_t(\tau_s - \tau) \quad (5.5)$$

Now if we had perfect linearity, the phase shift in the delay $\Delta\tau$ at f_{IF} would be (f_{IF}/f_t) times the quantity in (5.5), but due to nonlinearity we instead have a phase shift of

$$\phi_d(f_{IF}) = (f_{IF}/f_t)(1 + \zeta)\phi_d(f_t) \quad (5.6)$$

where ζ is a fractional linearity error. The total phase shift of the line is ideally $2\pi f_{IF}\tau_s$ at f_{IF} , but the nonlinearity causes it to become, from (5.5) and (5.6),

$$\begin{aligned} \phi(f_{IF}) &= 2\pi f_{IF}\tau + \phi_d(f_{IF}) \\ &= 2\pi f_{IF}\tau_s + 2\pi f_{IF}\zeta(\tau_s - \tau) \end{aligned} \quad (5.7)$$

If we assume that the linearity error ζ has zero mean, then the mean phase shift is $2\pi f_{IF}\tau_s$, and from (5.7) the phase error in a particular channel of the compensated system is

$$\delta_c = 2\pi f_{IF}\zeta(\tau_s - \tau) \quad (5.8)$$

and the r.m.s. phase error becomes

$$(\delta_c)_{\text{rms}} = 2\pi f_{\text{IF}} \zeta_{\text{rms}} [(\tau_{\text{rms}})^2 - 2\tau_s \bar{\tau} + (\tau_s)^2]^{1/2} \quad (5.9)$$

If $\tau_s \approx \bar{\tau}$, which is the case if the τ_{s2} characteristic is used and $\Delta\tau$ is not too large, then (5.9) can be approximated by

$$(\delta_c)_{\text{rms}} \approx \zeta_{\text{rms}} \delta_{\text{rms}} \quad (5.10)$$

where δ_{rms} is the r.m.s. phase error in the uncompensated system, as given by (5.4).

Since the phase error is reduced by a factor roughly equal to the r.m.s. fractional linearity error, satisfactory operation should result from maintaining the linearity of the delay lines within a few per cent. There is little point in attempting to achieve better linearity, since the phase errors from this source will become dominated by errors elsewhere in the compensation system. The uncertainty in the phase of the injected test signals will be the major source, the error here likely being of the order of 0.1° r.m.s. if a high-quality distribution system is used.

It is probable that the worst-case r.m.s. phase error resulting from delay variations in the transmission lines could be lowered by use of this compensation scheme to about 0.2° from the previously estimated value of 1.3° . This would reduce the overall r.m.s. phase error estimate (Table 4.1) from 1.5° to about 0.8° . More important, perhaps, than the actual reduction of errors is their increased stability and the elimination of the enormous task of periodic readjustment of the

electrical lengths of the lines. The initial trimming of the lines would also be simplified.

There are a number of difficulties which would have to be overcome in implementing this compensation system. One potential problem is associated with the assumption made in the preceding analysis that there is no significant dispersion in the transmission lines over the frequency range of interest. If this assumption is not valid, then one cannot assume that $\tau(f_t) = \tau(f_{IF})$, and equation (5.8) must be replaced by

$$\delta_c = 2\pi f_{IF} \{ (\kappa - 1) [\tau(f_t) - \overline{\tau(f_t)}] + (\zeta) [\tau_s - \tau(f_t)] \} \quad (5.11)$$

where $\kappa = \tau(f_{IF})/\tau(f_t)$ is a measure of the dispersion in the cable. It is clear from (5.11) that dispersion will tend to increase the r.m.s. phase errors, but the increase is not serious provided that κ does not exceed 0.01 or so. Judging from the discussion of dispersion in Sec.3.3.4, this criterion can probably be met by standard coaxial cables such as RG-62A/U.

Another possible source of problems is IM distortion in the second mixer due to products generated by the test signal. The test signal-to-noise ratio must be quite high if the compensator loop is to achieve low phase errors, so that we are injecting a relatively strong signal into the FDM spectrum. The choice of f_t must be made carefully in order to minimize this problem.

Recently developed continuously-variable analog delay lines using the "bucket-brigade" concept offer possibilities for delays having lower cost and better reproducibility than the lumped-constant type mentioned above. Bucket-brigade delay lines can be synthesized from discrete

components [79], or integrated on a chip using bipolar [80], MOS [81], or charge-coupled device [82] techniques. The major drawback of this method for the present application is that it makes use of sampling; the delay line consists basically of a series of sample-and-hold units forming what might be thought of as an analog shift register. As in a digital shift register, the delay time is a function of the clock frequency (sampling rate). A filter is needed at the output of the delay line to attenuate the unwanted products generated by the sampling process, which would otherwise add to the IM problems in the second mixer. The filter does not have to be an elaborate one, particularly if the sampling rate is well above the minimum (Nyquist rate) of twice the highest frequency present in the FDM spectrum; if channel filters are included in the FDM system, they would serve the purpose nicely.

If the FDM system parameters remain as given in Sec. 3.3.1, then the Nyquist rate would be in the neighborhood of 6 MHz. It would be preferable to use a sampling rate of at least 10 MHz to keep the sampling sidebands well separated from the original spectrum. For n bucket-brigade stages, the delay line provides a delay variation of [79]:

$$\Delta\tau(\max) - \Delta\tau(\min) = \frac{n}{2f_s(\min)} \left(1 - \frac{1}{a}\right) \quad (5.12)$$

where $f_s(\min)$ = minimum sampling rate used (not the theoretical minimum)

$$a = f_s(\max)/f_s(\min)$$

For example, if we had $n = 5$, $f_s(\min) = 10$ MHz, and $f_s(\max) = 10.5$ MHz, then the delay would be variable from 238 ns to 250 ns, thus providing the 12 ns range called for in equation (5.2). The system is obviously very flexible, with the delay range adjustable simply by changing the

frequency range of the voltage-controlled clock oscillator. The present maximum frequency of operation is of the order of 5 MHz for MOS and 20 MHz for charge-coupled devices [83], while bipolar bucket-brigades have been built [80] which operate at 30 MHz or more. Much of the research in the field of bucket-brigade electronics has concentrated on overcoming problems such as incomplete charge transfer [84] whose effects manifest themselves when the number of stages is very large, but these limitations should be of little concern in this application since only a small number of stages is needed. Other aspects of the devices such as noise figure would have to be investigated more closely due to the low level of signals involved.

In summary, the phase compensation system described appears to be feasible, its chief disadvantage being that its use is limited to the transmission lines. The design of the system is such that it could be omitted in the initial phase of array operation and added at a later date if it is felt to be needed. An amplitude compensation system based on the same concept could be developed if the disparity in cable attenuation-temperature coefficients proves to be larger than anticipated. Neither type of compensation system seems promising as a basis for an automatic FDM equalization scheme.

5.1.2 Discontinuous Compensation Systems

A more ambitious compensation scheme utilizing a test signal in the center of the radio telescope's passband has some distinct advantages over the system just described. More of the transmission and signal processing circuitry can be included in the compensation loop, and a continuously-variable delay line is not required. The phase and

amplitude equalization needed for the FDM system can also be provided by such a scheme. On the other hand, continuous operation of this type of compensation system is not possible, and one must therefore deal with the complications arising from periodic interruptions in observations. Since each channel is compensated separately, the system is a rather complex one.

One possible compensation system is outlined in Fig. 5.3. As usual, only two FDM channels are shown for clarity. This system is similar in some respects to one described by Smith [85] intended for coherent feeding of widely-spaced antennas; however, in the latter system the antenna output and the L0 signal share the same transmission path, no amplitude compensation is included, and no multiplexing of antenna outputs is involved.

The operation of the compensation system is as follows: A test signal at the center frequency of the array is generated by an oscillator at the observatory and distributed to the array elements by means of a distribution system similar to those used for the L0 signals. The test signal is coupled into the remote electronics in place of the antenna output, and it is picked off after transmission at a point preceding the beam-forming circuitry. The phase shift of the intervening path is compared to a reference phase shift, and the phase of the L0 signal at the second mixer is adjusted until the two become equal. A similar feedback scheme standardizes the channel gain by setting a variable attenuator.

The switching needed in the compensation system would likely be provided by diode switches, although electromechanical devices are also a possibility, particularly if a lightning protection system (Sec. 2.5)

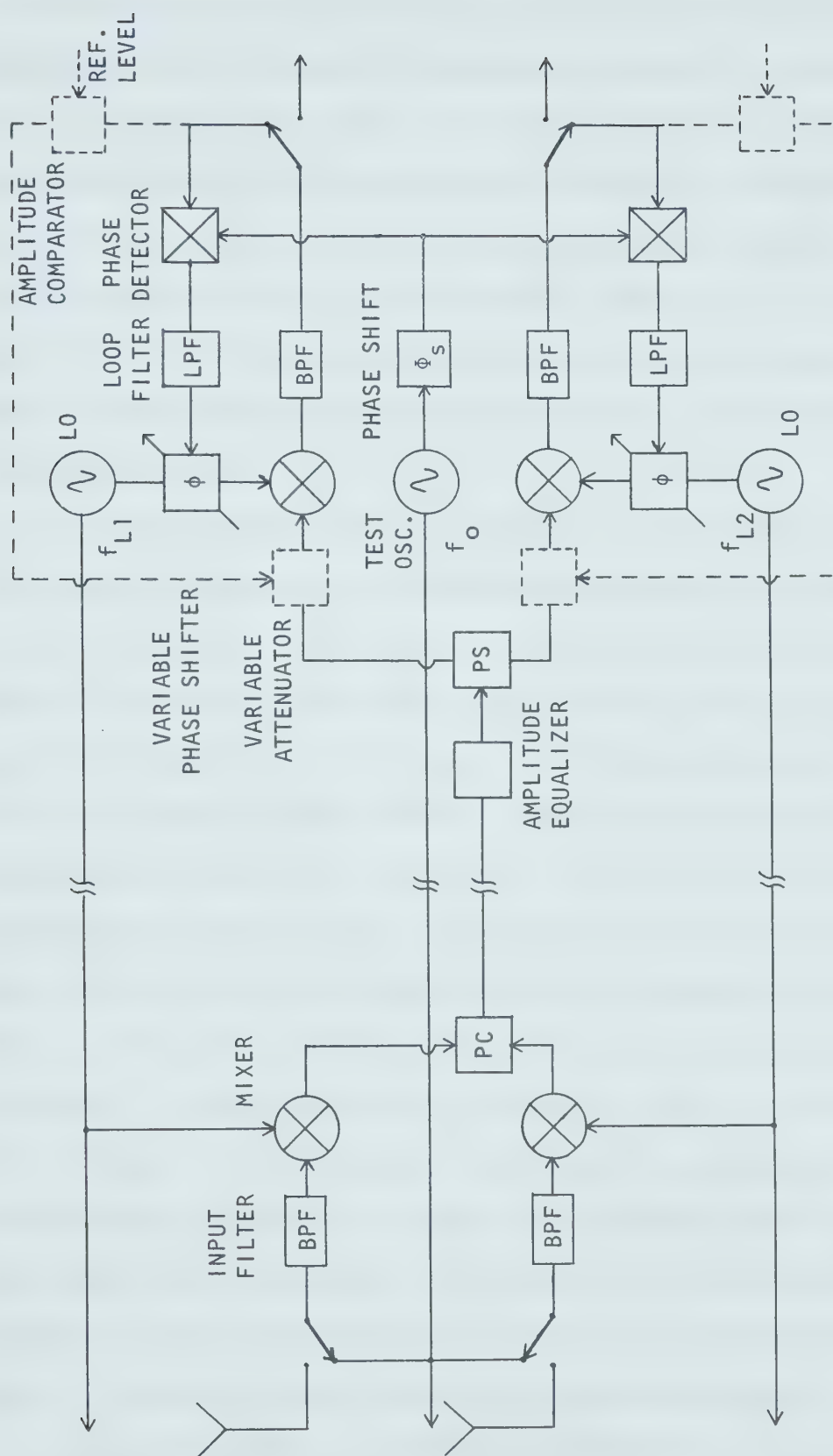


Fig. 5.3 FDM System With Discontinuous Phase and Amplitude Compensation

is incorporated into the switching arrangement. The time spent in "compensation mode" depends on the response times of the phase- and amplitude-control loops; since the changes needed will be small, the compensation period will probably be of the order of a second or less, so that the reduction in observation time would be negligible provided that the compensation is not performed too frequently. It is important that the phase shifters and attenuators have memory, allowing them to hold the values reached during compensation mode until the next compensation period.

It should be noted at this point that the L0 signal at the second mixer could be produced by a voltage-controlled oscillator (VCO) rather than derived from the first L0 via a phase shifter as shown in Fig. 5.3. We would then have a phase-locked loop configuration known as a translation loop [86]. If the loop filter is of second order, the loop will have frequency memory; that is, the VCO will tend to remain at the locked frequency when the input signal is removed, by virtue of the charge stored in the integrator. However, due to voltage offsets and other imperfections in the phase detector and integrator, the VCO will slowly be driven away from its initial frequency. Because of this drift, the interval between compensation periods would have to be kept very small. A phase shifter operated by some type of servomechanism which latched between compensation periods would probably provide superior performance. From the standpoint of changes in the transmission system, the interval could likely be several minutes, but the limitations in memory of the devices could prove to be the limiting factor.

Output from the test oscillator may have to be reduced during "observation mode" in order that radiation and switch leakage do not

result in a detectable signal in the receiver. There will undoubtedly be technical problems to be overcome in connection with the switching, such as transient suppression, but none of these are seen to be insurmountable.

To estimate the phase excitation errors which will occur when a compensation system of this type is employed, we return to the estimates of Table 4.1. There are several sources of phase error which are not included in the compensation; in this category are IM crosstalk, inter-channel crosstalk, and the beam-forming circuitry. For other sources, such as transmission line reflections and inter-cable crosstalk, the compensation is correct only at the center frequency of the channel. It may be possible to lower the errors in the beam-forming system from the previously-estimated values since this system is now relieved of the task of providing FDM phase equalization, but no reduction will be assumed here. The r.m.s. phase error within the compensation system should be about 0.2° , resulting mainly from errors in the test signal distribution system. Using this value and the estimates of Table 4.1 for the uncompensated error sources, the overall phase error estimate becomes

$$\delta_{\text{rms}} = 0.6^\circ \quad (5.13)$$

It must be kept in mind that those error sources which were excluded from the original estimates (i.e., positional errors, mutual coupling, and various unforeseen sources of small errors) take on even greater significance here, and this estimate should thus be treated with caution.

It has not yet been shown that the phase compensator performs adequately over the full bandwidth being transmitted. It is likely that the compensation will become less effective with increasing departure

from the center frequency, and we must ascertain whether this will significantly affect the estimate of (5.13). The total phase shift in a given channel is made up of frequency-dependent terms such as those resulting from the filters and transmission lines, plus terms which are independent of frequency (due to LO phase at the mixers). It is the frequency-dependent phase shifts which concern us here.

We begin by examining the action of the compensator for changes in the transmission lines, ignoring for the moment the other sources of phase shift in the channel. In a particular channel whose transmission line is identified in the following by the subscript 1, the total phase shift at the center of the IF passband f_j may be expressed as

$$\Phi_{1j} = 2\pi f_j \tau_{1j} + \Delta\phi_{1j} \quad (\text{radians}) \quad (5.14)$$

where τ_{1j} = the phase delay of the line at f_j

$\Delta\phi_{1j}$ = the remainder of the channel phase shift, including the variable phase shift of the compensator

The action of the compensator is to adjust $\Delta\phi_{1j}$ such that

$$\Phi_{1j} = \Phi_s \quad (5.15)$$

where Φ_s is the standard phase shift as shown in Fig. 5.3. Similarly, in a second channel transmitted at f_k over a cable having phase delay τ_{2k} at this frequency, we have a phase shift of

$$\Phi_{2k} = 2\pi f_k \tau_{2k} + \Delta\phi_{2k} = \Phi_s \quad (5.16)$$

and $\phi_{1j} = \phi_{2k}$ as desired.

Let us now examine the situation at the frequency $f_o + \Delta f$, which corresponds to $f_j - \Delta f$ and $f_k - \Delta f$ in the first and second channels, respectively. Assuming that Δf is sufficiently small that the phase delay at $f_j - \Delta f$ does not differ appreciably from the delay at f_j , the phase shift in the first channel at $f_j - \Delta f$ is

$$\begin{aligned}\phi_{1j}(f_j - \Delta f) &= 2\pi(f_j - \Delta f)\tau_{1j} + \Delta\phi_{1j} \\ &= \phi_s - 2\pi\Delta f\tau_{1j}\end{aligned}\tag{5.17}$$

A similar expression applies to the second channel. The difference in phase shift between the two channels is

$$\begin{aligned}\Delta\phi &= |\phi_{1j}(f_j - \Delta f) - \phi_{2k}(f_k - \Delta f)| \\ &= 2\pi\Delta f|\tau_{2k} - \tau_{1j}|\end{aligned}\tag{5.18}$$

If we assume for the moment that the delays in (5.18) have the same mean value $\bar{\tau}$ and r.m.s. value τ_{rms} independent of channel frequency, the r.m.s. phase error at $f_o + \Delta f$ is given by

$$\delta_{rms} = 2\pi\Delta f[(\tau_{rms})^2 - (\bar{\tau})^2]^{1/2}\tag{5.19}$$

Comparing this expression to the r.m.s. phase error for uncompensated cables given in equation (5.4), we see that (5.19) is identical to the latter except for a reduction in magnitude by the factor $\Delta f/f_{IF}$.

The dominant cause of random delay differences is the spread in phase-temperature coefficient K_p amongst the cables. In Sec. 2.4.4, the uncompensated error from this source was estimated at $\delta_{\text{rms}} = 0.72f_{\text{IF}}^\circ$ for RG-62A/U cable near the extremes of the temperature range; in the case of compensation, the error is eliminated at the center frequency and, according to (5.19), it is reduced to

$$\delta_{\text{rms}} = 0.72\Delta f \quad \text{degrees} \quad (5.20)$$

at the frequency $f_0 + \Delta f$, where Δf is expressed in MegaHertz. At the extremes of the maximum bandwidth of 200 KHz we have $\Delta f = 0.1$, which corresponds to an r.m.s. error, from (5.20), of 0.07° . The error is proportionately smaller as the center frequency is approached. It is clear that the compensator will do an adequate job of reducing the phase errors resulting from transmission line temperature changes even when the full bandwidth is considered, and no change in the error estimate of (5.13) is called for.

In the preceding analysis, the assumption was made that the cable delay is independent of frequency. While this assumption is fairly reasonable for the small frequency changes Δf which we are considering within a channel, there may be sufficient dispersion present to invalidate the assumption for the larger inter-channel differences. The phase equalization needed to combat dispersion (see Sec. 3.3.4) is not fully provided by the compensation system, and delay differences between channels of 0.1% (about 13 ns) will give rise to band-edge phase discrepancies of the order of 0.5° , according to (5.18). The solution would be to insert a fixed delay of

$$\Delta\tau_j = \overline{\tau(f_1)} - \overline{\tau(f_j)} \quad (5.21)$$

into each channel with $f_{IF} = f_j$ ($j=2,3,\dots,m$); f_1 is the lowest channel center frequency, corresponding to the maximum delay. Whether this expedient will be necessary depends on the results of dispersion measurements to be made on the cable after allocation of the channel frequencies. If the delay differences due to dispersion are reduced to the order of a few nanoseconds, then no significant deterioration in phase excitation should result.

The area in which the compensation system will be least effective is in the bandpass filters. The phase shift changes over the bandwidth will not be simply a constant phase offset or a change in slope of the phase characteristic. Although the compensator would likely provide some measure of error reduction in most instances, the amount of reduction is highly dependent on the nature of the changes. If, for example, the phase changes resulted from a shift in overall filter response to a slightly different center frequency, then virtually complete compensation is provided by a constant phase shift if the filter's phase characteristic is approximately linear. On the other hand, if the changes appear at the band edges but not at the center frequency, the compensator will fail to provide any error reduction. The actual performance will lie somewhere between these two extremes. Suppose we choose a conservative estimate of 25% reduction of phase errors (r.m.s.) in the bandpass filters; then, using the estimates of Table 4.1, the estimate of (5.13) for overall phase error in the compensated array is

$$\delta_{rms} = 0.7^\circ \quad (5.22)$$

One remaining component of the transmission system which has not yet been considered is the amplitude equalization network (Sec. 3.3.5). This is basically a highpass filter, but it will not have an abrupt attenuation characteristic, and its phase slope will likewise be quite gentle. The change in phase shift over an IF passband will probably be only a few degrees; in contrast, the four-stage Butterworth input filter has a phase shift which varies from -180° to $+180^\circ$ over its 3 dB bandwidth. The equalization network does not appear to pose any problems in regard to the effectiveness of the phase compensator.

The amplitude compensation portion of the compensator shown in Fig. 5.3 is perhaps of less importance than the phase compensation, but it would nevertheless be very useful. In particular, it would supplement the amplitude equalizer, making it adaptive to small changes in the channel gains. If the test signal distribution system is similar to the one described previously for L0 distribution, the r.m.s. amplitude error within the compensation system would be expected to be about 0.05 dB. Like the phase compensator, the amplitude compensator becomes less effective as the bandwidth increases, and this estimate may thus be overly optimistic. Again it is the filters which are most problematic; however, the amplitude changes may prove to be more amenable than phase changes to compensation at a single frequency. For instance, one change expected in the input filter is a variation in insertion loss caused by the dependence of inductor Q factor on temperature. This change is uniform over the passband and the compensation will hence be fully effective. If the r.m.s. amplitude errors in the filters are assumed to be reduced to approximately one-half of their estimated values with no compensation, and the other errors in the compensator are estimated at

5.8×10^{-3} (0.05 dB), then the estimate of Table 4.1 for overall r.m.s. amplitude error becomes

$$\Delta_{\text{rms}} = 0.014 \quad (1.4\%) \quad (5.23)$$

This error is dominated by the r.m.s. error in the beam-forming circuitry, which was previously estimated at 1.2%; if this figure can be improved upon in practice, the reduction of amplitude error level to less than that given by (5.23) may be possible.

On the basis of this preliminary analysis, a discontinuous compensation system would seem to be a highly useful adjunct to the array feeder system. There do not appear to be any insurmountable obstacles to implementing such a system, but experimental work will be needed to confirm the feasibility of the design and to study the technical problems involved. It may seem odd that the overall phase error reduction provided by this more elaborate compensator is apparently not a great deal better than for the continuous compensator of the previous section. The fact that the phase error estimates differ only slightly may be attributable in part to more pessimistic error estimates in the case of the discontinuous compensator, but the major reason is again the dominance of the beam-forming circuitry as a source of error.

There is another distinction between the two compensator systems which should be kept in mind. Many of the original error estimates of Chapter 4 were made with the proviso that calibration procedures be carried out frequently enough to maintain the error levels given. Since the continuous compensator includes only the transmission lines, the requirement for these procedures still remains insofar as the other

components are concerned. The discontinuous system, on the other hand, includes many of these components, notably the remote electronics; the need for frequent recalibration is thereby reduced or eliminated in these cases. In other words, the discontinuous compensator is superior in terms of maintaining a low level of excitation errors over a substantial period of time without demanding large amounts of time and labor on the part of the operators. This aspect of maintainability is of the utmost importance; because of it, a compensation system would definitely be an asset even if it provided no reduction in excitation errors. One further advantage of the discontinuous compensator is that it eliminates the need for having the same L0 phase, or at least a known phase, at each first mixer. The requirements on L0 amplitude uniformity can also be eased somewhat, but large departures from the nominal conversion gain are not acceptable. The L0 distribution system must have good short-term phase and amplitude stability, but it is no longer necessary to carefully choose the coupling points and adjust attenuators in order to get suitable L0 signals. Of course, the previous specifications demanded of the L0 system are now transferred to the test signal distribution system, but there is only one of these, compared to the m L0 distribution systems needed for m -channel FDM transmission. In this respect, as well as its abilities in the area of equalization mentioned earlier, the existence of a discontinuous compensation system would make FDM transmission a considerably more attractive proposition.

5.2 The Effects of Excitation Errors on Sidelobe Levels

Up to this point, no attempt has been made to relate the excitation errors to the antenna pattern produced, nor has the pattern needed to fulfil the astronomical objectives of the array been explicitly stated in terms of sidelobe levels. The reason for this omission is that complete answers to these questions are not yet available, and much work remains to be done in these areas. Some studies of the effects of errors on the patterns of the individual component arrays have been carried out [5], but the pattern of the Tee configuration after correlation has yet to be examined. As mentioned in Sec. 1.3.2, some criteria concerning the necessary r.m.s. sidelobe level have been formulated [2], but they have not been related to the particular power pattern of the Tee array. The intention of this section is to make a brief statistical study of the effects of excitation errors on certain sectors of the Tee pattern, in the hope of gaining some insight into the effect on the array pattern in general of errors of the magnitudes estimated in the preceding work.

5.2.1 Sidelobe Levels Off the Array Planes

We begin by considering the component arrays separately, under the assumption that they are rectangular arrays (no physical tapering) with Gaussian electrical tapering (to 6% in voltage at the extreme ends relative to the intersection of the Tee) on the long dimensions and no tapering on the short dimensions. The level of the sidelobes in the no-error patterns of these arrays has been shown to be of the order of -85 dB in directions which are well away from the fan beams [5]. If excitation errors are now introduced, the sidelobe levels will rise.

The field intensity v in a particular direction now becomes a random variable which is described statistically by a modified Rayleigh probability density function (p.d.f.) given by [87]:

$$p(v) = (2v/\sigma^2) \exp[-(a^2 + v^2)/\sigma^2] I_0(2av/\sigma^2) \quad (5.24)$$

where a = the field intensity of the no-error pattern in that direction

$I_0(x)$ = modified Bessel function of the first kind of order zero

and the parameter σ^2 is related to the excitation errors by

$$\sigma^2 = [(\Delta_{rms})^2 + (\delta_{rms})^2] \cdot [\sum_{p,q} (g_{pq})^2] / (\sum_{p,q} g_{pq})^2 \quad (5.25)$$

where Δ_{rms} = r.m.s. fractional amplitude error

δ_{rms} = r.m.s. phase error, radians

g_{pq} = voltage weighting of the array element whose position is denoted by the indices (p,q)

The factor multiplying the sum of the mean-square errors in equation (5.25) has been computed to be 1/905 for the east-west array and 1/1150 for the north-south array, assuming the use of the Gaussian electrical tapering as described at the beginning of this section.

For that part of the array pattern where the contribution of the errors to the field intensity predominates ($v^2 \gg a^2$), equation (5.24) can be simplified. Since $I_0(x) \approx 1$ for small arguments, the p.d.f. of (5.24) approaches the Rayleigh p.d.f.:

$$p(v) = (2v/\sigma^2) \exp(-v^2/\sigma^2) \quad (5.26)$$

The power pattern of the Tee array after cross-correlation is equal to the product of the voltage patterns of the component arrays, so that if the north-south and east-west arrays have normalized field intensities in a given direction of v_1 and v_2 respectively, then the normalized power pattern of the Tee has the value $W = v_1 v_2$ in this direction. In directions where the statistical patterns of the two arrays are dominant (i.e., away from the array planes), v_1 and v_2 may be considered to be independent random variables described by the p.d.f. of equation (5.26). The statistics of the Tee power pattern for these directions can thus be described by the p.d.f. of the product random variable W [88]:

$$\begin{aligned} p(W) &= \int_{-\infty}^{+\infty} \{ [p(v_1) p(W/v_1)] / |v_1| \} dv_1 \\ &= \int_0^{+\infty} \{ [p(v_1) p(W/v_1)] / v_1 \} dv_1 \end{aligned} \quad (5.27)$$

since $p(v) = 0$ for $v < 0$. To simplify the analysis, we shall assume that $p(v_1) = p(v_2)$, ignoring the difference in σ^2 for the two arrays. Substituting for $p(v_1)$ and $p(W/v_1)$ from (5.26) into (5.27), we get

$$p(W) = (4W/\sigma^4) \int_0^{\infty} \exp\{(-W/\sigma^2) [(v_1^2/W) + (W/v_1^2)]\} (dv_1/v_1) \quad (5.28)$$

If we make the substitution $u = \log_e (v_1^2/W)$, this becomes

$$p(W) = (2W/\sigma^4) \int_{-\infty}^{+\infty} \exp[(-2W/\sigma^2) (\cosh u)] du$$

$$\text{or,} \quad p(W) = (4W/\sigma^4) \int_0^{\infty} \exp[(-2W/\sigma^2)(\cosh u)] du \quad (5.29)$$

Using the relation [89]

$$K_0(x) = \int_0^{\infty} \exp[-x(\cosh u)] du \quad (5.30)$$

where $K_0(x)$ is the modified Bessel function of the second kind of order zero, we can write (5.29) in the form

$$p(W) = (4W/\sigma^4) K_0(2W/\sigma^2) \quad (5.31)$$

This p.d.f. is shown graphically in Fig. 5.4; its shape is not unlike that of the Rayleigh p.d.f. of equation (5.26). Since the mean value of the Rayleigh-distributed random variables v_1 and v_2 is $\sqrt{\pi}(\sigma/2)$, the mean sidelobe level is

$$\overline{W} = \overline{v_1} \overline{v_2} = \pi\sigma^2/4 \quad (5.32)$$

It is important to realize that this is not an average sidelobe level over the power pattern; it is rather an ensemble average for many identical Tee arrays with the same r.m.s. excitation error levels. It is valid for the directions in which the statistical patterns of the component arrays dominate the no-error patterns, which results in a relatively uniform sidelobe level for these directions.

A more enlightening function than the p.d.f. is the distribution function $P[W > W_0]$ giving the probability that a given sidelobe level W_0 will be exceeded:

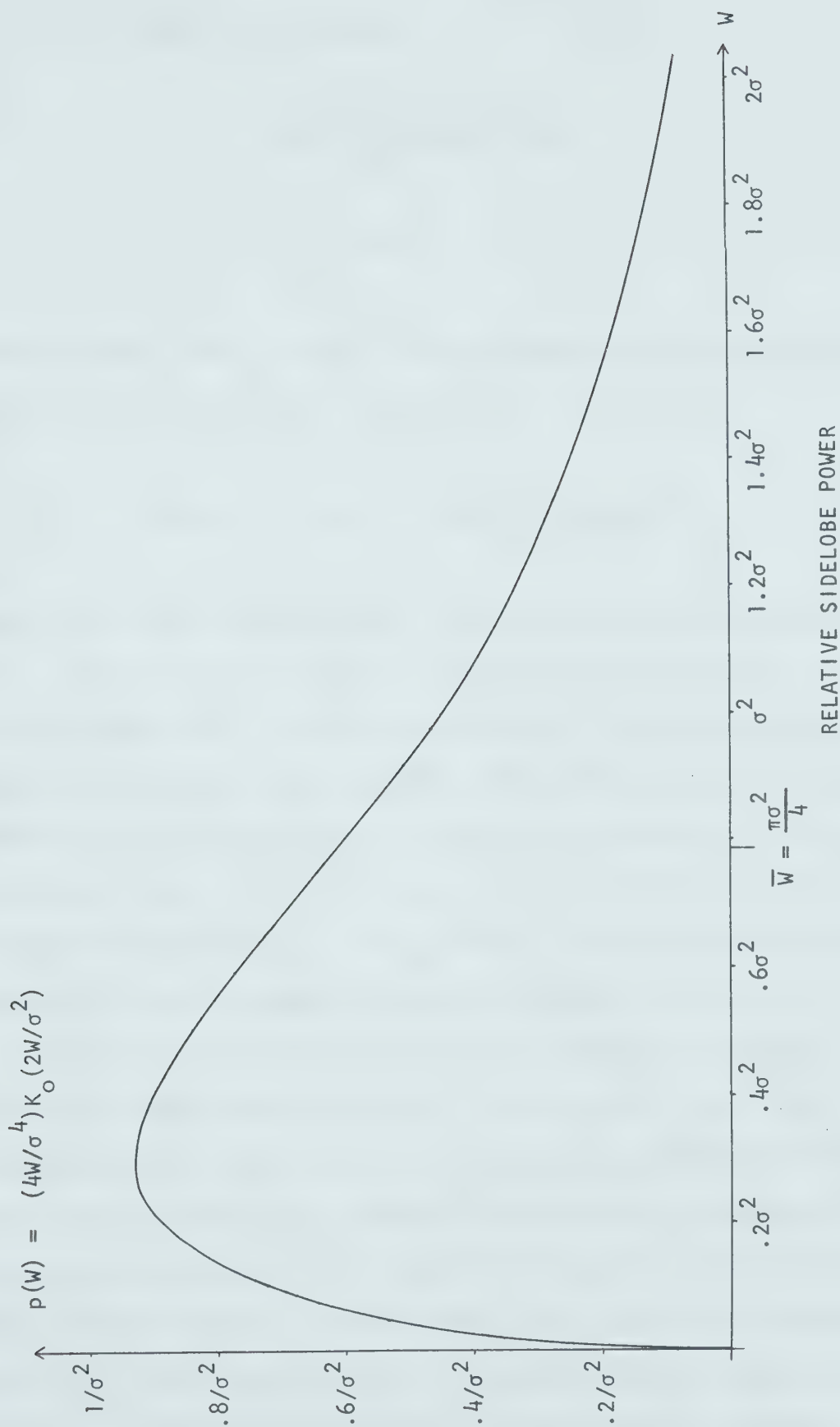


Fig. 5.4 Probability Density Function for Sidelobe Level Far from the Array Planes

$$\begin{aligned}
P[W > W_0] &= \int_{W_0}^{\infty} p(W) dW \\
&= (4/\sigma^4) \int_{W_0}^{\infty} W [K_0(2W/\sigma^2)] dW \\
&= \int_{z_0}^{\infty} z K_0(z) dz \tag{5.33}
\end{aligned}$$

where $z = 2W/\sigma^2$ and $z_0 = 2W_0/\sigma^2$. The integral in (5.33) can be evaluated from tables [90], yielding the relation

$$P[W > W_0] = z_0 K_1(z_0) = (2W_0/\sigma^2) K_1(2W_0/\sigma^2) \tag{5.34}$$

where $K_1(x)$ = the modified Bessel function of the second kind of order one.

The distribution function in equation (5.34) is shown in Fig. 5.4 for two cases; one is for the excitation error levels estimated in Chapter 4 (Table 4.1), and the other is for the reduced error levels resulting from the addition of a discontinuous compensation system, as estimated in Sec. 5.1.2. The value of σ^2 , as defined by equation (5.25), was approximated by $[(\Delta_{\text{rms}})^2 + (\delta_{\text{rms}})^2]/10^3$, which falls nearly midway between the values computed for the two component arrays.

Some of the salient features of the probability distribution just derived are summarized in Table 5.1. It can be seen from (5.32) that the compensator should give an average reduction in sidelobe level off the array planes of about 5 dB. Judging from preliminary studies of the Tee array pattern needed to fulfil certain astronomical objectives [2] and from the specifications placed on other arrays such as the Molonglo Cross [10], the proposed array will probably require a sidelobe level of -60 dB or better in these directions. To be reasonably confident, say

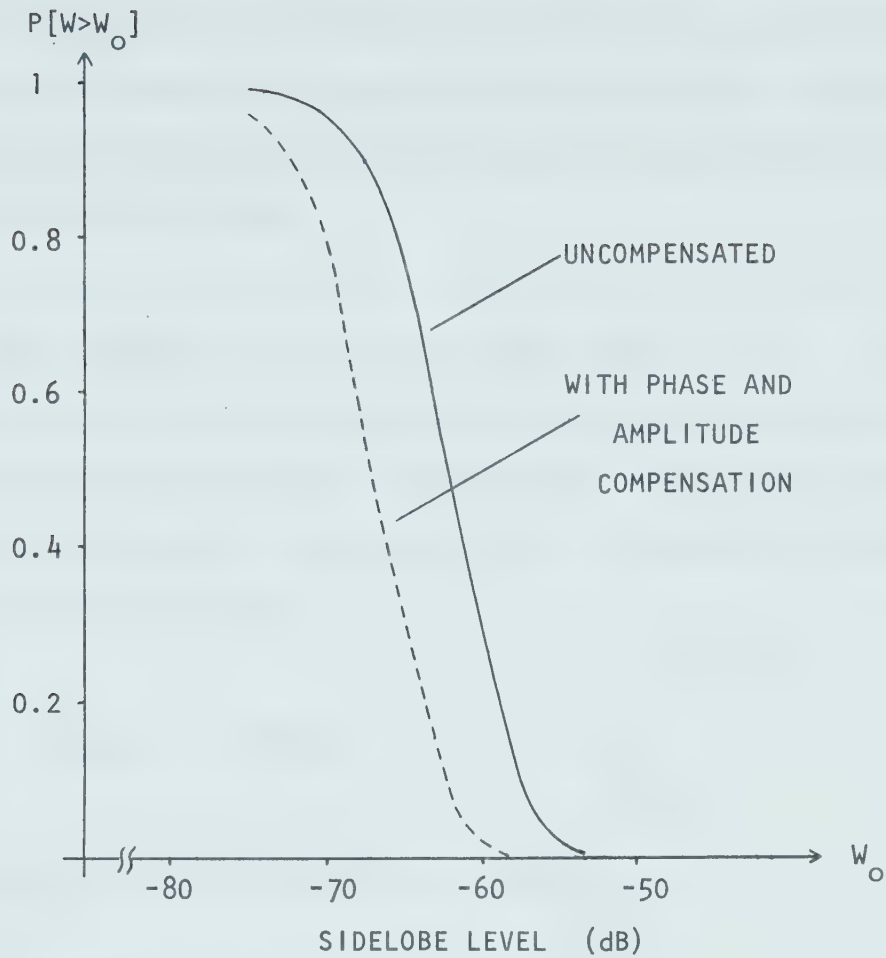


Fig. 5.5 Probability of Exceeding a Given Sidelobe Level

TABLE 5.1 Predicted Sidelobe Levels With and Without Compensation

Feeder System	σ^2	Sidelobe Level (dB) Far from Array Planes		
		Mean ($=\pi\sigma^2/4$)	Most Probable ($\approx 0.3\sigma^2$)	99% Confidence ($\approx 2.9\sigma^2$)
Uncompensated (Table 4.1)	11.2×10^{-7}	-61	-65	< -55
With Compensator (Sec. 5.1.2)	3.4×10^{-7}	-66	-70	< -60

90%, that this level is achieved, one must have r.m.s. excitation errors no greater than about 1° in phase and 2% in amplitude. The use of the compensator would significantly improve the chances of achieving or bettering the -60 dB level.

5.2.2 Sidelobe Levels In the Array Planes

We now consider those portions of the component array patterns in which the no-error pattern is dominant ($a^2 \gg \sigma^2$). This leads to another simplification of the general p.d.f. of equation (5.24). Using the asymptotic expression

$$I_0(x) \rightarrow e^{x/\sqrt{2\pi x}} \quad (5.35)$$

for large x , we find that (5.24) approaches

$$p(v) = (1/\sigma\sqrt{\pi}) \exp[-(v-a)^2/\sigma^2] \quad (5.36)$$

This is the p.d.f. for a Gaussian (normal) distribution with mean a and standard deviation $\sigma/\sqrt{2}$. In directions where the no-error pattern is very much larger than the statistical contribution, this p.d.f. approaches the Dirac delta function, and the approximation $v \approx a$ can be made. This is the case for most of the fan beam response of a component array. The sidelobe level for a particular zenith angle θ in the array plane of array #1 (north-south) can hence be given, except for very small and very large angles, as

$$W(\theta) = v_1 a_2(\theta) \quad (5.37)$$

where v_1 = the statistical sidelobe level at large angles for array #1,
as described by equation (5.26)

$a_2(\theta)$ = no-error sidelobe level in the fan beam of array #2 at zenith
angle θ

The sidelobe level in the other array plane can be similarly described
by $W = v_2 a_1$. The mainbeam of the Tee array is assumed to be aimed in the
direction of the zenith. To find the normalized fan beam response $a_i(\theta)$,
we make use of equation (1.1):

$$a_i(\theta) = \frac{\sin[\pi d_i N_i (\sin \theta)]}{N_i \sin[\pi d_i (\sin \theta)]} \quad (5.38)$$

where N_i = the number of elements across the short dimension of array #i
 d_i = the spacing of these elements, wavelengths

The distribution function for v_i is found by integrating the p.d.f.
in (5.26):

$$P[v_i > v_o] = \int_{v_o}^{\infty} p(v_i) dv_i = \exp(-v_o^2 / \sigma_i^2) \quad (5.39)$$

To illustrate the use of equation (5.37), suppose we are interested in
a particular direction in the north-south array plane for which the
east-west array fan beam has a relative field intensity of -20 dB, or
 $a_2 = 0.1$. We wish to predict the sidelobe level of the Tee array in this
direction; this is not possible, but we can state the probability that a
given level will not be exceeded. If, for example, we choose to find the
sidelobe level which we can be 95% certain of not exceeding, we set
 $P[v_i > v_o] = 0.05$ in (5.39) and find that $v_o = 1.73\sigma_i$. Recalling from Sec.
5.2.1 that $\sigma_1^2 = [(\Delta_{rms})^2 + (\delta_{rms})^2] / 1150$, and substituting $v_1 = 1.73\sigma_1$

and $a_2 = 0.1$ into (5.37), we have

$$\begin{aligned} W &= (0.1)(1.73)[(\Delta_{\text{rms}})^2 + (\delta_{\text{rms}})^2]^{1/2} / (1150)^{1/2} \\ &= 1.7 \times 10^{-4} \quad (-38 \text{ dB}) \end{aligned}$$

for the error estimates in the case of no compensation. In a similar fashion, one could estimate worst-case array plane response by choosing a suitable confidence level, finding the corresponding field intensity from (5.39), and multiplying the appropriate fan beam response from (5.38) by this field intensity. In connection with (5.38), the tentative parameter values for the proposed array are $N_1 = 8$, $d_1 = 5/8$ (north-south array), and $N_2 = 4$, $d_2 = 1/2$ (east-west array).

The analysis of this and the preceding section applies only to certain parts of the Tee array pattern; furthermore, the effects of making changes in the basic array structure, such as the removal of elements for physical tapering, cannot be deduced from these results. Despite these limitations, however, the results are indicative of how well the array can be expected to perform, and they will perhaps serve as a stimulus for further study in this important area.

5.3 Decorrelation and Delay Error Compensation

In a two-element correlation interferometer, the response in the direction of a given source is maximized by arranging that the antenna output signals resulting from this source are completely correlated at the detector input. If only a single frequency f_0 is received, the

correlation coefficient for the two signals is simply

$$\gamma = \cos 2\pi f_o \tau \quad (5.40)$$

where τ is the time delay between the arrivals at the two antennas of the wavefront from the source. To achieve unity correlation, a phase shift of $\phi = 2\pi f_o \tau$ radians must be inserted into the transmission line of the antenna nearest the source, assuming that the transmission lines are of equal length.

If we now accept a rectangular bandwidth B centered on f_o , the correlation coefficient departs from unity at frequencies other than f_o , and it is now given by

$$\gamma(f) = \cos 2\pi(f - f_o)\tau \quad (5.41)$$

for a given frequency f within the band. The overall correlation coefficient is obtained by integrating (5.41) over the bandwidth:

$$\gamma(B) = \frac{1}{B} \int_{f_1}^{f_2} \gamma(f) df = \frac{\sin \pi \tau B}{\pi \tau B} = \text{sinc } \tau B \quad (5.42)$$

where $f_1 = f_o - B/2$ and $f_2 = f_o + B/2$. The loss in sensitivity which results from $\gamma(B)$ falling below unity is known as a decorrelation loss. For unity correlation in this case, a time delay τ must be inserted into the appropriate transmission line.

In an instrument such as the proposed Tee array which is operated as a cross-correlation phased array, all of the element outputs within a component array are phase shifted and summed before correlation takes

place; the output voltage of the north-south array, for example, could be expressed in the form

$$V_{NS}(t) \propto \sum_{a,b} g_{ab} V_{ab}(t) \quad (5.43)$$

where $V_{ab}(t)$ = voltage output from element (a,b) after phasing, due to a point source in a given direction

g_{ab} = weighting of element (a,b) set by the grading function

Similarly, the east-west array has an output of

$$V_{EW}(t) \propto \sum_{c,d} g_{cd} V_{cd}(t) \quad (5.44)$$

The correlator performs the function of multiplying the array outputs, followed by time averaging (integration) of the product. The output of the correlator can thus be expressed as

$$\begin{aligned} V_O &= \overline{V_{NS}(t) V_{EW}(t)} \\ &\propto \sum_{a,b,c,d} g_{ab} g_{cd} \overline{V_{ab}(t) V_{cd}(t)} \\ &\propto \sum_{a,b,c,d} g_{ab} g_{cd} \gamma_{abcd} \end{aligned} \quad (5.45)$$

where the coefficient γ_{abcd} is, from (5.42),

$$\gamma_{abcd} = \text{sinc}(\Delta\tau_{abcd})B \quad (5.46)$$

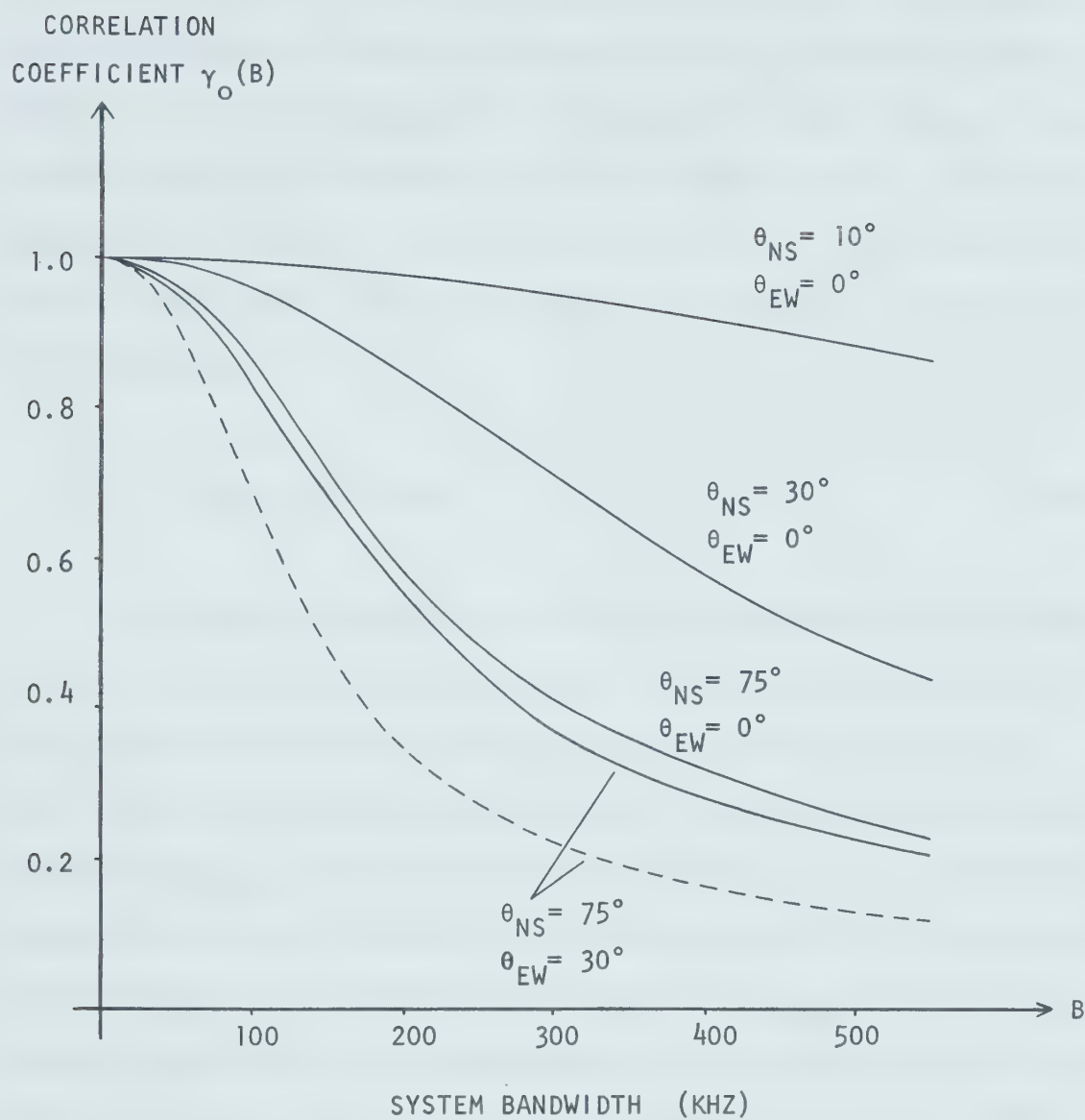
$\Delta\tau_{abcd}$ is the time difference in arrival at the correlator of the outputs

from elements (a,b) and (c,d) corresponding to the same wavefront from the source. Ideally, all of the correlation coefficients given by (5.46) will be unity; if they are not, the correlator output V_0 will be reduced from the maximum possible value by the factor

$$\gamma_0 = \frac{\sum_{a,b,c,d} g_{ab} g_{cd} \gamma_{abcd}}{\sum_{a,b,c,d} g_{ab} g_{cd}} \quad (5.47)$$

This coefficient, which is a function of bandwidth and source direction, indicates how the sensitivity of the radio telescope is reduced by the delay errors $\Delta\tau_{abcd}$. Without delay compensation, the array will have perfect correlation only for sources at the zenith (assuming an ideal feeder system having no delay errors). The coefficient of equation (5.47) is plotted in Fig. 5.6 as a function of bandwidth for the proposed Tee configuration. The delay errors were assumed to be solely a function of source direction and element position, and to simplify the computation the elements were partitioned into groups of 32 (four north-south by eight east-west), the arrival time of a wavefront being assumed to be the same for all members of a given group. It can be seen that the decorrelation loss becomes quite large, except in the case of directions near the zenith or very small bandwidths.

The problem of delay errors is more serious than it appears from the standpoint of loss of sensitivity. A delay error of the type under discussion is actually a systematic phase excitation error which appears when one attempts to scan away from the zenith. The error is zero at midband and linear across the bandwidth, and, unlike the phase errors discussed previously, it is entirely predictable. The delay error actually manifests itself as an amplitude error; as can be seen from



Key: ——— Gaussian Taper (to 6% at end of arms)
 - - - Uniform Aperture (no taper)

θ_{NS} = Zenith Angle in North-South Array Plane
 θ_{EW} = Zenith Angle in East-West Array Plane

Fig. 5.6 Correlation Versus Bandwidth for Various Scan Angles

equation (5.45), the coefficient γ_{abcd} has the effect of making the element weightings a function of source direction, which will result in changes in the array pattern as it is scanned. For this reason, it is customary (see [3], for example) to require that the r.m.s. value of γ_{abcd} be maintained at a value of 0.99 or greater. For the maximum bandwidth of 200 KHz, the delay difference corresponding to this value is, from (5.46),

$$\Delta\tau_{abcd} = 0.39 \mu\text{s} \quad (5.48)$$

To estimate the accuracy with which the compensating delays must be set, suppose that each element output passes through a delay which can be varied in steps of $\delta\tau$. The errors which appear due to this quantization have a uniform distribution from $-\delta\tau/2$ to $+\delta\tau/2$. The delay difference $\Delta\tau_{abcd}$ between the outputs of elements (a,b) and (c,d) after compensation will be the difference between the quantization errors for these elements. The probability distribution for $\Delta\tau_{abcd}$ is found by assuming these errors to be independent and convolving the uniform p.d.f. with itself; the result is a Simpson (triangular) distribution [88], whose p.d.f. is given by

$$p(\Delta\tau) = \begin{cases} \frac{\Delta\tau + \delta\tau}{(\delta\tau)^2} & \text{for } -\delta\tau \leq \Delta\tau \leq 0 \\ \frac{\delta\tau - \Delta\tau}{(\delta\tau)^2} & \text{for } 0 \leq \Delta\tau \leq \delta\tau \end{cases} \quad (5.49)$$

where $\Delta\tau_{abcd}$ has been abbreviated as $\Delta\tau$. The mean-square delay difference is then found to be

$$\overline{(\Delta\tau)^2} = \int_{-\delta\tau}^{+\delta\tau} (\Delta\tau)^2 p(\Delta\tau) d(\Delta\tau) = (\delta\tau)^2/6 \quad (5.50)$$

and the r.m.s. delay difference is

$$(\Delta\tau)_{\text{rms}} = \delta\tau/\sqrt{6} \quad (5.51)$$

Substituting the value for $\Delta\tau_{\text{abcd}}$ found in equation (5.48) for $(\Delta\tau)_{\text{rms}}$ in (5.51), we find that the maximum step size in the compensating delays for an r.m.s. correlation coefficient of 0.99 is

$$\delta\tau(\text{max}) = 0.96 \text{ } \mu\text{s} \quad (5.52)$$

for a bandwidth of 200 KHz. The actual delay step size will depend on the frequency at which the delays will operate; this will likely be the center frequency f_0 . Since it is desirable that the delay settings not interact with those of the phase shifters in the beam-forming network, the delay step size should be an integral multiple of $1/f_0$ (80.9 ns).

Placement of the compensating time delays in the transmission system would be feasible only if the multiple beams of the array were very closely spaced. Since we do not wish to place such a limitation on the flexibility of the array, at least a portion of the delays must be inserted within the beam-forming process, as was done in the Molonglo Cross delay compensation system [11]. Because the delays are so intimately connected with the beam-forming circuitry, they were not considered separately in the excitation error estimates of Chapter 4. It is possible, in fact, that variable delays rather than phase shifters could be used for beam formation. This possibility is practicable only if

the beam-forming network operates at f_o ; otherwise, the delays do not provide the phase shifts needed to scan the response of the array. The matter of beam formation is a complex one and will not be considered further here. Various methods of implementing variable delays were discussed in Sec. 5.1.1.

The range of compensating delays required for the array is a function of its size and the maximum angles from the zenith that the beam will be scanned. These angles were given in Sec. 1.3.2. For the east-west array, the maximum zenith angle will be about 30° , which corresponds to a delay gradient over the length of the array (5 km) of about $8.3 \mu\text{s}$. For the north-south array, the maximum angle will be about 67° , resulting in a gradient of $7.7 \mu\text{s}$ across this array. This is for beaming south of the zenith; the northern zenith angle need only be 38° to reach the north celestial pole, which gives a delay gradient of $5.1 \mu\text{s}$ in the opposite sense.

One possible system for organizing the compensating delays is to insert a fixed delay of $7.7 \mu\text{s}$ for the elements near the center of the Tee. Then the extreme northern elements of the north-south array would require delays variable from zero to $12.8 \mu\text{s}$, and the elements at the ends of the east-west array would require delays variable from 3.5 to $11.9 \mu\text{s}$. The delay range needed for the intermediate elements decreases proportionately as the center of the Tee is approached.

CHAPTER 6

SUMMARY AND CONCLUSIONS

The work of the preceding chapters obviously does not represent a complete feeder system design; numerous questions remain to be answered concerning the Tee array configuration and the type of signal processing to be done, and the ultimate design will be contingent on the results of further studies in these areas. Nevertheless, a basic framework has been developed, around which the array design can take shape as new information becomes available. Some potential pitfalls, and methods of avoiding them, have been pointed out. In summary, the following are some of the more important conclusions which have been reached regarding the feeder system design:

(1) The basic feeder configuration should consist of independent feedlines of equal length (approximately 2.5 km). The number of lines needed is N/mn , where N is the total number of elements, m is the number of FDM channels per line, and n is the subarray size. From considerations of cost, attenuation, and phase stability, RG-62A/U appears to be the best available coaxial transmission line for use in the feeder system.

(2) Frequency conversion before transmission offers a number of advantages over direct transmission at 12 MHz, including lower attenuation, smaller phase errors, and the possibility of using FDM. The most suitable range for IF transmission is approximately 1-4 MHz. The limits on this range are quite flexible; the upper limit is roughly equal to the frequency at which the cable attenuation equals the gain

of the remote electronics. The L0 signal needed for frequency conversion can be accurately distributed by means of the Swarup and Yang technique.

(3) Frequency-division multiplexing appears to be the only practicable method of transmitting several independent signals on a single transmission line. The implementation of FDM becomes quite simple if channel filters preceding the second mixers can be shown to be unnecessary. At present, a system of 4 to 6 channels is envisioned, with spacing between channel centers of about 0.5 MHz. A larger number of channels is conceivable, depending upon the outcome of investigations concerning IM crosstalk and automatic compensator systems.

(4) The r.m.s. excitation errors in the array (without automatic compensators) have been estimated at 1.5° in phase and 2.1% in amplitude. These values are based upon the supposition that a large amount of day-to-day maintenance and readjustment will be carried out. The r.m.s. errors can be reduced to an estimated 0.7° and 1.4% by the use of phase and amplitude compensation in the feeder system. The numbers involved are somewhat questionable; a more realistic statement regarding the feeder system excitation errors is that they likely can be reduced to the point where they are dominated by the other sources of error (notably the beam-forming system, mutual coupling of the array elements, and positional errors).

(5) A phase and amplitude compensation system is a necessity if accurate array excitation is to be maintained without expending an enormous number of man-hours re-trimming the transmission lines, adjusting attenuators, and so forth. A compensator such as the one described in Sec. 5.1.2 is preferred, since it encompasses virtually

all system components from antenna element to beam-forming network. It also simplifies the implementation of FDM by providing automatic equalization and by making LO distribution less difficult.

(6) The probability of achieving sidelobe levels of the order of -60 dB or better at angles far from the array planes appears to be quite high, especially if the discontinuous compensator is in use. It has not yet been ascertained whether the overall antenna pattern is adequate under these circumstances.

To consolidate these results and make the array design more definite, further studies are needed in a number of areas. Among them are:

(1) A detailed study of the Tee array radiation pattern, including the effects of mutual coupling, excitation errors, physical tapering, and subarrays, is required. The excitation error levels, subarray size, and other parameters must be related to their effects on the pattern, and decisions must then be made concerning the specifications needed to fulfill the astronomical objectives of the array.

(2) Other aspects of the antenna design such as the construction of the elements and their supports must be investigated. It has been shown that rather tight tolerances must be placed on element locations and orientations if positional errors are to be kept small with respect to electrical errors. Protection of the array from lightning damage is another important facet of the antenna design which demands further study.

(3) A thorough survey of beam-forming techniques must be carried

out to determine which is best suited to the proposed array. A number of interesting possibilities have been suggested, including the use of digital signal processing and the use of variable delays rather than phase shifters to scan the beams. Operation as a correlation array with electrooptical processing is another possibility.

(4) Experimental work on the proposed FDM system is needed to test its feasibility. In particular, IM crosstalk and the need for channel filters must be evaluated as suggested in Sec. 3.3.2.

(5) Experimental work on phase and amplitude compensator designs is required. The discontinuous nature of the more complex design of Sec. 5.1.2 poses a number of problems in the areas of switching, construction of a variable phase shifter with memory, and so on.

(6) Some questions concerning cable characteristics which have been raised in this work should be resolved by measurements. The spacing needed between cables to prevent significant inter-cable crosstalk levels must be determined. Phase delay measurements over the IF range must be made to determine whether small compensating delays are needed in the channels to combat dispersion.

(7) A good deal of work remains to be done in the area of electronics design, particularly in the remote units. The proposed eighth-order Butterworth input filter and other filter configurations should be studied with regard to their reproducibility and thermal stability. Other areas for further work include gain stability and IM performance of the mixers, design of the amplitude equalizer, and a general study of measurement and adjustment techniques by which the electronic components can be matched in phase and amplitude characteristics.

REFERENCES

- [1] F.S. Chute, C.G. Englefield, P.J.R. Harding, C.R. James, and D. Routledge, "Site-testing for a proposed 12 MHz radio telescope in Alberta," J. Roy. Astron. Soc. Can., vol. 65, no. 2, pp. 49-59, 1971.
- [2] W.R. Goddard, unpublished research report, Dept. of Elec. Eng., Univ. of Alberta, 1972.
- [3] M.I. Large and R.H. Frater, "The beam forming system for the Molonglo radio telescope," Proc. I.R.E.E. (Aust.), vol. 30, pp. 227-235, Aug. 1969.
- [4] W.N. Christiansen and J.A. Hogbom, Radiotelescopes. London, England: Cambridge Univ. Press, 1969.
- [5] D.A. Wynne, "Physical tapering of large antenna arrays," M.Sc. thesis, Dept. of Elec. Eng., Univ. of Alberta, 1973.
- [6] J.A. Galt, C.R. Purton, and P.A.G. Scheuer, "A large 10 MHz array for radio astronomy," Publ. Dominion Observatory, vol. 25, no. 10, pp. 295-304, 1967.
- [7] C.R. Purton, "Effect of mutual coupling in a 10-MHz antenna array," Bull. Radio Elec. Eng. Div., National Research Council of Canada, vol. 17, no. 2, pp. 4-12, 1967.
- [8] J.A. Galt and C.H. Costain, "Low-frequency radio astronomy," Trans. Roy. Soc. Can., vol. 3, series 4, pp. 419-430, 1965.
- [9] C.H. Costain, J.D. Lacey, and R.S. Roger, "Large 22-MHz array for radio astronomy," IEEE Trans. Antennas Propagat., vol. AP-17, pp. 162-169, Mar. 1969.
- [10] B.Y. Mills, R.E. Aitchison, A.G. Little, and W.B. McAdam, "The Sydney University cross-type radio telescope," Proc. I.R.E. (Aust.), vol. 24, pp. 156-165, Feb. 1963.
- [11] T.W. Clarke, H.S. Murdoch, and M.I. Large, "The delay line system for the Molonglo radio telescope," Proc. I.R.E.E. (Aust.), vol. 30, pp. 236-240, Aug. 1969.
- [12] R.E.B. Munro, H.S. Murdoch, and M.I. Large, "The multiple beam phasing of the Molonglo radio telescope," Proc. I.R.E.E. (Aust.), vol. 31, pp. 19-23, Jan. 1970.
- [13] W.C. Erickson, "The decametric arrays at the Clark Lake radio observatory," IEEE Trans. Antennas Propagat., vol. AP-13, pp. 422-427, May 1965.

- [14] W.C. Erickson, "A proposal for an electronics system for the Clark Lake Teepee Tee," Astronomy Program, Univ. of Maryland, Nov. 1970.
- [15] V.V. Vitkevich and P.D. Kalachev, "Design principles of the FIAN cross-type wide-range telescope," Proc. (Trudy) P.N. Lebedev Phys. Inst., vol. 28, pp. 1-6, Trans. Consultants Bureau, 1966.
- [16] Yu.P. Ilyasov and A.D. Kuzmin, "Wide-range exciter for a 'parabolic cylinder' antenna," Proc. (Trudy) P.N. Lebedev Phys. Inst., vol. 28, pp. 7-12, Trans. Consultants Bureau, 1966.
- [17] S.N. Ivanov, Yu.P. Ilyasov, and G.N. Khramov, "Wide-range exciter with an electrically scanned radiation pattern," Proc. (Trudy) P.N. Lebedev Phys. Inst., vol. 28, pp. 13-24, Trans. Consultants Bureau, 1966.
- [18] Yu.P. Ilyasov, "Basic parameters of the east-west antenna feed of the Lebedev Institute wideband cruciform radio telescope," Proc. (Trudy) P.N. Lebedev Phys. Inst., vol. 47, pp. 151-159, Trans. Consultants Bureau, 1971.
- [19] Yu.M. Bruk, N.Yu. Goncharov, A.V. Men, L.G. Sodin, and N.K. Sharykin, "A T-shaped radiotelescope with electrical beam scanning in the 10-25 Mc band," Izvestiya VUZ. Radiofizika, vol. 10, no. 5, pp. 608-619, 1967.
- [20] Yu.M. Bruk, N.Yu. Goncharov, I.N. Zhuk, G.A. Inyutin, A.V. Men, L.G. Sodin, and N.K. Sharykin, "Experimental study of the multielement antenna arrays of the UTR-1 radio telescope," Izvestiya VUZ. Radiofizika, vol. 11, no. 1, pp. 28-43, 1968.
- [21] B.Y. Mills, A.G. Little, K.V. Sheridan, and O.B. Slee, "A high resolution radio telescope for use at 3.5 M.," Proc. IRE, vol. 46, pp. 67-84, Jan. 1958.
- [22] C.A. Shain, "The Sydney 19.7-Mc radio telescope," Proc. IRE, vol. 46, pp. 85-88, Jan. 1958.
- [23] C.H. Costain and F.G. Smith, "The radio telescope for 7.9 metres wavelength at the Mullard Observatory," Mon. Not. Roy. Astr. Soc., vol. 121, no. 4, pp. 405-412, 1960.
- [24] J.H. Crowther and R.W. Clarke, "A pencil-beam radio telescope operating at 178 Mc/s," Mon. Not. Roy. Astr. Soc., vol. 132, no. 4, pp. 405-412, 1966.
- [25] J.P. Wild, "The Culgoora radioheliograph: 1 - specification and general design," Proc. I.R.E.E. (Aust.), vol. 28, pp. 279-291, Sept. 1967.
- [26] P.A. Hamilton and R.F. Haynes, "Observations of the southern sky at 10.02 MHz," Aust. J. Phys., vol. 21, pp. 895-902, 1968.

- [27] P.A. Hamilton, "An electronic phasing system for aerial arrays," Proc. I.R.E.E. (Aust.), vol. 29, pp. 56-57, Feb. 1968.
- [28] G.R.A. Ellis, "A receiver for observation of VLF noise from the outer atmosphere," Proc. IRE, vol. 48, pp. 1650-1651, Sept. 1960.
- [29] W.H. Kummer, "Feeding and phase scanning," Microwave Scanning Antennas, vol. 3 (R.C. Hansen, ed.). New York: Academic Press, 1966.
- [30] J.D. Kraus, Radio Astronomy. New York: McGraw-Hill, 1966, p. 102.
- [31] B.H. Andrew, "The spectrum of low radio frequency background radiation," Mon. Not. Roy. Astr. Soc., vol. 132, pp. 79-86, 1966.
- [32] B.F.C. Cooper, "Receivers in radio astronomy," Proc. I.R.E. (Aust.), vol. 24, pp. 113-119, Feb. 1963.
- [33] R.A. Batchelor, "Transistor r.f. and i.f. amplifiers for radio astronomy applications," Proc. I.R.E.E. (Aust.), vol. 30, pp. 99-105, Apr. 1969.
- [34] "RF transmission line catalog and handbook," no. TL-4, Times Wire and Cable Co., Wallingford, Conn., 1972.
- [35] "RF transmission lines and fittings," Military Standardization Handbook MIL-HDBK-216, Defence Supply Agency, Washington, D.C., May 1965.
- [36] N.A. Mackay, "A template method for equalization," Proc. I.R.E.E. (Aust.), vol. 30, pp. 142-146, May 1969.
- [37] A.M. Evans and R.L. Rhoads, "Wideband attenuation and phase measurements on high quality coaxial cables," IEEE WESCON Tech. Papers, vol. 13, Aug. 1969.
- [38] Loc. cit. [4], pp. 199-200.
- [39] G. Rodriguez, "Phase shift vs. temperature for braided coax," Microwaves, vol. 8, pp. 42-48, Feb. 1969.
- [40] A.M. Kushner, "Discussion of phase errors in coaxial transmission lines," Times Wire and Cable Co., Wallingford, Conn., Jan. 1965.
- [41] S. Reich, "MOSFET biasing techniques," EEE, vol. 18, pp. 62-68, Sept. 1970.
- [42] G. Swarup and K.S. Yang, "Phase adjustment of large antennas," IEEE Trans. Antennas Propagat., vol. AP-9, pp. 75-81, Jan. 1961.
- [43] C.G. Wynn-Williams, "Accurate measurement of the electrical length of long coaxial radio-frequency cables," Proc. Inst. Elec. Eng., vol. 119, pp. 113-116, Feb. 1972.

- [44] L.E. Sweeney, "A new swept-frequency technique for matching feedline lengths," Proc. IEEE (Lett.), vol. 59, pp. 1281-1282, Aug. 1971.
- [45] N.R. Labrum and K.R. McAlister, "The Culgoora radioheliograph: 3 - the transmission lines," Proc. I.R.E.E. (Aust.), vol. 28, pp. 297-301, Sept. 1967.
- [46] R.B. Read, "Two-element interferometer for accurate position determinations at 960 Mc," IRE Trans. Antennas Propagat., vol. AP-9, pp. 31-35, Jan. 1961.
- [47] "A proposal for a very large array radio telescope," vol. 2, p. 13-3, National Radio Astronomy Observatory, Green Bank, W.Va., Jan. 1967.
- [48] G.S. Eager, L. Jachimowicz, I. Kolodny, and D.E. Robinson, "Transmission properties of polyethylene-insulated telephone cables at voice and carrier frequencies," AIEE Trans., pt. 1 (Communication and Electronics), vol. 74, pp. 618-640, Nov. 1959.
- [49] D.P. Howson and J.G. Gardiner, "Image-cancelling mixers," Electron. Lett., vol. 8, pp. 352-354, 13 Jul. 1972.
- [50] A.G. Little, R.W. Hunstead, and G.G. Calhoun, "A constant phase local oscillator system for a cross type radio telescope," IEEE Trans. Antennas Propagat., vol. AP-14, pp. 645-646, Sept. 1966.
- [51] P.W. Arnold, "A 7-25 MHz high-power ten-element electronically scanned array for ionospheric backscatter measurements," IEEE Trans. Antennas Propagat., vol. AP-19, pp. 584-593, Sept. 1971.
- [52] B.P. McRae and A.V. Hromass, "A new approach to shielding against direct lightning strokes," Elec. Eng. Trans. (Inst. of Engineers, Aust.), vol. EE7, pp. 33-44, Sept. 1971.
- [53] K. Mukasa and Y. Kiyotani, "Lightning protection for a microwave relay station," Rev. Elec. Commun. Lab. (Nippon Telegraph and Telephone Corp.), vol. 18, pp. 898-912, Nov.-Dec. 1970.
- [54] D.L. Vines and P.K. Hardage, "An electronic lightning protector," Proc. Natl. Electron. Conf., vol. 24, pp. 374-376, Dec. 1968.
- [55] C.B. Feldman and W.R. Bennett, "Bandwidth and transmission performance," Bell Syst. Tech. J., vol. 28, pp. 490-595, July 1949.
- [56] F. Langford-Smith (ed.), Radiotron Designer's Handbook, 4th ed. Sydney, Australia: Wireless Press, 1953, pp. 1026 ff.
- [57] R.L. Wigington and N.S. Nahman, "Transient analysis of coaxial cables considering skin effect," Proc. IRE, vol. 45, pp. 166-174, Feb. 1957.

- [58] B.P. Lathi, Communication Systems. New York: Wiley, 1968, p. 249.
- [59] P.F. Panter, Modulation, Noise, and Spectral Analysis. New York: McGraw-Hill, 1965, pp. 524-527.
- [60] G.C. Hartley, P. Mornet, F. Ralph, and D.J. Tarran, Techniques of Pulse-Code Modulation in Communication Networks. London, England: Cambridge Univ. Press, 1967.
- [61] G.E. Hansell, Filter Design and Evaluation. New York: Van Nostrand Reinhold, 1969.
- [62] W.R. Bennett, "Cross-modulation requirements on multichannel amplifiers before overload," Bell Syst. Tech. J., vol. 19, pp. 587-610, Oct. 1940.
- [63] W.R. Bennett, Introduction to Signal Transmission. New York: McGraw-Hill, 1970, p. 217.
- [64] R.E. Matick, Transmission Lines for Digital and Communication Networks. New York: McGraw-Hill, 1969.
- [65] D.R. von Recklinghausen, "Theory and design of FET converters," IEEE Trans. Broadcast and Television Receivers, vol. BTR-12, pp. 43-50, Apr. 1966.
- [66] E.F. McKeon, "Cross-modulation effects in single-gate and dual-gate MOS field-effect transistors," Appl. Note AN-3435, Radio Corp. of America, Harrison, N.J., 1967.
- [67] J.M. Gutwein and J.F. Annese, "A double sideband quadrature carrier multiplex telemetry system," Proc. Int. Telemetry Conf., vol. 4, pp. 560-573, 1968.
- [68] D.L. Anderson, "A quadrature subcarrier technique for the transmission of two independent PCM channels," Proc. Natl. Telemetry Conf., 1963.
- [69] R. Aitchison, "Stability in electronic equipment," Progress in Radio Science 1963-66, part 2, Sept. 1966.
- [70] A.I. Zverev, Handbook of Filter Synthesis. New York: Wiley, 1967.
- [71] B.M. Oliver and J.M. Cage (ed.), Electronic Measurements and Instrumentation. New York: McGraw-Hill, 1971, p. 21.
- [72] H.P. Kalmus and A.L. Hedrich, "Precision phasemeter for small angles," Proc. IRE, vol. 47, p. 90, Jan. 1959.
- [73] D.E. Maxwell, "A 5 to 50 MHz direct-reading phase meter with hundredth-degree precision," IEEE Trans. Instr. Meas., vol. IM-15, pp. 304-310, Dec. 1966.

- [74] "Cable testing with time domain reflectometry," Appl. Note 67, Hewlett-Packard Co., Colorado Springs, Colo., 1965.
- [75] H. Stark, "Electrooptical processing for radio astronomy," Proc. IEEE (Lett.), vol. 60, pp. 1009-1010, Aug. 1972.
- [76] R.S. Elliott, "Mechanical and electrical tolerances for two-dimensional scanning antenna arrays," IRE Trans. Antennas Propagat., vol. AP-6, pp. 114-120, Jan. 1958.
- [77] R.C. Hansen (ed.), Microwave Scanning Antennas, vol. 2. New York: Academic Press, 1966.
- [78] P.W. Hannan, D.S. Lerner, and G.H. Knittel, "Impedance matching a phased-array antenna over wide scan angles by connecting circuits," IEEE Trans. Antennas Propagat., vol. AP-13, pp. 28-34, Jan. 1965.
- [79] W.J. Hannan, J.F. Schanne, and D.J. Woywood, "Automatic correction of timing errors in magnetic tape recorders," IEEE Trans. Military Electron., vol. MIL-9, pp. 246-254, July-Oct. 1965.
- [80] F.L.J. Sangster and K. Teer, "Bucket-brigade electronics - new possibilities for delay, time-axis conversion, and scanning," IEEE J. Solid-State Circuits, vol. SC-4, pp. 131-136, June 1969.
- [81] R.A. Mao, K.R. Keller, and R.W. Ahrons, "Integrated MOS analog delay line," IEEE J. Solid-State Circuits, vol. SC-4, pp. 196-201, Aug. 1969.
- [82] M.F. Tompsett and E.J. Zimany, "Use of charge-coupled devices for delaying analog signals," IEEE J. Solid-State Circuits, vol. SC-8, pp. 151-157, Apr. 1973.
- [83] L. Altman, "Bucket brigade devices pass from principle to prototype," Electronics, vol. 45, pp. 62-63, 28 Feb. 1972.
- [84] C.N. Berglund, "Analog performance limitations of charge-transfer dynamic shift registers," IEEE J. Solid-State Circuits, vol. SC-6, pp. 391-394, Dec. 1971.
- [85] P.G. Smith, "Phase compensation for widely-spaced antenna systems employing coherent signal combinations," IEEE Trans. Aerosp. Electron. Syst., vol. AES-3, pp. 91-98, Jan. 1967.
- [86] F.M. Gardner, Phaselock Techniques. New York: Wiley, 1966.
- [87] R.E. Collin and F.J. Zucker, Antenna Theory, part 1. New York: McGraw-Hill, 1969, pp. 232-233.
- [88] P. Beckmann, Elements of Applied Probability Theory. New York: Harcourt, Brace, and World, 1968, pp. 77-78.

[89] M. Abramowitz and I.A. Stegun, Handbook of Mathematical Functions.
Washington, D.C.: National Bureau of Standards, U.S. Government
Printing Office, 1964, p. 376.

[90] Ibid, p. 484.

B30064